Quantum Snake Walk on Graphs

by

Ansis Rosmanis

A thesis
presented to the University of Waterloo
in fulfillment of the
thesis requirement for the degree of
Master of Mathematics
in
Computer Science

Waterloo, Ontario, Canada, 2009

I hereby declare that I am the sole author of this thesis. This is a true copy of the thesis, including any required final revisions, as accepted by my examiners.

I understand that my thesis may be made electronically available to the public.

Abstract

Quantum walks on graphs have been proven to be a useful tool in quantum algorithm construction for various problems. In this thesis we introduce a new type of continuous-time quantum walk on graphs called the *quantum snake walk*, the basis states of which are fixed-length paths (*snakes*) in the underlying graph.

We first consider the quantum snake walk on the line. The analysis of the eigenvalues and the eigenvectors of the Hamiltonian governing the walk reveals that most states initially localized in a segment on the line always remain in that same segment. However, there are exponentially small (in the length of the snake) fraction of states which move on the line as wave packets with momentum inversely proportional to the length of the snake.

Next we show how an algorithm based on the quantum snake walk might be able to solve an extended version of the glued trees problem which asks to find a path connecting both roots of the glued trees graph. No efficient quantum algorithm solving this problem is known yet. For that reason we consider a specific extension of the glued trees graph and analyze how the quantum snake walk behaves on it. In particular we show that the quantum snake walk on the infinite binary tree, restricted to certain superpositions, in many aspects is very similar to the quantum snake walk on the line. We also argue why the quantum snake walk, initialized in certain superpositions on one side of the glued trees graph, after certain amount of time is likely to be found on the other side of the graph. This seems to be crucial if we want our algorithm to work.

Acknowledgements

I would like to thank my supervisor John Watrous for his invaluable support, advice and guidance throughout my Master's studies. It was his idea to consider quantum walks whose states are paths in graphs. I would also like to thank Richard Cleve for introducing me to the pathfinding problem in the glued trees graph. I am also grateful to Andrew Childs for numerous helpful discussions regarding my research. I would also like to thank my fellow graduate students at the Institute for Quantum Computing, especially Robin Kothari for his comments on my work.

I would like to thank all my friends who have made my stay at Waterloo an exciting experience. In particular, I would like to thank my dear friends Rina Baba and Rajasekhar Sappidi, without them this would not have been possible.

Last but not least, I would like to thank my family for their support and patience.

Dedication

In memory of Ināra Rosmane, a loving mother and the strongest supporter of my education since the first grade.

Contents

List of Figures

Chapter 1

Introduction

In the beginning of the last century scientists realized that the Universe does not quite behave as was believed. A new set of laws of physics was required in order to explain experimental observations made at the microscopic scale, and so the groundwork for a new theory called quantum mechanics was laid. Yet the principles of physical computational devices we use in practice today can be completely explained using our knowledge about the Universe before the discovery of quantum effects. Indeed, already in 1837 Charles Babbage described a design for a mechanical computer theoretically capable of computing all Turing-computable functions, long before Alan Turing was even born. So a couple of decades ago scientists started to ask why not to exploit our new knowledge of the reality around us to make possibly superior computational devices, and in 1985 Deutsch introduced the notion of a quantum computer as a universal computational device [17].

In 1994 Shor showed that quantum computers, once built, will be able to factor integers efficiently [28]. Integer factorization is a problem of great importance in cryptography, since the security of the most widely used cryptosystems is based on the assumption that we cannot factor integers efficiently. However, the true potential of quantum computers is still unclear. One step toward understanding it is to consider what are the differences between quantum and classical computers in a setting where we are given the input via a black-box oracle. Since we cannot know the inner workings of the oracle, it is easier to prove lower bounds in this model and therefore in many cases it is easier to show a separation between the best quantum and classical algorithms.

Ever since Deutsch presented a simple oracle problem that can be solved on a quantum computer using fewer oracle queries than on any classical computer [17], scientists have tried to come up with more and more problems for which quantum computers outperform their classical counterparts; some very artificial, some quite natural. Bernstein and Vazirani gave the first example of an oracle problem which can be solved in polynomial time on a quantum computer, but requires superpolynomial time on a classical computer [8]. Shortly after that Simon gave an example in which this separation is exponential [29]. Yet it is unclear what are the best methods for the construction of efficient quantum algorithms. While quantum Fourier sampling is probably the most popular such method so far, many algorithms are also based on the concept of quantum walk. In particular, continuous-time quantum walks

on graphs, introduced by Farhi and Gutmann [20], give rise to fast algorithms for NAND tree evaluation [18] and unstructured search [19, 14]. Continuous-time quantum walks are also known to be able to perform universal quantum computation [11], and they can solve some oracle problems exponentially faster than any classical algorithm [12, 16].

In this thesis we introduce a new type of continuous-time quantum walk on graphs, the basis states of which are not vertices of the graph, but paths in it of a fixed length n. We define this new walk on a unweighted undirected graph G as a regular continuous-time quantum walk (the one introduced by Farhi and Gutmann) on a more complex weighted undirected graph G_n which is constructed from the original graph G. Since to the author of this thesis the discrete-time classical counterpart of this walk in some sense resembles the behavior of a 'snake' of length n which is placed on a graph along its edges and which makes random decisions in which direction to go next, we call this new walk the *continuous-time quantum snake walk*. We analyze in detail the continuous-time quantum snake walk on the line and show its similarities to the regular continuous-time quantum walk on the line.

We do not introduce the continuous-time quantum snake walk just for the sake of introducing something new. As we discuss later, an algorithm based on this walk might be able to solve an extended version of the glued trees problem for which no efficient classical algorithm exists and no efficient quantum algorithm is known. Childs et al. introduced the *glued trees graph* consisting of two complete binary trees of the same height which are connected by a random cycle that alternates between the leaves of the trees [12]. Given a glued trees graph via a black-box oracle and the label of the root of one tree, the *glued trees problem* is to determine the label of the root of the other tree. While there is an efficient quantum algorithm based on the continuous-time quantum walk which solves this problem [12], no efficient quantum algorithm which *finds* a path connecting these two roots is known. This yet unsolved problem is the main motivation for the continuous-time quantum snake walk.

This thesis is a report on ongoing research, and, since the analysis of the continuous quantum snake walk is somewhat technically involved, we make certain assumptions in some parts of it. Wherever necessary, we point out assumptions we make and why it is reasonable to make them.

The structure of the thesis is as follows. In Chapter 2 we discuss some already known results about continuous-time quantum walks. These results in later chapters help us to analyze the continuous-time quantum snake walk, which we precisely define at the end of this chapter. Chapter 3 is completely devoted to the analysis of the quantum snake walk on the line. We use a similar analysis in Chapter 4 to analyze the quantum snake walk on the glued trees graph. There we also intuitively sketch an algorithm which might efficiently find a path connecting the roots of the glued trees graph. Finally, we conclude in Chapter 5 with comments and potential future work.

Chapter 2

Continuous-time quantum walk

Let $G = (V, w)$ be a weighted undirected graph, where V is a set of vertices and w is a weight function, which assigns a weight $w(v_1, v_2) \in \mathbb{R}$ to every pair $(v_1, v_2) \in V^2$. Since G is undirected, we have $w(v_1, v_2) = w(v_2, v_1)$ for all $v_1, v_2 \in V$. Unweighted graphs can be considered as a special case when each weight is either 1, if there is an edge, or 0, if there is not. Let $\mathbb{C}^V$ be a Hilbert space having an orthonormal basis $\{|v\rangle : v \in V\}$ called the *standard basis*. Let H_G be a linear operator acting on $\mathbb{C}^V$ such that $\langle v_1|H_G|v_2\rangle = w(v_1, v_2)$ for all $v_1, v_2 \in V$. Since G is undirected with all weights being real, H_G is Hermitian. The *continuous-time quantum walk* on G is defined as a quantum evolution in the space $\mathbb{C}^V$ governed by the Hamiltonian H_G according to the Schrödinger equation. If we fix an initial state of the walk to be $|\psi(0)\rangle \in \mathbb{C}^V$, then we can look on the walk as a function which maps time $t \geq 0$ to the state $|\psi(t)\rangle = e^{-\mathrm{i}H_G t}|\psi(0)\rangle \in \mathbb{C}^V$.

It is not always possible to simulate a continuous-time quantum walk by a quantum circuit efficiently, simply because there are too many graphs to consider. Still, as the theorem below states, it is always possible to do so for sparse graphs.

We call a graph $G = (V, w)$ *sparse* if for all vertices $v_1 \in V$ the number of vertices $v_2 \in V$ such that $w(v_1, v_2) \neq 0$ is bounded by $\mathrm{poly}(\log |V|)$. Suppose all vertices are labeled by bit strings, and let $\bar{v}$ denote the label of a vertex v. We call the graph G *computable* if there exists an efficient algorithm that, given $\bar{v}_1$ as an input, outputs a list $\{\, (\bar{v}_2, w(v_1, v_2)) \,:\, v_2 \in V, w(v_1, v_2) \neq 0 \,\}$. Lemma 1 in [2] states the following:

Theorem 2.1. *If a graph $G = (V, w)$ is sparse and computable, and all its weights are bounded by* $\mathrm{poly}(\log |V|)$*, then we can simulate the continuous-time quantum walk on G efficiently, that is, we can implement a unitary transformation U such that $||U - e^{-iH_G t}|| < \epsilon$ using* $\mathrm{poly}(\log |V|, t, 1/\epsilon)$ *elementary quantum operations for all $\epsilon > 0$.*

Better techniques for simulating sparse Hamiltonians were later given by [10, Section 1.3] and [9].

2.1 Continous time quantum walk on the line

One of the simplest examples of how the continuous-time quantum walk works is the walk on the line. The behavior of both the continuous-time and the discrete-time quantum walks on the line are similar and well understood [3, 5, 7, 25]. However, we repeat the analysis of the continuous-time case here because it helps us to analyze the more complex model of the continuous-time quantum snake walk later.

By the line we mean the graph $G = (V, E)$, where $V = \mathbb{Z}$ is the set of vertices and $E = \{(x, x \pm 1) : x \in \mathbb{Z}\}$ is the set of edges. In this case the Hamiltonian governing the continuous-time quantum walk is $H = \sum_{x\in\mathbb{Z}} (|x-1\rangle\langle x| + |x+1\rangle\langle x|)$ (for convenience we omit the subscript G for H_G and denote it just by H).

Let us start by finding the eigenvalues and the eigenvectors of H. For any real number k let us define $|\tilde{k}\rangle = \frac{1}{\sqrt{2\pi}} \sum_{x\in\mathbb{Z}} e^{\mathrm{i}kx}|x\rangle$. We have

$$\sum_{x\in\mathbb{Z}} |x-1\rangle\langle x| \cdot |\tilde{k}\rangle = \frac{1}{\sqrt{2\pi}} \sum_{x\in\mathbb{Z}} e^{\mathrm{i}kx}|x-1\rangle = e^{\mathrm{i}k} \frac{1}{\sqrt{2\pi}} \sum_{x\in\mathbb{Z}} e^{\mathrm{i}k(x-1)}|x-1\rangle = e^{\mathrm{i}k}|\tilde{k}\rangle \tag{2.1}$$

and similarly $\sum_{x\in\mathbb{Z}} |x+1\rangle\langle x| \cdot |\tilde{k}\rangle = e^{-\mathrm{i}k}|\tilde{k}\rangle$. Hence

$$H|\tilde{k}\rangle = e^{\mathrm{i}kx}|\tilde{k}\rangle + e^{-\mathrm{i}kx}|\tilde{k}\rangle = 2\cos k|\tilde{k}\rangle. \tag{2.2}$$

We have $\langle\tilde{k_2}|\tilde{k_1}\rangle = \delta(k_1 - k_2 \bmod 2\pi)$, where δ is the Dirac delta function, (see [11]) and

$$H = \int_0^{2\pi} 2\cos k\, |\tilde{k}\rangle\langle\tilde{k}|\, \mathrm{d}k. \tag{2.3}$$

Here we demonstrate two types of approaches for the analysis. In the first case we analyze a walk starting from a standard basis state. This analysis, which uses the Bessel function, is precise. In the second case we consider a wave packet as an initial state of the walk, and then, using approximate analysis, we see how the wave packet moves.

2.1.1 Precise analysis using Bessel functions

Now we show how the walk works if the initial state of it is a standard basis state $|x\rangle$, where $x \in \mathbb{Z}$. Let us consider what is the probability (or the amplitude, to be precise) that we start from the state $|x\rangle$ and after time t we are in a state $|y\rangle$, where $y \in \mathbb{Z}$. That is, what is the value of $\langle y|e^{-iHt}|x\rangle$. We get

$$\begin{aligned}
\langle y|e^{-\mathrm{i}Ht}|x\rangle =& \langle y| \left(\int_0^{2\pi} e^{-2\mathrm{i}t\cos k} |\tilde{k}\rangle\langle\tilde{k}|\, \mathrm{d}k \right) |x\rangle \\
=& \frac{1}{2\pi} \int_0^{2\pi} e^{-2\mathrm{i}t\cos k} e^{\mathrm{i}ky - \mathrm{i}kx}\, \mathrm{d}k \\
=& \frac{(-1)^{y-x}}{\pi} \int_0^{\pi} e^{2\mathrm{i}t\cos k}\, \frac{(e^{\mathrm{i}k(y-x)} + e^{\mathrm{i}k(x-y)})}{2}\, \mathrm{d}k \\
=& (-\mathrm{i})^{y-x} J_{y-x}(2t),
\end{aligned} \tag{2.4}$$

where $J_m(z)$ denotes the Bessel function of the first kind, which for integer order m can be defined as

$$J_m(z) = \frac{\mathrm{i}^{-m}}{\pi} \int_0^\pi e^{\mathrm{i}z\cos\theta} \cos(m\theta)\,\mathrm{d}\theta \tag{2.5}$$

[1, Chapter 9]. By the properties of the Bessel function, this implies that the state $|x\rangle$ evolves as two, left and right moving wave packets, each propagating with momentum 2 [10, Section 3.3.2]. The same conclusion can be achieved using the method of stationary phase approximation [3].

2.1.2 A wave packet as an initial state

As shown in the previous section, we can analyze the continuous-time quantum walk on the line precisely. We are able to do so because we know the full eigenspectrum of the operator H. However, later we consider a walk governed by a Hamiltonian for which we do not know how to obtain the full eigenspectrum, therefore it is important to explore good approximation methods.

Let $p_{(\mu,\sigma)}$ be the probability density function of a normal distribution with a mean μ and a variance σ^2. That is

$$p_{(\mu,\sigma)}(z) = \frac{1}{\sigma\sqrt{2\pi}} e^{-\frac{(z-\mu)^2}{2\sigma^2}}. \tag{2.6}$$

For some values of parameters μ and σ let the initial state of the walk be

$$|\xi_{\mu,\sigma}\rangle = c_\sigma \int_{-\infty}^{\infty} \sqrt{p_{(\mu,\sigma)}(k)}\,|\tilde{k}\rangle\,\mathrm{d}k, \tag{2.7}$$

where $c_\sigma > 0$ is the normalization factor. In order to see that the initial state looks like a Gaussian-shaped wave packet, we need to cover some mathematical background first.

The error function is defined as

$$\mathrm{erf}(z) = \frac{2}{\sqrt{\pi}} \int_0^z e^{-\theta^2}\mathrm{d}\theta, \tag{2.8}$$

and therefore $\mathrm{d}(\mathrm{erf}(z))/\mathrm{d}z = 2e^{-z^2}/\sqrt{\pi}$. This allows us to see that

$$\int e^{az^2+bz}\mathrm{d}z = \frac{-\mathrm{i}\sqrt{\pi}}{2\sqrt{a}} e^{-\frac{b^2}{4a}} \mathrm{erf}\left(\mathrm{i}\frac{b+2az}{2\sqrt{a}}\right) \tag{2.9}$$

and

$$\int e^{az^2+bz} z\,\mathrm{d}z = \frac{1}{2a} e^{az^2+bz} + \frac{\mathrm{i}b\sqrt{\pi}}{4a^{3/2}} e^{-\frac{b^2}{4a}} \mathrm{erf}\left(\mathrm{i}\frac{b+2az}{2\sqrt{a}}\right) \tag{2.10}$$

(the latter integral we use only later in Section 3.3). It is known that $\mathrm{erf}(-z) = -\mathrm{erf}(z)$, $\mathrm{erf}(\overline{z}) = \overline{\mathrm{erf}(z)}$ and $\mathrm{erf}(z) \to 1$ as $z \to \infty$ in $|\arg z| < \frac{\pi}{2}$ [1, Chapter 7]. Hence, if $\mathrm{Re}(a) < 0$, then from (2.9) we get

$$\int_{-\infty}^{\infty} e^{az^2+bz}\mathrm{d}z = \sqrt{\frac{\pi}{-a}} e^{-\frac{b^2}{4a}}. \tag{2.11}$$

Let $\kappa = k - \mu$. (2.11) gives us

$$\begin{aligned}
|\xi_{\mu,\sigma}\rangle =& c_\sigma \left(\sum_{x\in\mathbb{Z}} |x\rangle\langle x|\right) \int_{-\infty}^{\infty} \sqrt{\frac{1}{\sigma\sqrt{2\pi}} e^{-\frac{(k-\mu)^2}{2\sigma^2}}}\, |\tilde{k}\rangle \,\mathrm{d}k \\
=& \frac{c_\sigma}{\sqrt{\sigma}(2\pi)^{3/4}} \sum_{x\in\mathbb{Z}} \left(\int_{-\infty}^{\infty} e^{-\frac{\kappa^2}{4\sigma^2}}\, e^{\mathrm{i}(\mu+\kappa)x}\,\mathrm{d}\kappa\right) |x\rangle \\
=& c_\sigma \sqrt[4]{\frac{2\sigma^2}{\pi}} \sum_{x\in\mathbb{Z}} e^{\mathrm{i}\mu x} e^{-\frac{x^2}{2(1/2\sigma^2)}} |x\rangle.
\end{aligned} \tag{2.12}$$

Therefore we can see that the amplitudes of $|\xi_{\mu,\sigma}\rangle$ correspond (up to some global factor and a local phase $e^{\mathrm{i}\mu x}$) to the normal distribution in x with mean 0 and variance $1/2\sigma^2$. We can also see that the larger σ we choose, the more localized the state $|\xi_{\mu,\sigma}\rangle$ becomes, and vice versa. We are interested in the case when σ is small because it makes a couple of approximations possible. For small σ (how small σ must be we specify later) we have

$$\langle\xi_{\mu,\sigma}|\xi_{\mu,\sigma}\rangle = c_\sigma^2 \frac{1}{(1/2\sigma)\sqrt{2\pi}} \sum_{x\in\mathbb{Z}} e^{-\frac{x^2}{2(1/2\sigma)^2}} = c_\sigma^2 \sum_{x\in\mathbb{Z}} p_{(0,\,1/2\sigma)}(x) \approx c_\sigma^2, \tag{2.13}$$

which gives us $c_\sigma \approx 1$. The approximation in (2.13) is due to the fact that for large variances (which is $(1/2\sigma)^2$ in our case) the binomial distribution with the success probability $1/2$ is very well approximated by the normal distribution [26, Part II].

Now let us see how the state $|\xi_{\mu,\sigma}\rangle$ evolves in time. We choose σ to be small enough so that most of the contribution to the integral (2.7) comes from values of k close to μ. We also have to assume that the time t is small enough to use the approximation below. Using the first three terms from the Taylor series of $\cos k$ around μ we have

$$e^{\mathrm{i}t\cos k} \approx e^{\mathrm{i}t(\cos\mu - \kappa\sin\mu - \frac{\kappa^2}{2}\cos\mu)}. \tag{2.14}$$

This approximation gives us

$$\begin{aligned}
e^{-\mathrm{i}Ht}|\xi_{\mu,\sigma}\rangle =& c_\sigma \left(\sum_{x\in\mathbb{Z}} |x\rangle\langle x|\right) \int_{-\infty}^{\infty} e^{-2\mathrm{i}t\cos k} \sqrt{\frac{1}{\sigma\sqrt{2\pi}} e^{-\frac{(k-\mu)^2}{2\sigma^2}}}\, |\tilde{k}\rangle \,\mathrm{d}k \\
\approx& c_\sigma \frac{1}{\sqrt{\sigma}(2\pi)^{3/4}} \sum_{x\in\mathbb{Z}} \left(\int_{-\infty}^{\infty} e^{-2\mathrm{i}t(\cos\mu - \kappa\sin\mu - \frac{\kappa^2}{2}\cos\mu)}\, e^{-\frac{\kappa^2}{4\sigma^2}}\, e^{\mathrm{i}(\mu+\kappa)x}\,\mathrm{d}\kappa\right) |x\rangle \\
=& c_\sigma \frac{e^{-2\mathrm{i}t\cos\mu}}{\sqrt{\sigma}(2\pi)^{3/4}} \sum_{x\in\mathbb{Z}} e^{\mathrm{i}\mu x} \left(\int_{-\infty}^{\infty} e^{(\mathrm{i}t\cos\mu - \frac{1}{4\sigma^2})\kappa^2 + \mathrm{i}(x+2t\sin\mu)\kappa}\,\mathrm{d}\kappa\right) |x\rangle \\
=& c_\sigma \frac{e^{-2\mathrm{i}t\cos\mu}}{\sqrt{\sigma}(2\pi)^{3/4}} \sum_{x\in\mathbb{Z}} e^{\mathrm{i}\mu x} \sqrt{\frac{\pi}{\frac{1}{4\sigma^2} - \mathrm{i}t\cos\mu}}\, e^{-\frac{(x+2t\sin\mu)^2}{(\frac{1}{\sigma^2} - 4\mathrm{i}t\cos\mu)}} |x\rangle \\
=& f(t,\mu,\sigma) \sum_{x\in\mathbb{Z}} e^{\mathrm{i}g(x,t,\mu,\sigma)} \cdot p_{\left(-2t\sin\mu,\,\sqrt{\frac{1}{2\sigma^2} + 8\sigma^2 t^2\cos^2\mu}\right)}(x)\, |x\rangle,
\end{aligned} \tag{2.15}$$

where f and g are real-valued functions and we assume $t\cos\mu < \frac{1}{4\sigma^2}$ in order to use the integral (2.11). $f(t,\mu,\sigma)$ is a global normalization factor, while $e^{\mathrm{i}g(x,t,\mu,\sigma)}$ is a local phase,

and here we do not care about their exact values. If we choose $\mu \in [\frac{\pi}{2}, \frac{3\pi}{2}]$, the condition $t \cos \mu < \frac{1}{4\sigma^2}$ is always satisfied.

From (2.15) we see that $e^{-\mathrm{i}Ht}|\xi_{\mu,\sigma}\rangle$ has the highest amplitudes for the basis states corresponding to integers close to $-2t \sin \mu$. That implies that the walk propagates as a wave packet moving with momentum $-2 \sin \mu$. Also we can see that the wave packet becomes more diffused as the variance $(\frac{1}{2\sigma^2} + 8\sigma^2 t^2 \cos^2 \mu)$ increases in time - the front of the wave packet moves a bit faster than the rear. This diffusion can be explained by the Heisenberg uncertainty principle: we cannot know both the position and the momentum of the walk to arbitrary precision. It is known that the same behavior remains even when the time t is large and we cannot use the approximation (2.14) anymore [11]. It can be shown using the method of stationary phase approximation, an application of which we demonstrate later in Section 3.3.

These wave packets, which, as (2.15) shows, can move with any chosen momentum up to 2, are useful in algorithm construction. Even though one might guess that the faster wave packet we choose, the better an algorithm works, this in not the case: while the continuous-time quantum walk algorithm for NAND tree evaluation indeed uses wave packets of momentum 2 [18], the universal computation using continuous-time quantum walk presented in [11] requires wave packets of momentum $\sqrt{2}$. This is because, when we put an 'obstacle' (a modification of the line graph) in the way of a wave packet, the probabilities of the packet either going though or being reflected from the obstacle depend on its momentum. When later in Chapter 4 we discuss how the continuous-time quantum snake walk behaves on the glued trees graph, we have to consider which momenta are good for our purposes as well.

2.2 Glued trees problem

It was an important development in the area of quantum algorithm design when Childs et al. showed that quantum algorithms using quantum walks can solve certain black-box problems exponentially faster than any classical algorithm [12]. For this purpose they introduced the glued trees graph. The *glued trees graph* consists of two complete binary trees of height N, which are connected by a random cycle that alternates between the leaves of the two trees. An example of the graph is shown in Figure 2.1 (for $N = 3$). Let us also call N and the roots of both trees, respectively, the height and the roots of the glued trees graph.

Suppose we are given a glued trees graph via a black-box oracle (given the label of a node as an input, the oracle outputs labels of all its neighbors) and the label of one root r_1. The *glued trees problem* is to determine the label of the other root r_2 (see Figure 2.1). Childs et al. show that, if we start a continuous-time quantum walk at the root r_1, the walk quickly (in poly N time) traverses the graph and ends up in a superposition state which has a large overlap on the root r_2 [12]. According to Theorem 2.1, we can implement this walk efficiently in the quantum circuit model which uses the black-box oracle of the graph. It is also shown in [12] that no classical query algorithm can solve this problem efficiently.

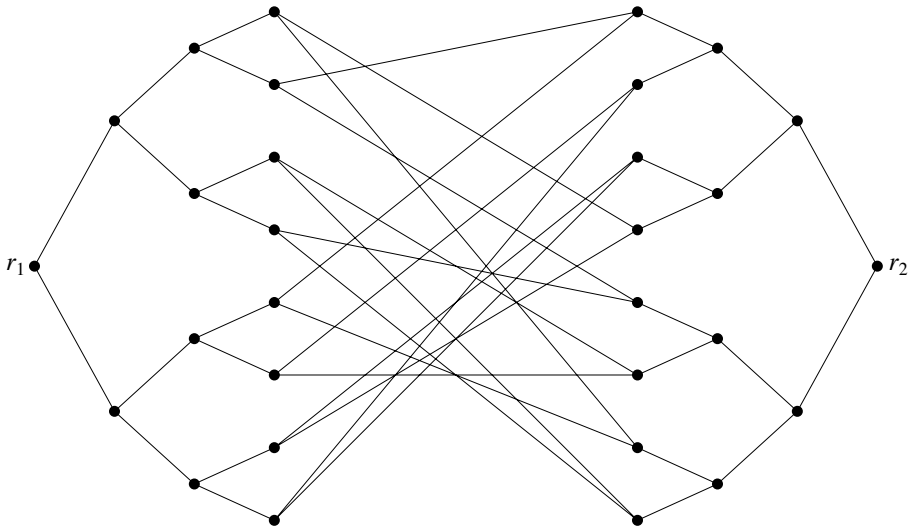

Figure 2.1: A glued trees graph of height 3.

The first step used in [12] to analyze the quantum walk on the glued trees graph is to reduce it to a walk on a much smaller and simpler graph. Let us demonstrate this method, because it is also useful for us later in Chapter 4.

Suppose we have two disjoint finite sets X and Y, and a complex Euclidean space $\mathcal{Z}$ such that $\operatorname{span}\{|z\rangle : z \in X \cup Y\}$ is its subspace. We also have an Hermitian operator A acting on $\mathcal{Z}$ satisfying a promise that there are two non-negative numbers $m(X,Y)$ and $m(Y,X)$ such that $\sum_{y\in Y}\langle y|A|x\rangle = m(X,Y)$ for all $x \in X$ and $\sum_{x\in X}\langle x|A|y\rangle = m(Y,X)$ for all $y \in Y$. Let $|X\rangle$ and $|Y\rangle$ be uniform superpositions over elements of X and Y respectively.

Lemma 2.2. *$A|X\rangle = \sqrt{m(X,Y)\cdot m(Y,X)}|Y\rangle + |Y^\perp\rangle$, where $\langle y|Y^\perp\rangle = 0$ for all $y \in Y$.*

Proof. For every $y \in Y$ we have $\langle y|A|X\rangle = \overline{\langle X|A|y\rangle} = \sum_{x\in X}\frac{1}{\sqrt{|X|}}\overline{\langle x|A|y\rangle} = \frac{m(Y,X)}{\sqrt{|X|}}$. Hence $A|X\rangle = \sqrt{\frac{|Y|}{|X|}}m(Y,X)|Y\rangle + |Y^\perp\rangle$, where $|Y^\perp\rangle$ satisfies the required condition. $\langle Y|A|X\rangle \in \mathbb{R}$ implies $\langle Y|A|X\rangle = \langle X|A|Y\rangle$, and therefore by symmetry $\sqrt{\frac{|Y|}{|X|}}m(Y,X) = \sqrt{\frac{|X|}{|Y|}}m(X,Y)$. The lemma holds trivially if $m(Y,X) = 0$, therefore let $m(Y,X) > 0$. We get $\frac{|Y|}{|X|} = \frac{m(X,Y)}{m(Y,X)}$, which gives $A|X\rangle = \sqrt{m(X,Y)\cdot m(Y,X)}|Y\rangle + |Y^\perp\rangle$. □

In terms of graphs, we can consider X and Y to be disjoint subsets of vertices of an unweighted graph and A to be the adjacency matrix of the graph. Then the condition $\sum_{y\in Y}\langle y|A|x\rangle = m(X,Y)$ for all $x \in X$ means that every vertex in X is connected to $m(X,Y)$ vertices in Y. (This would be just slightly more complicated for weighted graphs.)

Now consider a glued trees graph of height N and its adjacency matrix A. For $l \in [0\,..\,2N+1]$ let X_l be the set of all vertices which are at distance l from the root r_1. First of all, we can see that $m(X_{l_1}, X_{l_2}) = 0$ whenever $|l_1 - l_2| \neq 1$, because, obviously, there

is no edge connecting any two vertices for which distance from r_1 differs by at least 2. For $l \in [0\,..\,N-1]$, each vertex in X_l is connected to two vertices in X_{l+1} while each vertex in X_{l+1} is connected to one vertex in X_l. This gives us that $\langle X_l|A|X_{l+1}\rangle = \sqrt{2}$ for $l \in [0\,..\,N-1]$. By symmetry, $\langle X_l|A|X_{l+1}\rangle = \sqrt{2}$ also for $l \in [N+1\,..\,2N]$. For the glued part we have that each vertex in X_N is connected to two vertices in X_{N+1} and vice versa, giving us $\langle X_N|A|X_{N+1}\rangle = \sqrt{4} = 2$. Note that this holds independently of which random cycle we have. Now, by Lemma 2.2 we can see that, if we start a walk from a state in the subspace $\mathcal{X} = \text{span}\{|X_l\rangle \,:\, l \in [0\,..\,2N+1]\}$, the system will always remain in a state in this subspace. That is, $\mathcal{X}$ is invariant under A, and in $\mathcal{X}$ the operator A acts the same way as the operator

$$A_{\mathcal{X}} = 2(\,|X_N\rangle\langle X_{N+1}| + |X_{N+1}\rangle\langle X_N|\,) + \sum_{\substack{l\in[0\,..\,2N]\\ l\neq N}} \sqrt{2}(\,|X_l\rangle\langle X_{l+1}| + |X_{l+1}\rangle\langle X_l|\,). \quad (2.16)$$

Since $|r_1\rangle = |X_0\rangle \in \mathcal{X}$, the walk on the glued trees graph starting from r_1 can be reduced to the walk on the line segment of length $2N+1$ with all weights $\sqrt{2}$ except the middle weight being 2 (see Figure 2.2). Then, analyzing the eigenspectrum of this simplified graph and using the concept of the quantum mixing time, Childs et al. show that in a polynomial time we can obtain a state having a large overlap with $|X_{2N+1}\rangle = |r_2\rangle$.

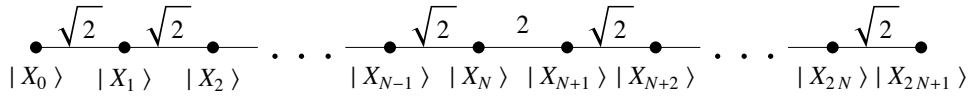

Figure 2.2: A walk on a glued trees graph reduced to a line segment.

2.2.1 The extended glued trees problem - a motivation for quantum snake walks

Given a glued trees graph via a black-box oracle and the label of one of its two roots r_1, the *extended glued trees problem* is to find a path in the graph connecting r_1 to the opposite root r_2. As Childs et al. mention in their paper, even though the algorithm starting from the root r_1 finds the root r_2, it does not find a path connecting r_1 and r_2 [12]. As far as I know, there is still no quantum algorithm known which would find such a path efficiently. Even more, it is not even known if such an efficient algorithm exists [10, Section 5.4].

If we want to find such a path efficiently, we obviously cannot simply take the quantum walk solving the regular glued trees problem and measure in which state it is after some fixed time intervals (and store the results of measurements in a classical memory). Such measurements would destroy a quantum interference, which is a key feature why the algorithm finds r_2 quickly.

An algorithm solving the extended glued trees problem efficiently most likely would have to employ quantum interference of some sort. In order for constructive interference to take place, we might have to avoid measurements, which, in turn, means that we must

store any information about path connecting r_1 and r_2 in quantum, not classical, memory. This is the main motivation why we consider quantum snakes, which, in principle, are arrays of registers, where each register contains a label of a vertex, satisfying a particular promise.

2.3 The definition and simulation of quantum snake walk

Suppose $G = (V, E)$ is an undirected unweighted graph, where V is a set of vertices and $E \subset V^2$ is a set of edges. Let $S_n(G)$ be the set of all paths in G which have length n. Here we assume that a path can visit a vertex multiple times. Let us call an element of $S_n(G)$ a snake of length n. That is, a snake of length n is a vector $s = (v_0, \ldots, v_n) \in V^{n+1}$ such that $(v_{l-1}, v_l) \in E$ for all $l \in [1\,..\,n]$. Note that we assume all paths are directed ($(v_0, v_1, \ldots, v_n)$ and $(v_n, v_{n-1}, \ldots, v_0)$ are not the same snake).

Let $s = (v_0, \ldots, v_n) \in S_n(G)$ be a snake of length n. We say that s can move forward to a snake $t \in S_n(G)$ if there exists a vertex $v_{n+1} \in V$ such that $t = (v_1, \ldots, v_{n+1})$, and we write $m_f(s, t)$ (we think of m_f as a predicate). Similarly, we say that s can move backward to $t \in S_n(G)$ if there exists $v_{-1} \in V$ such that $t = (v_{-1}, \ldots, v_{n-1})$, and we write $m_b(s, t)$. We also consider $m_f(s, t)$ as a binary function on $S_n(G)^2$ taking a value 1 if and only if the predicate m_f is true for a pair (s, t), and similar for m_b. Let $a_{s,t} = m_f(s, t) + m_b(s, t) \in \{0, 1, 2\}$, and let $A_n(G)$ be a matrix whose rows and columns are labeled by the elements of $S_n(G)$ and $A_n(G)_{s,t} = a_{s,t}$ for all $s, t \in S_n(G)$.

Clearly $m_f(s, t)$ if and only if $m_b(t, s)$, and therefore $A_n(G)$ is a symmetric matrix. We can look on $A_n(G)$ as the adjacency matrix of a graph having $S_n(G)$ as the set of vertices, and possibly some edges having weight 2 instead of 1. As a matter of fact, $A_n(G)_{s,t} = 2$ if and only if there are two adjacent vertices u and v such that $s = (u, v, u, v, \ldots)$ and $t = (v, u, v, u, \ldots)$.

Definition. Let G_n be a weighted graph with the set of vertices $S_n(G)$ and the matrix of weights $A_n(G)$. The *continuous-time quantum snake walk* on the graph G is defined as a continuous-time quantum walk on the weighted graph G_n.

Since we consider only continuous-time walks, we often refer to continuous-time quantum walks and continuous-time quantum snake walks, respectively, as quantum snake walks and regular quantum walks. Let S be a quantum register corresponding to the Hilbert space $\mathbb{C}^{S_n(G)}$. Sometimes we use the word snake to refer to the content of the register S, and we call the elements of $S_n(G)$ the positions of the snake. In some sense, we can think of the snake as being a path which can move form one position in the graph to another. In what sense the word snake is used should be clear from the context.

If we want to simulate a quantum snake walk using the quantum circuit model, the most reasonable way to store a snake in quantum memory seems to be by using an array

of $n+1$ quantum registers each containing a label of a vertex. Suppose for every vertex $v \in V$ a unique L bit label $\bar{v}$ is assigned and we assume that the label $w_\emptyset = 1 \ldots 1$ is not assigned to any vertex. Let d be the maximum vertex degree in G. For each vertex $v \in V$ having d_v adjacent vertices let $u_1(v), \ldots, u_{d_v}(v)$ be the labels those vertices (here we assume that these vertices are sorted according to some fixed, but not necessarily known, ordering). Let all $u_{d_v+1}(v), \ldots, u_d(v)$ be $w_\emptyset$. The quantum black-box oracle for G is the unitary transformation O which maps $|\bar{v}\rangle|b_1, \ldots, b_d\rangle$ to $|\bar{v}\rangle|b_1 \oplus u_1(v), \ldots, b_d \oplus u_d(v)\rangle$ for $v \in V$, where $b_1, \ldots, b_d$ are arbitrary L bit strings, and when $\bar{v}$ is not the label of any vertex O works as the identity operator.

It is known that given an access to a quantum black-box oracle of a graph G having the vertex degree $d \in O(\mathrm{poly}\, L)$, one can simulate the continuous-time quantum walk on G efficiently (Theorem 2.1). Here we show that in the sparse case the continuous-time quantum snake walk can also be efficiently implemented.

Given a snake $s = (v_0, \ldots, v_n) \in S_n(G)$ and the quantum black-box oracle of G, we can quickly obtain the list of vertices adjacent to v_n and therefore, assuming $n \in O(\mathrm{poly}\, L)$, also the list of all snakes $t \in S_n(G)$ satisfying $m_f(s,t)$. The same way we obtain the list of all $t \in S_n(G)$ satisfying $m_b(s,t)$. This allows us to compute the list of pairs $\{(t, a_{s,t}) : a_{s,t} > 0\}$ efficiently. This list has at most $2d$ pairs (independent of the length of the snake). Note that, since O is its own inverse, we can carry this computation without producing any 'garbage' bits (see [27, Section 3.2.5] on reversible computation). Therefore the weighted graph G_n with the set of vertices $S_n(G)$ and the adjacency matrix $A_n(G)$ is computable according to the definition given on page 3. Thus, Theorem 2.1 implies that the continuous-time quantum walk on G_n, which is the snake walk on G, can be simulated efficiently.

Chapter 3

Snakes on line

As an example of a continuous-time quantum snake walk, let us consider the quantum snake walk on the line. This example is relatively simple compared to quantum snake walks on other graphs. Nonetheless, understanding this walk later helps us to analyze snake walks on more complex graphs.

In Section 3.1 we present the Hamiltonian governing the continuous-time quantum snake walk on the line and describe its eigenspectrum. As it turns out, only an exponentially small (in the length of the snake) portion of its eigenvalues and their corresponding eigenvectors are useful in the sense that they give rise to an interesting behavior of the walk. Unfortunately, these eigenvalues are exactly the ones for which we do not have closed-form expressions. However, in Section 3.2 we are able to obtain some nice properties of those eigenvalues, which later in Section 3.3 allow us to demonstrate an interesting instance of that walk. That is, we give a specific initial state and show that, under some reasonable assumptions, it moves as a wave packet with constant momentum.

3.1 The Hamiltonian

The graph of our consideration is $G = (V, E)$, where $V = \mathbb{Z}$ and $E = \{(x, x \pm 1) : x \in \mathbb{Z}\}$. It is convenient to think of the line also as X-axis. For every snake $(v_0, \ldots, v_n) \in V^{n+1}$ on G of length n let $x = v_0$ be the start vertex of the snake and for $l \in [1\,..\,n]$ let $j_l = 0$ if the l-th edge of the snake is pointed in the negative direction of X-axis and $j_l = 1$ if it is pointed in the positive direction, that is, $j_l \in \{0, 1\}$ is such that $v_l = v_{l-1} - (-1)^{j_l}$. This gives a one-to-one relation between the set of snakes $S_n(G)$ and the set $\mathbb{Z} \times \{0, 1\}^n$. From now on let us consider any snake s to be given as a pair $(x, j_1 \ldots j_n) \in \mathbb{Z} \times \{0, 1\}^n$, and let $|x\rangle|j_1 \ldots j_n\rangle$ denote $|s\rangle$.

Since each vertex of G has two adjacent vertices, every snake can move forward to two other snakes, and it can move backward to two other snakes. If a snake $(x, j_1 \ldots j_n)$ moves forward, then the start vertex of the new snake is determined by j_1. Its end vertex can either move in the positive or the negative direction of X-axis. In other words, we have

$$m_f((x, j_1 \ldots j_n), (x-(-1)^{j_1}, j_2 \ldots j_n 0)) \quad \& \quad m_f((x, j_1 \ldots j_n), (x-(-1)^{j_1}, j_2 \ldots j_n 1)) \tag{3.1}$$

for each $j \in \{0,1\}^n$. If a snake moves backward, a direction in which its start vertex moves is opposite to the direction of the first edge of the new snake. That is,

$$m_b((x, j_1 \dots j_n), (x-1, 1 j_1 \dots j_{n-1})) \quad \& \quad m_b((x, j_1 \dots j_n), (x+1, 0 j_1 \dots j_{n-1})) \tag{3.2}$$

for each $j \in \{0,1\}^n$. Notice that on any graph there is no conceptual difference between forward and backward motion of a snake, and the only reason why (3.1) and (3.2) look different is because we choose x to represent the start vertex of a snake, not the end vertex. The Hamiltonian governing the quantum snake walk on the line $A_n(G)$, which for convenience we denote by H, is therefore

$$\begin{aligned} H \;=\; & \sum_{x' \in \mathbb{Z},\, j' \in \{0,1\}^n} \; \sum_{\substack{x'' \in \mathbb{Z},\, j'' \in \{0,1\}^n \\ m_f((x',j'),(j'',j''))}} |x'', j''\rangle\langle x', j'| \\ & + \sum_{x' \in \mathbb{Z},\, j' \in \{0,1\}^n} \; \sum_{\substack{x'' \in \mathbb{Z},\, j'' \in \{0,1\}^n \\ m_b((x',j'),(j'',j''))}} |x'', j''\rangle\langle x', j'| \\ = & \sum_{x \in \mathbb{Z}} \sum_{j \in \{0,1\}^{n-1}} (\, |x-1, j0\rangle\langle x, 0j| + |x-1, j1\rangle\langle x, 0j| \,) \\ & + \sum_{x \in \mathbb{Z}} \sum_{j \in \{0,1\}^{n-1}} (\, |x+1, j0\rangle\langle x, 1j| + |x+1, j1\rangle\langle x, 1j| \,) \\ & + \sum_{x \in \mathbb{Z}} \sum_{j \in \{0,1\}^{n-1}} (\, |x-1, 1j\rangle\langle x, j0| + |x+1, 0j\rangle\langle x, j0| \,) \\ & + \sum_{x \in \mathbb{Z}} \sum_{j \in \{0,1\}^{n-1}} (\, |x-1, 1j\rangle\langle x, j1| + |x+1, 0j\rangle\langle x, j1| \,); \end{aligned} \tag{3.3}$$

$$\begin{aligned} H \;=\; & \sum_{x \in \mathbb{Z}} |x-1\rangle\langle x| \otimes \sum_{j \in \{0,1\}^{n-1}} (\, |j0\rangle\langle 0j| + |j1\rangle\langle 0j| + |1j\rangle\langle j0| + |1j\rangle\langle j1| \,) \\ & + \sum_{x \in \mathbb{Z}} |x+1\rangle\langle x| \otimes \sum_{j \in \{0,1\}^{n-1}} (\, |j0\rangle\langle 1j| + |j1\rangle\langle 1j| + |0j\rangle\langle j0| + |0j\rangle\langle j1| \,). \end{aligned} \tag{3.4}$$

It might be helpful to understand a structure of H by thinking of it as an adjacency matrix. For example, for $n = 3$ the H is the adjacency matrix of the graph given in Figure 3.1, where each vertex corresponds to a snake.

In order to analyze the quantum snake walk on G it is helpful to understand the eigenspectrum of H. One can see that H is invariant under the translation $\sum_{x \in \mathbb{Z}} |x-1\rangle\langle x| \otimes \mathbb{I}$, where $\mathbb{I}$ is the identity operator on the space $\mathbb{C}^{\{0,1\}^n}$. We already know the eigenvalues and eigencevtors of $\sum_{x \in \mathbb{Z}} |x-1\rangle\langle x|$ and $\sum_{x \in \mathbb{Z}} |x+1\rangle\langle x|$ from Section 2.1: for $k \in \mathbb{R}$ and $|\tilde{k}\rangle = \frac{1}{\sqrt{2\pi}} \sum_{x \in \mathbb{Z}} e^{\mathrm{i}kx} |x\rangle$ we have

$$\sum_{x \in \mathbb{Z}} |x-1\rangle\langle x| \cdot |\tilde{k}\rangle = e^{\mathrm{i}k} |\tilde{k}\rangle \qquad \& \qquad \sum_{x \in \mathbb{Z}} |x+1\rangle\langle x| \cdot |\tilde{k}\rangle = e^{-\mathrm{i}k} |\tilde{k}\rangle. \tag{3.5}$$

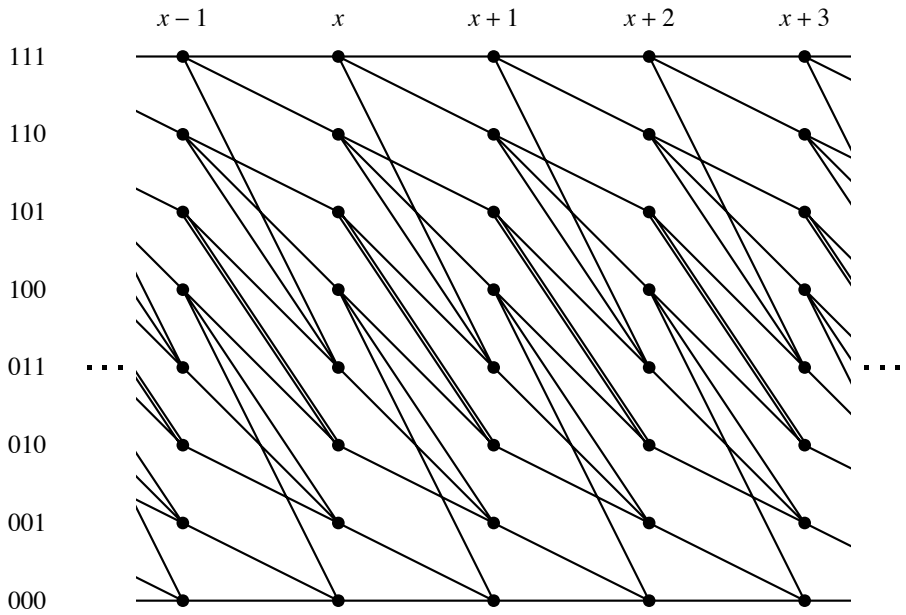

Figure 3.1: The graph corresponding to the adjacency matrix H (for $n = 3$).

This together with (3.4) give us

$$H(|\tilde{k}\rangle \otimes \mathbb{I}) = |\tilde{k}\rangle \otimes H_{n,k}, \tag{3.6}$$

where

$$\begin{aligned} H_{n,k} \;=\; & \sum_{j\in\{0,1\}^{n-1}} e^{\mathrm{i}k}(\,|j0\rangle\langle 0j| + |j1\rangle\langle 0j| + |1j\rangle\langle j0| + |1j\rangle\langle j1|\,) \\ & + \sum_{j\in\{0,1\}^{n-1}} e^{-\mathrm{i}k}(\,|j0\rangle\langle 1j| + |j1\rangle\langle 1j| + |0j\rangle\langle j0| + |0j\rangle\langle j1|\,). \end{aligned} \tag{3.7}$$

From (3.6) we get that for any value k, if $|\psi\rangle$ is an eigenvector of $H_{n,k}$ with an eigenvalue λ, then $|\tilde{k}\rangle|\psi\rangle$ is an eigenvector of H with the same eigenvalue λ. Because of the periodicity, we can restrict k to be in $[0, 2\pi)$. For example,

$$H_{3,k} = \begin{pmatrix} e^{\mathrm{i}k}+e^{-\mathrm{i}k} & e^{-\mathrm{i}k} & 0 & 0 & e^{-\mathrm{i}k} & 0 & 0 & 0 \\ e^{\mathrm{i}k} & 0 & e^{-\mathrm{i}k} & e^{-\mathrm{i}k} & e^{-\mathrm{i}k} & 0 & 0 & 0 \\ 0 & e^{\mathrm{i}k} & 0 & 0 & e^{-\mathrm{i}k} & 2e^{-\mathrm{i}k} & 0 & 0 \\ 0 & e^{\mathrm{i}k} & 0 & 0 & 0 & e^{-\mathrm{i}k} & e^{-\mathrm{i}k} & e^{-\mathrm{i}k} \\ e^{\mathrm{i}k} & e^{\mathrm{i}k} & e^{\mathrm{i}k} & 0 & 0 & 0 & e^{-\mathrm{i}k} & 0 \\ 0 & 0 & 2e^{\mathrm{i}k} & e^{\mathrm{i}k} & 0 & 0 & e^{-\mathrm{i}k} & 0 \\ 0 & 0 & 0 & e^{\mathrm{i}k} & e^{\mathrm{i}k} & e^{\mathrm{i}k} & 0 & e^{-\mathrm{i}k} \\ 0 & 0 & 0 & e^{\mathrm{i}k} & 0 & 0 & e^{\mathrm{i}k} & e^{\mathrm{i}k}+e^{-\mathrm{i}k} \end{pmatrix}, \tag{3.8}$$

where rows and columns are labeled by 000, 001, 010 etc.

3.1.1 Change of basis

Now let us fix k and focus on finding the eigenvalues and eigenvectors of $H_{n,k}$. This task becomes much easier if we express $H_{n,k}$ in a different basis. Consider two pairs of orthonormal vectors: $|u_{0,k}\rangle = \frac{1}{\sqrt{2}}\left(e^{-ik}|0\rangle + e^{ik}|1\rangle\right)$ and $|u_{1,k}\rangle = \frac{1}{\sqrt{2}}\left(e^{-ik}|0\rangle - e^{ik}|1\rangle\right)$, and $|v_0\rangle = \frac{1}{\sqrt{2}}\left(|0\rangle + |1\rangle\right)$ and $|v_1\rangle = \frac{1}{\sqrt{2}}\left(|0\rangle - |1\rangle\right)$. For $m \in [0\,..\,2^n - 1]$ and a fixed k let us define a unit vector $|\widehat{m}\rangle$ as follows. First, let $|\widehat{0}\rangle = -\mathrm{i}|u_{0,k}\rangle^{\otimes n}$. For $m \in [1\,..\,2^n - 1]$, let m written in binary using $\lfloor \log_2(m) \rfloor + 1$ bits be $1m_{\lfloor \log_2(m) \rfloor} \ldots m_1$. Then for $m \in [1\,..\,2^n - 1]$ we define

$$|\widehat{m}\rangle = |u_{0,k}\rangle^{\otimes n - \lfloor \log_2(m) \rfloor - 1}|u_{1,k}\rangle|v_{m_{\lfloor \log_2(m) \rfloor}}\rangle \ldots |v_{m_1}\rangle. \tag{3.9}$$

It is not hard to see that $B_{n,k} = \{|\widehat{0}\rangle, \ldots, |\widehat{2^n - 1}\rangle\}$ is an orthonormal basis of $\mathbb{C}^{\{0,1\}^n}$, and we call $B_{n,k}$ the hat basis. Let us keep in mind that these basis vectors depend on the value of k. As an example, for $n = 3$ we have

$$\begin{aligned}
|\widehat{0}\rangle &= -\mathrm{i}|u_{0,k}\rangle|u_{0,k}\rangle|u_{0,k}\rangle,\\
|\widehat{1}\rangle &= |u_{0,k}\rangle|u_{0,k}\rangle|u_{1,k}\rangle,\\
|\widehat{2}\rangle &= |u_{0,k}\rangle|u_{1,k}\rangle|v_0\rangle,\\
|\widehat{3}\rangle &= |u_{0,k}\rangle|u_{1,k}\rangle|v_1\rangle,\\
|\widehat{4}\rangle &= |u_{1,k}\rangle|v_0\rangle|v_0\rangle,\\
|\widehat{5}\rangle &= |u_{1,k}\rangle|v_0\rangle|v_1\rangle,\\
|\widehat{6}\rangle &= |u_{1,k}\rangle|v_1\rangle|v_0\rangle,\\
|\widehat{7}\rangle &= |u_{1,k}\rangle|v_1\rangle|v_1\rangle.
\end{aligned} \tag{3.10}$$

Let us express $H_{n,k}$ in the hat basis. We start by rewriting $H_{n,k}$: using (3.7) and the definitions of $|u_{0,k}\rangle$ and $|v_0\rangle$ we get

$$\begin{aligned}
H_{n,k} =& \sqrt{2} \sum_{j \in \{0,1\}^{n-1}} \left(|u_{0,k}\rangle|j\rangle\langle j0| + |u_{0,k}\rangle|j\rangle\langle j1| + |j0\rangle\langle u_{0,k}|\langle j| + |j1\rangle\langle u_{1,k}|\langle j| \right)\\
=& \, 2 \sum_{j \in \{0,1\}^{n-1}} \left(|u_{0,k}\rangle|j\rangle\langle j|\langle v_0| + |j\rangle|v_0\rangle\langle u_{0,k}|\langle j| \right).
\end{aligned} \tag{3.11}$$

Therefore, for arbitrary $|\phi_n\rangle, |\phi_1\rangle \in \mathbb{C}^2$ and $|\phi_{n-1\,..\,2}\rangle \in \mathbb{C}^{2^{n-2}}$ we have

$$H_{n,k}|\phi_n\rangle|\phi_{n-1\,..\,2}\rangle|\phi_1\rangle = 2\langle v_0|\phi_1\rangle \, |u_{0,k}\rangle|\phi_n\rangle|\phi_{n-1\,..\,2}\rangle + 2\langle u_{0,k}|\phi_n\rangle \, |\phi_{n-1\,..\,2}\rangle|\phi_1\rangle|v_0\rangle. \tag{3.12}$$

This equality turns out to be very useful if we consider how $H_{n,k}$ acts on the vectors of

$B_{n,k}$. For $|\widehat{0}\rangle$ and $|\widehat{1}\rangle$ it gives

$$\begin{aligned}
H_{n,k}|\widehat{0}\rangle &= -\mathrm{i}H_{n,k}|u_{0,k}\rangle^{\otimes n} \\
&= -\mathrm{i}(2\,(e^{\mathrm{i}k}+e^{-\mathrm{i}k})/2\,|u_{0,k}\rangle^{\otimes n} + 2\,|u_{0,k}\rangle^{\otimes n-1}|v_0\rangle) \\
&= -\mathrm{i}((e^{\mathrm{i}k}+e^{-\mathrm{i}k})\,|u_{0,k}\rangle^{\otimes n} + 2\,|u_{0,k}\rangle^{\otimes n-1}((e^{\mathrm{i}k}+e^{-\mathrm{i}k})/2\,|u_{0,k}\rangle + (e^{\mathrm{i}k}-e^{-\mathrm{i}k})/2\,|u_{1,k}\rangle)) \\
&= 2(e^{\mathrm{i}k}+e^{-\mathrm{i}k})\,(-\mathrm{i}|u_{0,k}\rangle^{\otimes n}) + \mathrm{i}(e^{-\mathrm{i}k}-e^{\mathrm{i}k})\,|u_{0,k}\rangle^{\otimes n-1}|u_{1,k}\rangle \\
&= 4\cos k\,|\widehat{0}\rangle + 2\sin k\,|\widehat{1}\rangle, \qquad (3.13) \\
H_{n,k}|\widehat{1}\rangle &= H_{n,k}|u_{0,k}\rangle^{\otimes n-1}|u_{1,k}\rangle \\
&= 2\,\mathrm{i}(e^{-\mathrm{i}k}-e^{\mathrm{i}k})/2\,(-\mathrm{i}|u_{0,k}\rangle^{\otimes n}) + 2\,|u_{0,k}\rangle^{\otimes n-2}|u_{1,k}\rangle|v_0\rangle \\
&= 2\sin k\,|\widehat{0}\rangle + 2\,|\widehat{2}\rangle. \qquad (3.14)
\end{aligned}$$

For the rest of the basis vectors $|\widehat{m}\rangle$, where $m \in [2\,..\,2^n-1]$, let us distinguish the following four cases and use (3.12) for all of them.

1. m is odd and $m \geq 2^{n-1}$. Then $|\widehat{m}\rangle = |u_{1,k}\rangle|\Psi_m\rangle|v_1\rangle$ for some $|\Psi_m\rangle \in \mathbb{C}^{2^{n-2}}$. Thus $H_{n,k}|\widehat{m}\rangle = H_{n,k}|u_{1,k}\rangle|\Psi_m\rangle|v_1\rangle = 0$.
2. m is even and $m \geq 2^{n-1}$. Then $|\widehat{m}\rangle = |u_{1,k}\rangle|\Psi_m\rangle|v_0\rangle$ for some $|\Psi_m\rangle \in \mathbb{C}^{2^{n-2}}$. Thus $H_{n,k}|\widehat{m}\rangle = H_{n,k}|u_{1,k}\rangle|\Psi_m\rangle|v_0\rangle = 2\,|u_{0,k}\rangle|u_{1,k}\rangle|\Psi_m\rangle = 2\,|\widehat{m/2}\rangle$.
3. m is odd and $m < 2^{n-1}$. Then $|\widehat{m}\rangle = |u_{0,k}\rangle|\Psi_m\rangle|v_1\rangle$ for some $|\Psi_m\rangle \in \mathbb{C}^{2^{n-2}}$. Thus $H_{n,k}|\widehat{m}\rangle = H_{n,k}|u_{0,k}\rangle|\Psi_m\rangle|v_1\rangle = 2\,|\Psi_m\rangle|v_1\rangle|v_0\rangle = 2\,|\widehat{2m}\rangle$.
4. m is even and $m < 2^{n-1}$. Then $|\widehat{m}\rangle = |u_{0,k}\rangle|\Psi_m\rangle|v_0\rangle$ for some $|\Psi_m\rangle \in \mathbb{C}^{2^{n-2}}$. Thus $H_{n,k}|\widehat{m}\rangle = H_{n,k}|u_{0,k}\rangle|\Psi_m\rangle|v_0\rangle = 2\,|u_{0,k}\rangle|u_{0,k}\rangle|\Psi_m\rangle + 2\,|\Psi_m\rangle|v_0\rangle|v_0\rangle = 2\,|\widehat{m/2}\rangle + 2\,|\widehat{2m}\rangle$.

To summarize: for all $m \in [2\,..\,2^n-1]$, $H_{n,k}$ maps $|\widehat{m}\rangle$ to $2|\widehat{2m}\rangle$ if $2m \leq 2^n-1$ and to $2|\widehat{m/2}\rangle$ if m is even. Hence,

$$H_{n,k} = 4\cos k\,|\widehat{0}\rangle\langle\widehat{0}| + 2\sin k\,(|\widehat{1}\rangle\langle\widehat{0}| + |\widehat{0}\rangle\langle\widehat{1}|) + 2\sum_{m=1}^{2^{n-1}-1}(|\widehat{2m}\rangle\langle\widehat{m}| + |\widehat{m}\rangle\langle\widehat{2m}|). \qquad (3.15)$$

From (3.15) we see that $\langle\widehat{m_1}|H_{n,k}|\widehat{m_2}\rangle = 0$ whenever m_1 and m_2 have different greatest odd divisors, where we assume that the greatest odd divisor of 0 is 1. Therefore we can block diagonalize $H_{n,k}$ with respect to $B_{n,k}$ into 2^{n-1} blocks. To be more precise, let us define 2^{n-1} orthogonal projectors $\Pi_1 = |\widehat{0}\rangle\langle\widehat{0}| + \sum_{j=0}^{n-1}|\widehat{2^j}\rangle\langle\widehat{2^j}|$ and $\Pi_l = \sum_{j=0}^{n-\lceil\log_2 l\rceil}|\widehat{l\cdot 2^j}\rangle\langle\widehat{l\cdot 2^j}|$ for odd $l \in [3\,..\,2^n-1]$. We have $\Pi_{l_1}H_{n,k}\Pi_{l_2} = 0$ whenever $l_1 \neq l_2$. Therefore, in order to get the full eigenspectrum of $H_{n,k}$, we consider the eigenvalues of each block separately.

3.1.2 *k*-dependent eigenvalues

We start with the first block $\Pi_1 H_{n,k} \Pi_1$. Consider a linear k-dependent isometry

$$U_k = \sum_{y=1}^{n} |\widehat{2^{n-y}}\rangle\langle\overline{y}| + |\widehat{0}\rangle\langle\overline{n+1}|, \tag{3.16}$$

where $\{|\overline{1}\rangle, \ldots, |\overline{n+1}\rangle\}$ is some fixed, k-independent basis (we use the k-independence later, when we talk about derivatives of eigenvectors). We have

$$\begin{aligned} \Phi_k = U_k^* H_{n,k} U_k =& 2\sum_{y=1}^{n-1} (|\overline{y+1}\rangle\langle\overline{y}| + |\overline{y}\rangle\langle\overline{y+1}|) \\ &+ 2\sin k\,(|\overline{n+1}\rangle\langle\overline{n}| + |\overline{n}\rangle\langle\overline{n+1}|) + 4\cos k\,|\overline{n+1}\rangle\langle\overline{n+1}|, \end{aligned} \tag{3.17}$$

which is the adjacency matrix of the graph given in Figure 3.2.

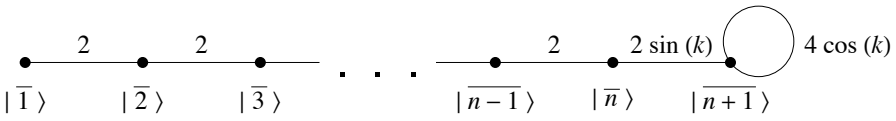

Figure 3.2: The graph corresponding to the adjacency matrix Φ_k.

If $k \in \{0, \pi\}$ then $\sin k = 0$ and thus Φ_k is the sum of two orthogonal operators $2M_{n-1}$ and $\pm 4|\overline{n+1}\rangle\langle\overline{n+1}|$, where we define

$$M_l = \sum_{y=1}^{l} (|\overline{y+1}\rangle\langle\overline{y}| + |\overline{y}\rangle\langle\overline{y+1}|). \tag{3.18}$$

M_l is basically the adjacency matrix of the line segment of length l and its eigenvalues and eigenvectors are well known (for example, see [3]). That is, for $p \in \{\frac{\pi}{l+2}, \frac{2\pi}{l+2}, \ldots, \frac{(l+1)\pi}{l+2}\}$ and $|p\rangle = \sqrt{\frac{2}{l+2}} \sum_{y=1}^{l+1} \sin yp\,|\overline{y}\rangle$ we have

$$M_l|p\rangle = 2\cos p\,|p\rangle \quad \text{and} \quad \langle p|p\rangle = 1. \tag{3.19}$$

Therefore for $k \in \{0, \pi\}$ the eigenvalues of Φ_k are $4\cos\frac{\pi}{n+1}, 4\cos\frac{2\pi}{n+1}, \ldots, 4\cos\frac{n\pi}{n+1}$ and $4\cos k$. Note that all of them are distinct. Next we show that all the eigenvalues are distinct for any value of k. Without loss of generality, we assume all eigenvectors of Φ_k are in reals with a non-negative amplitude of $|\overline{1}\rangle$.

Lemma 3.1. *Let $k \notin \{0, \pi\}$ and let $|\phi\rangle \in \mathbb{R}^{n+1}$ be a unit vector such that $\Phi_k|\phi\rangle = \lambda|\phi\rangle$ for some eigenvalue $\lambda \in \mathbb{R}$. Then there exist unique $p \in (0, \pi)$ and $c > 0$ such that $|\phi\rangle = c\sum_{y=1}^{n} \sin yp|\overline{y}\rangle + c\frac{\sin(n+1)p}{\sin k}|\overline{n+1}\rangle$ and $\lambda = 4\cos p$.*

Proof. The maximum absolute column sum norm of (3.7) is at most 4 (it is exactly 4 unless $n = 1$), which implies that all the eigenvalues of $H_{n,k}$ are at most 4 by the absolute value, and therefore so are the eigenvalues of Φ_k. That is, $|\lambda| \leq 4$. It can be easily shown that $|\lambda| = 4$ only in the case when $|\phi\rangle = |\overline{n+1}\rangle$ and $k \in \{0, \pi\}$. It is also the only case when $\langle\overline{1}|\phi\rangle = 0$.

Hence let $|\lambda| < 4$ and let $p \in (0, \pi)$ be the unique value such that $\lambda = 4\cos p$. Let $|\phi\rangle = \sum_{y=1}^{n+1} a_y|\overline{y}\rangle$ for some real numbers $a_1, \ldots, a_{n+1}$. We have

$$\lambda a_1 = \lambda\langle\overline{1}|\phi\rangle = \langle\overline{1}|\Phi_k|\phi\rangle = 2\langle\overline{2}|\phi\rangle = 2a_2. \tag{3.20}$$

Since $\sin p > 0$, we have a unique $c > 0$ satisfying $a_1 = c\sin p$. From (3.20) we get $a_2 = 2\cos p \cdot c\sin p = c\sin 2p$. Now let us use induction. Let $2 \leq l < n$, and let us assume $a_y = c\sin yp$ for all $y \in [1\,..\,l]$. We have

$$\lambda a_l = \lambda\langle\bar{l}|\phi\rangle = \langle\bar{l}|\Phi_k|\phi\rangle = (2\langle\overline{l-1}| + 2\langle\overline{l+1}|)|\phi\rangle = 2a_{l-1} + 2a_{l+1}, \tag{3.21}$$

$$4\cos p \cdot c\sin lp = 2c\sin(l-1)p + 2a_{l+1}, \tag{3.22}$$

$$a_{l+1} = 2c\cos p\,\sin lp - c(\cos p\,\sin lp - \cos lp\,\sin p) = c\sin(l+1)p. \tag{3.23}$$

Therefore, by the induction, $a_y = c\sin yp$ for $y \in [1\,..\,n]$. Finally,

$$\lambda a_n = \lambda\langle\overline{n}|\phi\rangle = \langle\overline{n}|\Phi_k|\phi\rangle = (2\langle\overline{n-1}| + 2\sin k\,\langle\overline{n+1}|)|\phi\rangle = 2a_{n-1} + 2a_{n+1}\sin k \tag{3.24}$$

similarly as above gives us

$$a_{n+1} = c\frac{\sin((n+1)p)}{\sin k}. \tag{3.25}$$

□

From Lemma 3.1 we see that an eigenvalue of Φ_k uniquely determines the eigenvector corresponding to it. This implies that all the eigenvalues of Φ_k are distinct.

Let us see what properties p must satisfy in order for $4\cos p$ to be an eigenvalue of Φ_k. By Lemma 3.1, the eigenvector corresponding to the eigenvalue $4\cos p$ is $|\phi\rangle = c\sum_{y=1}^{n}\sin yp|\overline{y}\rangle + c\frac{\sin(n+1)p}{\sin k}|\overline{n+1}\rangle$ for some $c > 0$. Similarly as in the proof of the lemma, we can see that $\langle\overline{y}|\Phi_k|\phi\rangle = 4\cos p\langle\overline{y}|\phi\rangle$ for all values of p and all $y \in [1\,..\,n]$, so any value of p for which $\langle\overline{n+1}|\Phi_k|\phi\rangle = 4\cos p\langle\overline{n+1}|\phi\rangle$ holds gives a valid eigenvalue. We have

$$\begin{aligned} 4\cos p \cdot c\frac{\sin(n+1)p}{\sin k} &= 4\cos p\langle\overline{n+1}|\phi\rangle = \langle\overline{n+1}|\Phi_k|\phi\rangle = (2\sin k\langle\overline{n}| + 4\cos k\langle\overline{n+1}|)|\phi\rangle \\ &= 2\sin k \cdot c\sin np + 4\cos k \cdot c\frac{\sin(n+1)p}{\sin k}, \end{aligned} \tag{3.26}$$

which gives us the necessary and sufficient condition

$$2(\cos p - \cos k)\sin((n+1)p) = \sin^2 k\sin np. \tag{3.27}$$

Note that even in the case $k \in \{0, \pi\}$ this condition is both necessary and sufficient for $4\cos p$ to be an eigenvalue. We sometimes refer to (3.27) as the *p-equation* or the *p-condition*. Unfortunately we do not know how to solve the p-equation (it possibly does not even have a closed for solution). Nevertheless, in Section 3.2 we show that it helps us to obtain some useful information about the eigenvalues.

3.1.3 *k*-independent eigenvalues

Let us consider the rest of the blocks of $H_{n,k}$ expressed in the hat basis. Recall that for odd $l \in [1\,..\,2^n-1]$ we have $H_{n,k} = \sum_l \Pi_l H_{n,k} \Pi_l$, where $\{\Pi_l \,:\, l \text{ is odd}\}$ is a set of orthogonal projectors (see page 16). So far we have considered eigenvalues only of the block $\Pi_1 H_{n,k} \Pi_1$. For odd $l \geq 3$ we have $\Pi_l = \sum_{j=0}^{n-\lceil \log_2 l \rceil} |\widehat{l \cdot 2^j}\rangle\langle\widehat{l \cdot 2^j}|$, and therefore from (3.15) we get that

$$\Pi_l H_{n,k} \Pi_l = 2 \sum_{j=0}^{n-\lceil \log_2 l \rceil - 1} (|\widehat{l \cdot 2^{j+1}}\rangle\langle\widehat{l \cdot 2^j}| + |\widehat{l \cdot 2^j}\rangle\langle\widehat{l \cdot 2^{j+1}}|) = 2 V_{k,l} M_{n-\lceil \log_2 l \rceil} V_{k,l}^*, \tag{3.28}$$

where $V_{k,l} = \sum_{y=1}^{n-\lceil \log_2 l \rceil + 1} |\widehat{l \cdot 2^{y-1}}\rangle\langle\overline{y}|$ is a linear isometry and $M_{n-\lceil \log_2 l \rceil}$ is defined in (3.18) as the adjacency matrix of the line segment of length $n - \lceil \log_2 l \rceil$. We already know the eigenvalues of $M_{n-\lceil \log_2 l \rceil}$ (see page 17), but, even more importantly, we know that they are k-independent. And therefore, so they are for every block $\Pi_l H_{n,k} \Pi_l$ with $l \geq 3$. This means that only $n+1$ out of all 2^n eigenvalues of $H_{n,k}$ depend on k. Next we show that those $n+1$ are the ones we care about.

Every eigenvector $|\phi\rangle$ of $M_{n-\lceil \log_2 l \rceil}$ is also k-independent. $V_{k,l}|\phi\rangle$ is an eigenvector of $\Pi_l H_{n,k} \Pi_l$ and, since each vector of the hat basis can be expressed in the form

$$\frac{1}{\sqrt{2^n}} \sum_{j \in \{0,1\}^n} (e^{\mathrm{i} k m_j})|j\rangle, \tag{3.29}$$

where $m_j \in [-n\,..\,n]$ for all j, we have

$$V_{k,l}|\phi\rangle\langle\phi|V_{k,l}^* = \sum_{j',j'' \in \{0,1\}^n} \left(\sum_{m=-2n}^{2n} \alpha_{(j',j'',m)} e^{\mathrm{i} k m} \right) |j''\rangle\langle j'|, \tag{3.30}$$

where $\alpha_{(j',j'',m)} \in \mathbb{R}$ for all j', j'' and m. For $m \in \mathbb{Z}$ we have

$$\int_0^{2\pi} |\tilde{k}\rangle\langle\tilde{k}| \otimes H_{n,k}\, \mathrm{d}k = H \quad \text{and} \quad \int_0^{2\pi} e^{\mathrm{i} k m} |\tilde{k}\rangle\langle\tilde{k}|\, \mathrm{d}k = \sum_{x \in \mathbb{Z}} |x-m\rangle\langle x|. \tag{3.31}$$

Hence,

Lemma 3.2. *Let Λ be the set of the eigenvalues of $M_0, M_2, \ldots, M_{n-2}$. There exists a (unique) complete set of orthogonal projectors $\{\Pi''_K\} \cup \{\Pi'_\lambda \,:\, \lambda \in \Lambda\}$ such that $H = K + \sum_{\lambda \in \Lambda} \lambda \Pi'_\lambda$, where $\Pi''_K = \int_0^{2\pi} |\tilde{k}\rangle\langle\tilde{k}| \otimes \Pi_1\, \mathrm{d}k$ and $K = \Pi''_K H \Pi''_K$. Let $\mathbb{I}$ be the identity operator on $\mathbb{C}^{\{0,1\}^n}$. We have $(\langle x + \Delta x| \otimes \mathbb{I})\Pi'_\lambda(|x\rangle \otimes \mathbb{I}) = 0$ for all $\lambda \in \Lambda$ and all $x \in \mathbb{Z}$ whenever $|\Delta x| > 2n$.*

Let K, Λ and $\{\Pi'_\lambda \,:\, \lambda \in \Lambda\}$ be such as in Lemma 3.2. Then for all $j', j'' \in \{0,1\}^n$ we have

$$\begin{aligned} \langle x'', j''|e^{-\mathrm{i}Ht}|x', j'\rangle &= \langle x'', j''| \left(e^{-\mathrm{i}Kt} + \sum_{\lambda \in \Lambda} e^{-\mathrm{i}\lambda t} \Pi'_\lambda \right) |x', j'\rangle \\ &= \langle x'', j''|e^{-\mathrm{i}Kt}|x', j'\rangle \end{aligned} \tag{3.32}$$

whenever $|x' - x''| > 2n$. This means that, if we want the snake to move further than $2n$ units on the line, we need to consider only how the operator K acts on it. And K is exactly the part of H which corresponds to k-dependent eigenvalues of $H_{n,k}$.

3.2 Even n and the median eigenvalue

We do not know how to solve the p-equation (3.27), the solution of which would give us the full eigenspectrum of $H_{n,k}$. Despite that, the p-equation allows us to obtain good approximations of eigenvalues and their derivatives. But let us first show that we can treat k-dependent eigenvalues (and therefore all eigenvalues) as differentiable functions of k.

3.2.1 Holomorphy and some general results

Definition. A complex-valued function is *holomorphic* if it is complex-differentiable in a neighborhood of every point in its domain.

Holomorphic functions are known to be infinitely differentiable, and their Taylor series converge at every point of their domain (the radius of convergence being the distance between the point and its nearest singularity) [23, Section 81]. The class of holomorphic functions include polynomials, the exponential function, sine and cosine [23, Chapter 7]. The notion of holomorphic functions can be generalized to vector-valued and operator-valued functions in an obvious way. From [22, Chapter II, §6.2] we have the following lemma

Lemma 3.3. *Let $\mathcal{X}$ be a finite complex Euclidean space of dimension m. Consider a holomorphic operator-valued function T which maps complex numbers to linear operators over $\mathcal{X}$ such that $T(k)$ is Hermitian for all $k \in \mathbb{R}$. Then for $k \in \mathbb{R}$ there exist a family of orthonormal basis $\{\phi_l(k) : l \in [1\,..\,m]\}$ of $\mathcal{X}$ consisting of eigenvectors of $T(k)$ and a family $\{\lambda_l(k) : l \in [1\,..\,m]\}$ consisting of eigenvalues of $T(k)$ such that $\lambda_l(k)$ and $\phi_l(k)$ are holomorphic functions of k for all $l \in [1\,..\,m]$.*

Let $\lambda_l(k)$ be the l-th largest eigenvalue of Φ_k. Since all the eigenvalues of Φ_k are distinct and Φ_k is holomorphic in k (which can be easily seen from (3.17)), then according to Lemma 3.3 $\lambda_l(k)$ is a holomorphic function in k for all $l \in [1\,..\,n+1]$. In order to give some intuition about the eigenspectrum of Φ_k, we show how the eigenvalues of Φ_k (Figure 3.3) and their derivatives (Figure 3.4) depend on $k \in [0, 2\pi)$ in the case when $n = 8$. These plots are obtained via numerical computation.

The plots suggest some interesting properties of $\lambda_l(k)$. Let us use a prime to denote derivatives with respect to k. For example, it seems that:

1. the range of the functions $\lambda_{l_1}(k)$ and $\lambda_{l_2}(k)$, where $l_1 \neq l_2$, do not overlap, except for the endpoints when $|l_1 - l_2| = 1$;

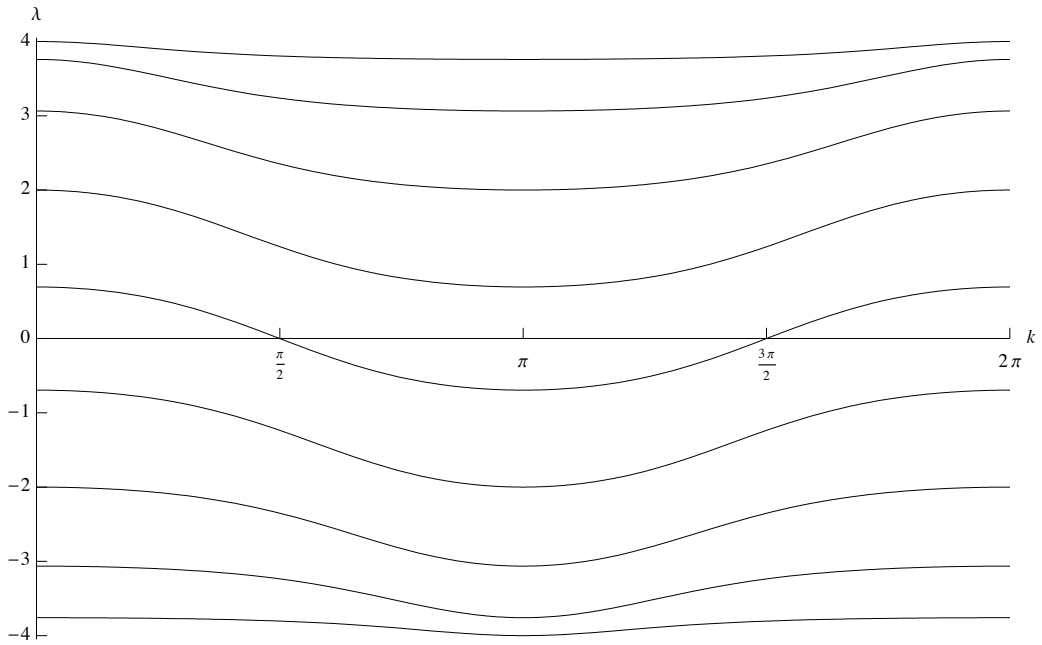

Figure 3.3: k-dependent eigenvalues for $n = 8$.

2. for every l the function $\lambda_l'(k)$ is negative for all $k \in (0, \pi)$ and positive for all $k \in (\pi, 2\pi)$;

3. there exists a constant $c > 0$ such that $\max_l |\lambda_l'(k)|$ is 'closely' bounded from above by $c|\sin k|$ for all values of k;

4. for every l there are unique $k_{l,1} \in (0, \pi)$ and $k_{l,2} \in (\pi, 2\pi)$ such that $\lambda_l''(k_{l,1}) = \lambda_l''(k_{l,2}) = 0$.

We prove below that observation 2 is true, and it easily implies that observation 1 also holds. As we see in Section 3.3.2, it is important for observation 4 to be true. So far we are not able to prove it, but in Section 3.2.2 we argue why it should hold for one specific choice of l.

The following lemma shows that by using the p-equation for some values of k we can calculate the derivatives of eigenvalues precisely. Lemma 3.4 was originally intended as a part of the proof of Theorem 3.5, but turned out not to be necessary. However, it still well exhibits usefulness of the p-equation.

Lemma 3.4. $\lambda_l'(\frac{\pi}{2}) = -\frac{8}{n+2} \sin^2 \frac{l\pi}{n+2}$ *for every* $l \in [1\,..\,n+1]$.

Proof. Let $\lambda_l(k) = 4\cos p_l(k)$, and therefore $p_l(k) = \arccos(\lambda_l(k)/4)$. One can verify that $k = \frac{\pi}{2}$ and every $p \in \{\frac{\pi}{n+2}, \frac{2\pi}{n+2}, \ldots, \frac{(n+1)\pi}{n+2}\}$ satisfies the p-condition. Hence, $p_l(\frac{\pi}{2}) = \frac{l\pi}{n+2}$ and $\lambda_l(\frac{\pi}{2})/4 \neq \pm 1$, which means that $p_l(k)$ is differentiable at $k = \frac{\pi}{2}$. For short, let

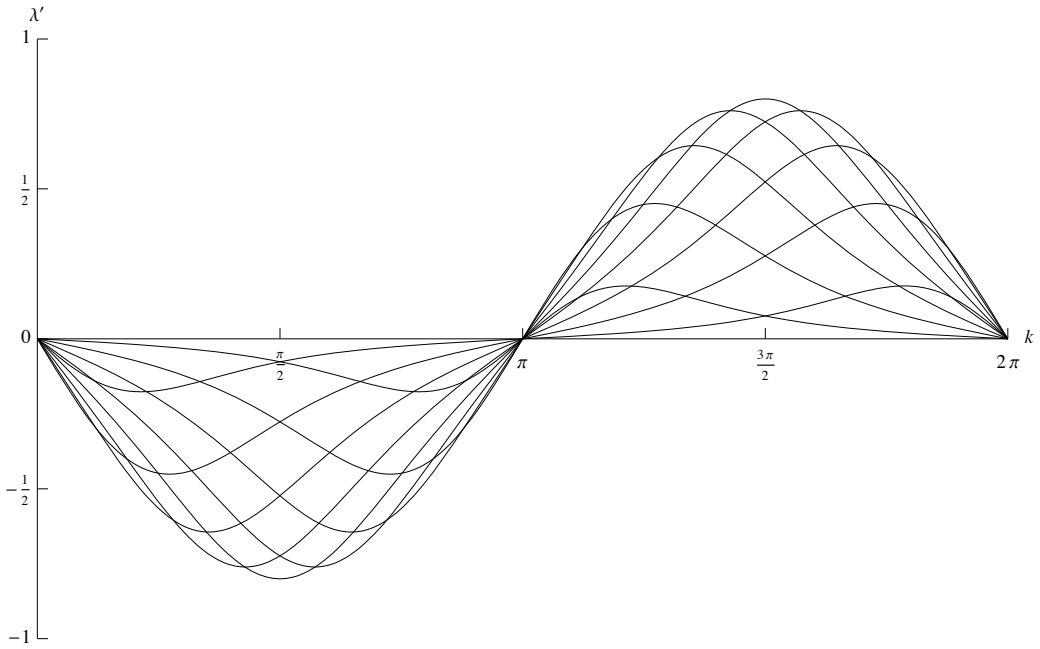

Figure 3.4: Derivatives of k-dependent eigenvalues for $n = 8$.

$p_l^{(1)} = p_l'(\frac{\pi}{2})$. By taking the derivatives of both sides of the p-equation we obtain

$$\begin{aligned} &2\left(-p_l'(k)\sin p_l(k) + \sin k\right)\sin((n+1)p_l(k)) \\ &+ 2(n+1)p_l'(k)(\cos p_l(k) - \cos k)\cos((n+1)p_l(k)) \\ &= 2\sin k\cos k\sin np_l(k) + np_l'(k)\sin^2 k\cos np_l(k), \end{aligned} \tag{3.33}$$

which for $k = \frac{\pi}{2}$ is

$$2\left(-p_l^{(1)}\sin\frac{l\pi}{n+2} + 1\right)\sin\frac{(n+1)l\pi}{n+2} + 2(n+1)p_l^{(1)}\cos\frac{l\pi}{n+2}\cos\frac{(n+1)l\pi}{n+2} = np_l^{(1)}\cos\frac{nl\pi}{n+2}. \tag{3.34}$$

Then $\sin\frac{(n+1)l\pi}{n+2} = -(-1)^l\sin\frac{l\pi}{n+2}$, $\cos\frac{(n+1)l\pi}{n+2} = (-1)^l\cos\frac{l\pi}{n+2}$ and $\cos\frac{nl\pi}{n+2} = (-1)^l\cos\frac{2l\pi}{n+2}$, and some simple derivations give us $p_l^{(1)} = \frac{2}{n+2}\sin\frac{l\pi}{n+2}$. Finally,

$$\lambda_l'(\pi/2) = (4\cos p_l(k))'|_{k=\pi/2} = 4p_l'(\pi/2)(-\sin p_l(\pi/2)) = -\frac{8}{n+2}\sin^2\frac{l\pi}{n+2}. \tag{3.35}$$

□

Theorem 3.5. *For every $l \in [1\,..\,n+1]$ the eigenvalue function $\lambda_l(k)$ is strictly decreasing in the interval $(0,\pi)$ and strictly increasing in the interval $(\pi, 2\pi)$.*

Proof. Fix l. We know that $\lambda_l(\pi) < \lambda_l(0) = \lambda_l(2\pi)$ (see page 17), therefore it is enough to show that the derivative of $\lambda_l(k)$ is non-zero whenever $k \notin \{0,\pi\}$. Now suppose the contrary: there exists $k_0 \in (0,\pi)\cup(\pi,2\pi)$ such that k_0 is the stationary point of $\lambda_l(k)$.

Since k_0 is the stationary point of $p_l(k) = \arccos(\lambda_l(k)/4)$ too, when we take the derivatives of both sides of the p-equation, we get

$$2 \sin k_0 \sin((n+1)p_l(k_0)) = 2 \sin k_0 \cos k_0 \sin np_l(k_0). \tag{3.36}$$

If $\sin((n+1)p_l(k_0)) = 0$, then $p_l(k_0) = \frac{m\pi}{n+1}$ for some $m \in [1\,..\,n]$ (recall that $|\lambda_l(k_0)| \neq 4$), which, in turn, implies $\sin np_l(k_0) \neq 0$ and $\sin k_0 = 0$ by the p-equation. We know that $\sin k_0 \neq 0$, thus (3.36) gives that all $\sin((n+1)p_l(k_0))$, $\cos k_0$ and $\sin np_l(k_0)$ are nonzero. Hence, by combining the p-equation and (3.36) we have

$$2(\cos p_l(k_0) - \cos k_0) \cos k_0 = \sin^2 k_0, \tag{3.37}$$

$$\cos p_l(k_0) = \frac{1}{2}\left(\frac{1}{\cos k_0} + \cos k_0\right). \tag{3.38}$$

Therefore k_0 must be either 0 or π for $\cos p_l(k_0)$ to be in $[-1, 1]$, which is a contradiction. □

It seems likely that an argument similar to one used in the proof of Theorem 3.5 might prove that $\lambda_l''(k) = 0$ for only two values of $k \in [0, 2\pi)$.

3.2.2 Median eigenvalue for asymptotically large n

For the rest of the chapter we consider only the case when n is even because it makes some calculations easier. Also, out of all $n+1$ k-dependent eigenvalues of $H_{n,k}$, let $\lambda(k)$ be the middle one, that is, the $\frac{n+2}{2}$-th largest; we consider only this particular eigenvalue. The reasons for considering this particular eigenvalue is the fact that it can be well approximated for values of k close to $\frac{\pi}{2}$ and it seems to have the largest derivative, which is good for a fast-moving snake. We know $\lambda(0) = 4\cos\frac{\frac{n}{2}\pi}{n+1}$ and $\lambda(\pi) = 4\cos\frac{(\frac{n}{2}+1)\pi}{n+1}$, therefore a corollary of Theorem 3.5 is that $|\lambda(k)| \leq 4\sin\frac{\pi}{2n+2}$. Let $p(k) \in [\frac{n\pi}{2n+2}, \frac{(n+2)\pi}{2n+2}]$ be such that $\lambda(k) = 4\cos p(k)$. By Lemma 3.3 $\lambda(k)$ is holomorphic, therefore $p(k)$ is infinitely differentiable.

From the definition of $H_{n,k}$ (3.7) one can easily see that $H_{n,-\kappa}$ is the transpose of $H_{n,\kappa}$, where $\kappa \in \mathbb{R}$, while $H_{n,\frac{\pi}{2}-\kappa}$ is minus the transpose of $H_{n,\frac{\pi}{2}+\kappa}$. Hence, the eigenspectra of $H_{n,-\kappa}$ and $H_{n,\kappa}$ are equal, while the eigenspectrum of $H_{n,\frac{\pi}{2}-\kappa}$ is minus the eigenspectrum of $H_{n,\frac{\pi}{2}+\kappa}$ (each eigenvalue of $H_{n,\frac{\pi}{2}-\kappa}$ multiplied by -1). By a little thought, this implies that $\lambda(-\kappa) = \lambda(\kappa)$ and $\lambda(\frac{\pi}{2} - \kappa) = -\lambda(\frac{\pi}{2} + \kappa)$ for all $\kappa \in \mathbb{R}$. Obviously, $\lambda(2\pi + \kappa) = \lambda(\kappa)$.

The function $\lambda(k)$ is holomorphic, and therefore it has a convergent Taylor series at every point $k \in \mathbb{R}$. In particular, let us consider the point $k = \frac{\pi}{2}$. Let $\lambda^{(0)}$ denote $\lambda(\frac{\pi}{2})$ and let $\lambda^{(m)}$ denote the value of m-th derivative of $\lambda(k)$ at $k = \frac{\pi}{2}$; similarly we use $p^{(0)}$ and $p^{(m)}$. Since $\lambda(k) = 4\cos p(k)$, and $p(k)$ is infinitely differentiable, we can easily obtain $\lambda^{(m)}$ for any order m, assuming we know $p^{(0)}, p^{(1)}, \ldots, p^{(m)}$. Luckily enough, getting derivatives of $p(k)$ at $\frac{\pi}{2}$ is not a problem: from Lemma 3.4 and its proof we already know that $p^{(0)} = \frac{\pi}{2}$ and $p^{(1)} = \frac{2}{n+2}$, and the values of further derivatives can be obtained from the p-equation (3.27). That is, since n is even, we have $\sin np^{(0)} = \cos(n+1)p^{(0)} = 0$ and

$\cos np^{(0)} = \sin(n+1)p^{(0)} \neq 0$. In order to get $p^{(m)}$, we compute values $p^{(0)}, p^{(1)}, \ldots, p^{(m-1)}$ first, and then substitute them and $k = \frac{\pi}{2}$ in the m-th derivative of the p-equation. This way we end up with a linear equation for $p^{(m)}$, whose coefficients can be shown (by induction) to be rational functions in n.

Since $\lambda(k)$ and $p(k)$ are n-dependent functions, for a moment let us denote them by, respectively, $\lambda_{[n]}(k)$ and $p_{[n]}(k)$ instead, and let $T_{[n]}(k)$ denote the Taylor series of $\lambda_{[n]}(k)$ at $k = \frac{\pi}{2}$. We do not know what is the convergence radius of $T_{[n]}(k)$ since we do not know how $\lambda_{[n]}(k)$ can be defined for complex k. Because of $\lambda_{[n]}(\frac{\pi}{2} - \kappa) = -\lambda_{[n]}(\frac{\pi}{2} + \kappa)$, for even m we have $\lambda_{[n]}^{(m)} = 0$ (and $p_{[n]}^{(m)} = 0$ if $m \neq 0$). Carrying out symbolic computation which uses the method described in the previous paragraph we obatin that for odd $m \in \{1, 3, \ldots, 29\}$ both $p_{[n]}^{(m)}$ and $\lambda_{[n]}^{(m)}$ are rational functions with denominator $(n+2)^m$ and some polynomials of degree $m-1$ as numerators. For example, for $m = 1$, $m = 3$, $m = 5$ and $m = 7$ we have:

$$
\begin{aligned}
p_{[n]}^{(1)} &= \frac{2}{n+2}, & \lambda_{[n]}^{(1)} &= -\frac{8}{n+2}, \\
p_{[n]}^{(3)} &= -\frac{6n^2}{(n+2)^3}, & \lambda_{[n]}^{(3)} &= \frac{8(3n^2+4)}{(n+2)^3}, \\
p_{[n]}^{(5)} &= \frac{10(9n^4 - 16n^3 - 16n^2)}{(n+2)^5}, & \lambda_{[n]}^{(5)} &= -\frac{8(45n^4 - 80n^3 + 40n^2 + 16)}{(n+2)^5},
\end{aligned} \tag{3.39}
$$

and

$$
\begin{aligned}
p_{[n]}^{(7)} &= -\frac{14(249n^6 - 976n^5 - 208n^4 + 1536n^3 + 768n^2)}{(n+2)^7}, \\
\lambda_{[n]}^{(7)} &= \frac{8(1743n^6 - 6832n^5 + 4844n^4 + 4032n^3 + 336n^2 + 64)}{(n+2)^7}.
\end{aligned} \tag{3.40}
$$

Assuming this pattern holds for derivatives of all orders, $\lim_{n\to\infty}(n+2)\lambda_{[n]}^{(m)} = \alpha_m$ exists, and it is nonzero for odd m. Therefore the sequence of series $4T_{[2]}(k)$, $6T_{[4]}(k)$, $8T_{[6]}(k)$, ... converge to a series

$$
T_\infty(\pi/2+\kappa) = \sum_{m\in\mathbb{N}} \frac{\alpha_m}{m!}\kappa^m = -8\kappa + \frac{24}{3!}\kappa^3 - \frac{360}{5!}\kappa^5 + \frac{13944}{7!}\kappa^7 - \frac{1005000}{9!}\kappa^9 + \frac{116437464}{11!}\kappa^{11} - \ldots \tag{3.41}
$$

The coefficients of T_∞ seem to increase, so it might be the case that the convergence radius of T_∞, if non-zero, is at least less than 1.

Even though $T_\infty(k)/(n+2)$ may not be a good approximation of $\lambda_{[n]}(k)$, numerical results suggest that $4\lambda_{[2]}(k)$, $6\lambda_{[4]}(k)$, $8\lambda_{[6]}(k)$, ... converge to some function $\lambda_\infty(k)$. When we plot the values of $(n+2)\lambda_{[n]}(k)$, $(n+2)\lambda'_{[n]}(k)$ and $(n+2)\lambda''_{[n]}(k)$ for $k \in [0, 2\pi)$, the plots change less and less as n increases. In Figure 3.5 we plot $(n+2)\lambda_{[n]}(k)$ and its first and second derivatives in the case when $n = 500$. This plot looks hardly different if we choose $n = 20$, $n = 50$ or $n = 200$, therefore it seems likely that, if the function $\lambda_\infty(k)$ exists, Figure 3.5 well represents $\lambda_\infty(k)$ and its first two derivatives.

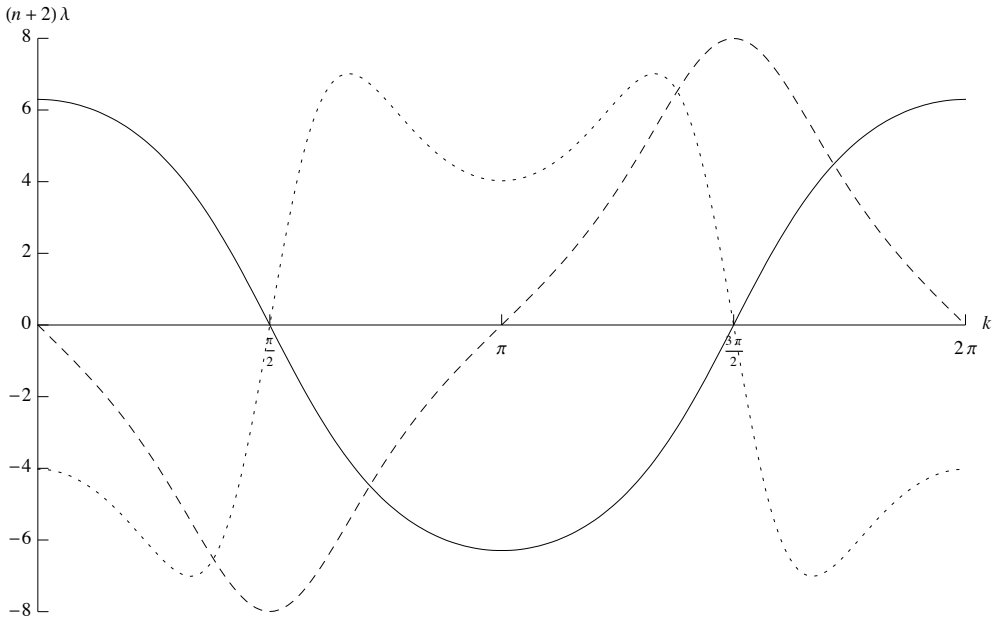

Figure 3.5: $(n+2)\lambda(k)$ (solid line), $(n+2)\lambda'(k)$ (dashed line) and $(n+2)\lambda''(k)$ (dotted line) for $n = 500$.

This plot suggests that the second derivative of $\lambda(k)$ is 0 only if $k = \{\frac{\pi}{2}, \frac{3\pi}{2}\}$. Plus, which is also important in our analysis later: $\lambda''(k)$ is bounded, but also it is not close to 0 for many values of k, and, when it is, it changes rapidly. The existence of $\lambda_\infty(k)$ would suggest that this hold for all n, therefore let us assume the following hypothesis.

Hypothesis 3.6. *Consider $k \in [0, 2\pi)$ and an arbitrary even n. $\lambda''(k) = 0$ if and only if $k = \{\frac{\pi}{2}, \frac{3\pi}{2}\}$, and for all values of k: $(n+2)|\lambda''(k)| \le 8$ and, if $(n+2)|\lambda''(k)| < 4$, then $(n+2)|\lambda'''(k)| > 4\sqrt{3}$.*

Similarly as we get derivatives of $\lambda(k)$ at $k = \frac{\pi}{2}$, at $k = \pi$ we get

$$\lambda''(\pi) = \frac{4\left(\cos\frac{\pi}{4n+4} + \sin\frac{\pi}{4n+4}\right)\cos\frac{\pi}{2n+2}}{(n+1)\left(\cos\frac{\pi}{4n+4} - \sin\frac{\pi}{4n+4}\right)}; \tag{3.42}$$

therefore the constant 4 in Hypothesis 3.6. The bounds $4\sqrt{3}$ and 8 come from the case $n = 2$: for $n = 2$ we have $\lambda(k) = 2\cos k$, $\lambda''(2\pi/3) = 1$ and $\lambda'''(2\pi/3) = \sqrt{3}$.

The following rough approximation favors the existence of $\lambda_\infty(k)$. Assume that n is large (and even), and let $p(k) = \frac{\pi}{2} + \frac{\theta(k)}{n+1}$, where $\theta(k) \in [-\frac{\pi}{2}, \frac{\pi}{2}]$. By substituting this in the p-equation and doing some trivial trigonometric derivations we get

$$2\left(-\sin\left(\frac{1}{n+1}\theta(k)\right) - \cos k\right)\cos\theta(k) = \sin^2 k \sin\left(\frac{n}{n+1}\theta(k)\right). \tag{3.43}$$

Since n is large, we can roughly approximate $\sin\left(\frac{1}{n+1}\theta(k)\right)$ by 0 and $\sin\left(\frac{n}{n+1}\theta(k)\right)$ by $\sin\theta(k)$. Therefore

$$-2\cos k\cos\theta(k) \approx \sin^2 k \sin\theta(k), \tag{3.44}$$

which gives us

$$\theta_{n,k} \approx \arctan\left(\frac{-2\cos k}{\sin^2 k}\right). \tag{3.45}$$

Hence

$$\lambda(k) = 4\cos\left(\frac{\pi}{2} + \frac{\theta(k)}{n+1}\right) = -4\sin\frac{\theta(k)}{n+1} \approx \frac{-4\theta(k)}{n+1} \approx \frac{4}{n+1}\arctan\left(\frac{2\cos k}{\sin^2 k}\right). \tag{3.46}$$

The plot for $4\arctan\left(\frac{2\cos k}{\sin^2 k}\right)$ and its first two derivatives (see Figure 3.6) very well resembles Figure 3.5, the plot for $(n+2)\lambda(k)$ and its first two derivatives when $n = 500$. This indicates that Hypothesis 3.6 might indeed be true. However, more precise analysis must be done in the future.

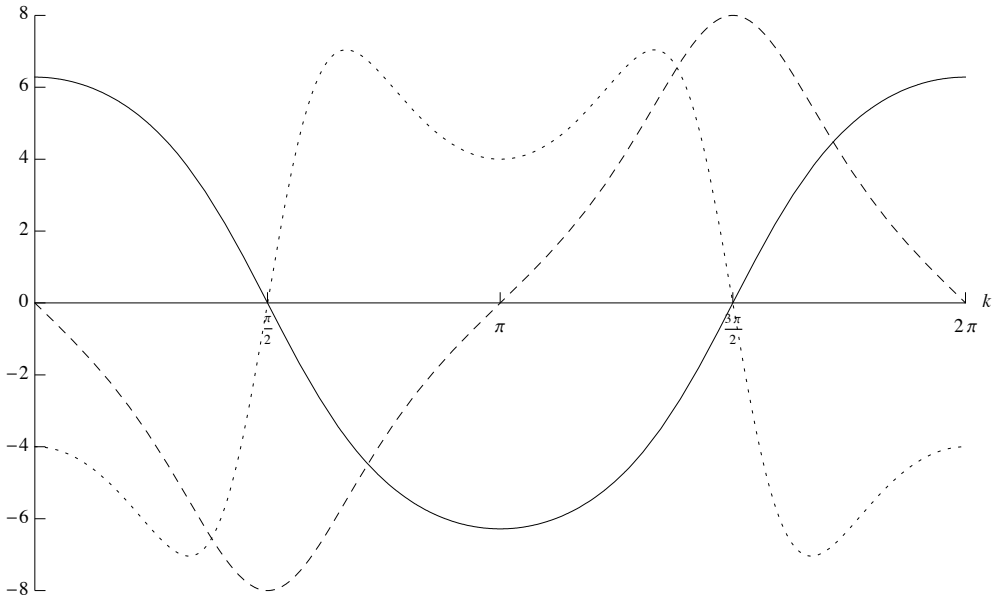

Figure 3.6: $4\arctan\left(\frac{2\cos k}{\sin^2 k}\right)$ (solid line) and its first and second derivatives (dashed and dotted lines, respectively).

3.2.3 Perturbed eigenvalues and eigenvectors

Recall that for any $k \in [0, 2\pi)$

$$U(k) = \sum_{y=2}^{n+1} |\widehat{2^{y-2}}(k)\rangle\langle\overline{n+2-y}| + |\widehat{0}(k)\rangle\langle\overline{n+1}| \tag{3.47}$$

and

$$\begin{aligned}\Phi(k) = {} & 2\sum_{y=1}^{n-1}\left(|\overline{y+1}\rangle\langle\overline{y}| + |\overline{y}\rangle\langle\overline{y+1}|\right) \\ & + 2\sin k\left(|\overline{n+1}\rangle\langle\overline{n}| + |\overline{n}\rangle\langle\overline{n+1}|\right) + 4\cos k\,|\overline{n+1}\rangle\langle\overline{n+1}|\end{aligned} \tag{3.48}$$

as they are, respectively, defined in (3.16) and (3.17), where $\{\,|\overline{y}\rangle\,:\,y\in[1\,..\,n+1]\,\}$ is an orthonormal k-independent basis, and the orthonormal k-dependent basis $\{\,|\widehat{m}(k)\rangle\,:\,m\in[0\,..\,2^n-1]\,\}$ is defined on page 15 (here we write (k) to stress dependence on k). Let n still be even and $\lambda(k)$ be the $\frac{n+2}{2}$-th largest eigenvalue of $\Phi(k)$. Lemma 3.3 states that there is a holomorphic vector-valued function $|\phi_0(k)\rangle$ such that $\Phi(k)|\phi_0(k)\rangle=\lambda(k)|\phi_0(k)\rangle$ and $\langle\phi_0(k)|\phi_0(k)\rangle=1$. For any holomorphic function $a(k)$ let $a^{(0)}=a(\frac{\pi}{2})$ and $a^{(1)}=a'(\frac{\pi}{2})$, which is a notation common in perturbation theory. From

$$(\langle\phi_0(k)|\phi_0(k)\rangle)'=\langle\phi_0'(k)|\phi_0(k)\rangle+\langle\phi_0(k)|\phi_0'(k)\rangle=0 \tag{3.49}$$

we get that $\langle\phi_0^{(0)}|\phi_0^{(1)}\rangle=\mathrm{i}b$ for some $b\in\mathbb{R}$. Let $|\phi(k)\rangle=e^{-\mathrm{i}bk}|\phi_0(k)\rangle$, for which we have $\langle\phi^{(0)}|\phi^{(1)}\rangle=0$. And finally, let $|\psi(k)\rangle=U(k)|\phi(k)\rangle$. The functions $\lambda(k)$ and $|\phi(k)\rangle$ are holomorphic, and therefore all the functions mentioned above are holomorphic.

Note that $|\psi(k)\rangle$ is an eigenvector of $H_{n,k}$ corresponding to the eigenvalue $\lambda(k)$. Our aim here is to express $|\psi^{(0)}\rangle$ and $|\psi^{(1)}\rangle$ in the orthonormal basis $\{\,|\widehat{m}^{(0)}\rangle\,:\,m\in[0\,..\,2^n-1]\,\}$, and show that they are orthogonal. Vectors $|\psi^{(0)}\rangle$ and $|\psi^{(1)}\rangle$ are important in Section 3.3, where we talk how the continuous-time quantum snake walk behaves for one specific initial state. We have

$$|\psi^{(0)}\rangle=U^{(0)}|\phi^{(0)}\rangle\quad\text{and}\quad|\psi^{(1)}\rangle=U^{(1)}|\phi^{(0)}\rangle+U^{(0)}|\phi^{(1)}\rangle. \tag{3.50}$$

$U^{(0)}$ is already known. We obtain $U^{(1)}$ by considering the values of the derivatives of hat vectors at $k=\frac{\pi}{2}$. $|\phi^{(0)}\rangle$ is an eigenvector of $\Phi^{(0)}$, which is simply twice the adjacency matrix of the line segment of length n, whose eigenvalues and eigenvectors are well known. Then we use the perturbation theory for the operator $\Phi(k)$ to obtain $|\phi^{(1)}\rangle$.

Let us start by $|\psi^{(0)}\rangle$. We have $\Phi^{(0)}=2\sum_{y=1}^{n}(|\overline{y+1}\rangle\langle\overline{y}|+|\overline{y}\rangle\langle\overline{y+1}|)$, and for every $p\in P=\{\frac{\pi}{n+2},\frac{2\pi}{n+2},\ldots,\frac{(n+1)\pi}{n+2}\}$ the operator $\Phi^{(0)}$ has an eigenvalue $4\cos p$ with corresponding eigenvector

$$|p\rangle=\sqrt{\frac{2}{n+2}}\sum_{y=1}^{n+1}\sin yp\,|\overline{n+2-y}\rangle \tag{3.51}$$

(which is equal to $\sqrt{\frac{2}{n+2}}\sum_{y=1}^{n+1}\sin yp\,|\overline{y}\rangle$ up to a global phase). The $\frac{n+2}{2}$-th largest eigenvalue of $\Phi^{(0)}$ corresponds to the $\frac{n+2}{2}$-th smallest element in P, which is $\frac{\pi}{2}$. Therefore we have $\lambda^{(0)}=4\cos(\frac{\pi}{2})=0$ and

$$|\phi^{(0)}\rangle=\sqrt{\frac{2}{n+2}}\sum_{y=1}^{n+1}\sin(y\pi/2)\,|\overline{n+2-y}\rangle=\sqrt{\frac{2}{n+2}}\sum_{\substack{y=1\\ y\text{ is odd}}}^{n+1}(-1)^{\frac{y-1}{2}}\,|\overline{n+2-y}\rangle. \tag{3.52}$$

When we multiply this with $U^{(0)}$, we get

$$|\psi^{(0)}\rangle=\sqrt{\frac{2}{n+2}}\left(|\widehat{0}^{\,(0)}\rangle+\sum_{\substack{y=2\\ y\text{ is even}}}^{n}\mathrm{i}^y\,|\widehat{2^{y-1}\,(0)}\rangle\right) \tag{3.53}$$

Next, let us obtain $|\phi^{(1)}\rangle$ by using the perturbation theory. We have

$$\Phi'(k) + 2\cos k\,(|\overline{n+1}\rangle\langle\overline{n}| + |\overline{n}\rangle\langle\overline{n+1}|) - 4\sin k\,|\overline{n+1}\rangle\langle\overline{n+1}|, \tag{3.54}$$

from which we get that $\Phi^{(1)} = -4\,|\overline{n+1}\rangle\langle\overline{n+1}|$. Then, according to [21, Section 1.2], we have

$$\lambda^{(1)} = \langle\phi^{(0)}|\Phi^{(1)}|\phi^{(0)}\rangle = -\frac{8}{n+2} \tag{3.55}$$

(which we already know from Lemma 3.4) and

$$\begin{aligned}
|\phi^{(1)}\rangle &= \sum_{p\in P\setminus\{\pi/2\}} \frac{\langle p|\,\Phi^{(1)}\,|\phi^{(0)}\rangle}{\lambda^{(0)} - 4\cos p}\,|p\rangle \\
&= \frac{2}{n+2} \sum_{p\in P\setminus\{\pi/2\}} \frac{\sin p}{\cos p}|p\rangle \\
&= \left(\frac{2}{n+2}\right)^{3/2} \sum_{y=1}^{n+1} \left(\sum_{p\in P\setminus\{\pi/2\}} \frac{\sin p\,\sin yp}{\cos p} \right) |\overline{n+2-y}\rangle.
\end{aligned} \tag{3.56}$$

Lemma 3.7. *For $y \in [0\,..\,n+1]$ let $S_n(y) = \sum_{p\in P\setminus\{\pi/2\}} \frac{\sin p\,\sin yp}{\cos p}$. Then we have $S_n(y) = 0$ for odd y and $S_n(y) = -(-1)^{y/2}(n+2-y)$ for positive even y.*

Proof. If y is odd, then

$$\sum_{p\in P\setminus\{\pi/2\}} \frac{\sin p\,\sin yp}{\cos p} = -\sum_{p\in P\setminus\{\pi/2\}} \frac{\sin(\pi-p)\,\sin y(\pi-p)}{\cos(\pi-p)} = -\sum_{p\in P\setminus\{\pi/2\}} \frac{\sin p\,\sin yp}{\cos p}, \tag{3.57}$$

which implies $S_n(y) = 0$. Suppose y is even. One can verify that

$$\frac{\sin p\,\sin yp}{\cos p} = 2\sin p\,\sin(y-1)p - \frac{\sin p\,\sin(y-2)p}{\cos p} \tag{3.58}$$

holds, which gives us

$$S_n(y) = -S_n(y-2) + 2\sum_{p\in P\setminus\{\pi/2\}} \sin p\,\sin(y-1)p. \tag{3.59}$$

Using the facts that $\sin x = \mathrm{i}(e^{-\mathrm{i}x} - e^{\mathrm{i}x})/2$ and $\sin p\,\sin(y-1)p = \sin(\pi+p)\,\sin((y-1)(\pi+p))$ for even y, we can evaluate the sum on the right. For even $y \in [2\,..\,n]$:

$$\begin{aligned}
\sum_{p\in P\setminus\{\pi/2\}} \sin p\,\sin((y-1)p) &= (-1)^{y/2} + \sum_{p\in\{0\}\cup P} \sin p\,\sin((y-1)p) \\
&= (-1)^{y/2} + \frac{1}{2} \sum_{\rho\in[0\,..\,2n+3]} \sin\frac{\rho\pi}{n+2}\,\sin\frac{(y-1)\rho\pi}{n+2} \\
&= (-1)^{y/2} - \frac{1}{8} \sum_{\rho\in[0\,..\,2n+3]} \left(e^{-\mathrm{i}\frac{y\rho\pi}{n+2}} + e^{\mathrm{i}\frac{y\rho\pi}{n+2}} - e^{-\mathrm{i}\frac{(y-2)\rho\pi}{n+2}} - e^{\mathrm{i}\frac{(y-2)\rho\pi}{n+2}} \right) \\
&= (-1)^{y/2} + \frac{n+2}{2}\delta_{y,2}.
\end{aligned} \tag{3.60}$$

Obviously $S_n(0) = 0$. From (3.59) and (3.60) we have $S_n(2) = -2 + n + 2 = n$ and $S_n(y) = 2(-1)^{y/2} - S_n(y-2)$ for other even values of y. Then the lemma follows by induction. □

Hence

$$|\phi^{(1)}\rangle = -\left(\frac{2}{n+2}\right)^{3/2} \sum_{\substack{y=2 \\ y \text{ is even}}}^{n} (-1)^{y/2}(n+2-y)|\overline{n+2-y}\rangle. \tag{3.61}$$

All that is left is to find $U^{(1)}$. In order to do that we need to find the derivatives of the hat vectors which span the range of the operator $U(k)$. The derivatives of vectors

$$\begin{aligned} |u_{0,k}\rangle &= \frac{1}{\sqrt{2}}(e^{-\mathrm{i}k}|0\rangle + e^{\mathrm{i}k}|1\rangle), \quad |u_{1,k}\rangle = \frac{1}{\sqrt{2}}(e^{-\mathrm{i}k}|0\rangle - e^{\mathrm{i}k}|1\rangle), \\ |v_0\rangle &= |+\rangle = \frac{1}{\sqrt{2}}(|0\rangle + |1\rangle), \quad |v_1\rangle = |-\rangle = \frac{1}{\sqrt{2}}(|0\rangle - |1\rangle) \end{aligned} \tag{3.62}$$

are, respectively,

$$|u'_{0,k}\rangle = -\mathrm{i}|u_{1,k}\rangle, \quad |u'_{1,k}\rangle = -\mathrm{i}|u_{0,k}\rangle, \quad |v'_0\rangle = 0, \quad |v'_1\rangle = 0. \tag{3.63}$$

Note that $|u_{0,\frac{\pi}{2}}\rangle = -\mathrm{i}|-\rangle$ and $|u_{1,\frac{\pi}{2}}\rangle = -\mathrm{i}|+\rangle$. The hat vectors we care about in the context of $U^{(0)}$ and $U^{(1)}$ turns out to be

$$\begin{aligned} |\widehat{0}(k)\rangle &= -\mathrm{i}|u_{0,k}\rangle^{\otimes n}, \\ |\widehat{2^{l_1}}(k)\rangle &= |u_{0,k}\rangle^{\otimes n-l_1-1}|u_{1,k}\rangle|v_0\rangle^{\otimes l_1}, \\ |\widehat{2^{l_2}-2^{l_1}}(k)\rangle &= |u_{0,k}\rangle^{\otimes n-l_2}|u_{1,k}\rangle|v_1\rangle^{\otimes l_2-l_1-1}|v_0\rangle^{\otimes l_1}, \end{aligned} \tag{3.64}$$

where $0 \le l_1 < l_2 \le n$. Thus

$$\begin{aligned} |\widehat{0}^{\,(0)}\rangle &= (-\mathrm{i})^{n+1}|-\rangle^{\otimes n}, \\ |\widehat{2^{l_1}}^{\,(0)}\rangle &= (-\mathrm{i})^{n-l_1}|-\rangle^{\otimes n-l_1-1}|+\rangle^{\otimes l_1+1}, \\ |\widehat{2^{l_2}-2^{l_1}}^{\,(0)}\rangle &= (-\mathrm{i})^{n-l_2+1}|-\rangle^{\otimes n-l_2}|+\rangle|-\rangle^{\otimes l_2-l_1-1}|+\rangle^{\otimes l_1}. \end{aligned} \tag{3.65}$$

Now, for $l \in [0\,..\,n-1]$ we have

$$\begin{aligned} |\widehat{0}\,'(k)\rangle &= -\sum_{j=0}^{n-1} |u_{0,k}\rangle^{\otimes n-1-j}|u_{1,k}\rangle|u_{0,k}\rangle^{\otimes j}, \\ |\widehat{2^l}\,'(k)\rangle &= -\mathrm{i}|u_{0,k}\rangle^{\otimes n-l}|v_0\rangle^{\otimes l} - \mathrm{i}\sum_{j=0}^{n-l-2} |u_{0,k}\rangle^{\otimes n-l-2-j}|u_{1,k}\rangle|u_{0,k}\rangle^{\otimes j}|u_{1,k}\rangle|v_0\rangle^{\otimes l}. \end{aligned} \tag{3.66}$$

It is convenient to define $|\widehat{2^{-1}}(k)\rangle = |\widehat{0}(k)\rangle$, $|\widehat{2^{-2}}^{(0)}\rangle = 0$ and $|\widehat{2^{n}}^{(0)}\rangle = 0$. From (3.65) and (3.66) we get

$$\begin{aligned}
|\widehat{2^{-1}}^{(1)}\rangle =& |\widehat{0}^{(1)}\rangle = -(-\mathrm{i})^n \sum_{j=0}^{n-1} |-\rangle^{\otimes n-1-j}|+\rangle|-\rangle^{\otimes j} \\
=& |\widehat{2^{-1-1}}^{(0)}\rangle - |\widehat{2^{-1+1}}^{(0)}\rangle - \sum_{j=1}^{n-(-1)-2} \mathrm{i}^{-j}|2^{-1+1}\widehat{(2^{j+1}-1)}^{(0)}\rangle, \\
|\widehat{2^{l}}^{(1)}\rangle =& (-\mathrm{i})^{n-l+1}|-\rangle^{\otimes n-l}|+\rangle^{\otimes l} + (-\mathrm{i})^{n-l+1} \sum_{j=0}^{n-l-2} |-\rangle^{\otimes n-l-2-j}|+\rangle|-\rangle^{\otimes j}|+\rangle^{\otimes l+1} \\
=& |\widehat{2^{l-1}}^{(0)}\rangle - |\widehat{2^{l+1}}^{(0)}\rangle - \sum_{j=1}^{n-l-2} \mathrm{i}^{-j}|2^{l+1}\widehat{(2^{j+1}-1)}^{(0)}\rangle.
\end{aligned} \tag{3.67}$$

Therefore

$$U^{(0)} = \sum_{y=1}^{n+1} |\widehat{2^{y-2}}^{(0)}\rangle\langle\overline{n+2-y}| \tag{3.68}$$

and

$$U^{(1)} = \sum_{y=1}^{n+1} \left(|\widehat{2^{y-3}}^{(0)}\rangle - |\widehat{2^{y-1}}^{(0)}\rangle - \sum_{j=1}^{n-y} \mathrm{i}^{-j}|2^{y-1}\widehat{(2^{j+1}-1)}^{(0)}\rangle \right) \langle\overline{n+2-y}|. \tag{3.69}$$

By combining the expressions for $|\phi^{(0)}\rangle$, $|\phi^{(1)}\rangle$, $U^{(0)}$ and $U^{(1)}$ we get

$$\begin{aligned}
|\psi^{(1)}\rangle =& \sqrt{\frac{2}{n+2}} \sum_{\substack{y=1 \\ y \text{ is odd}}}^{n+1} (-1)^{\frac{y-1}{2}} \left(|\widehat{2^{y-3}}^{(0)}\rangle - |\widehat{2^{y-1}}^{(0)}\rangle - \sum_{j=1}^{n-y} \mathrm{i}^{-j}|2^{y-1}\widehat{(2^{j+1}-1)}^{(0)}\rangle \right) \\
& - \left(\frac{2}{n+2}\right)^{3/2} \sum_{\substack{y=2 \\ y \text{ is even}}}^{n} (-1)^{y/2}(n+2-y)|\widehat{2^{y-2}}^{(0)}\rangle \\
=& \sqrt{\frac{2}{n+2}} \sum_{\substack{y=0 \\ y \text{ is even}}}^{n} (-1)^{y/2}|\widehat{2^{y-2}}^{(0)}\rangle + \sqrt{\frac{2}{n+2}} \sum_{\substack{y=2 \\ y \text{ is even}}}^{n+2} (-1)^{y/2}|\widehat{2^{y-2}}^{(0)}\rangle \\
& - \sqrt{\frac{2}{n+2}} \sum_{\substack{y=0 \\ y \text{ is even}}}^{n} (-1)^{y/2} \sum_{j=1}^{n-y-1} \mathrm{i}^{-j}|2^{y}\widehat{(2^{j+1}-1)}^{(0)}\rangle \\
& - \left(\frac{2}{n+2}\right)^{3/2} \sum_{\substack{y=2 \\ y \text{ is even}}}^{n} (-1)^{y/2}(n+2-y)|\widehat{2^{y-2}}^{(0)}\rangle =
\end{aligned}$$

$$= \sqrt{\frac{2}{n+2}} \left(\frac{2}{n+2} \sum_{\substack{y=2 \\ y \text{ is even}}}^{n} \mathrm{i}^y \, y \, |\widehat{2^{y-2}\,(0)}\rangle - \sum_{\substack{y=0 \\ y \text{ is even}}}^{n-2} \sum_{j=1}^{n-y-1} \mathrm{i}^{y-j} |2^y (\widehat{2^{j+1}-1})\,(0)\rangle \right). \tag{3.70}$$

Since all vectors in this sum are distinct, we have

$$\langle \psi^{(1)} | \psi^{(1)} \rangle = \frac{2}{n+2} \left(\frac{4}{(n+2)^2} \sum_{\substack{y=2 \\ y \text{ is even}}}^{n} y^2 + \sum_{\substack{y=0 \\ y \text{ is even}}}^{n-2} \sum_{j=1}^{n-y-1} 1 \right) = \frac{n(3n^2+14n+8)}{6(n+2)^2}. \tag{3.71}$$

One can easily see that $|\psi^{(0)}\rangle$ and $|\psi^{(1)}\rangle$ are superpositions over disjoint subsets of $\{\, |\widehat{m}^{(0)}\rangle \,:\, m \in [0\,..\,2^n-1]\,\}$, and therefore they are orthogonal.

3.3 A wave packet of snakes

In Section 2.1.2 we have already shown that in the case of the regular continuous-time quantum walk on the line we can prepare a specific initial state which then propagates as a Gaussian-shaped wave packet with any momentum up to 2. Here we show that something very similar is possible in the case of the continuous-time quantum snake walk on the line.

Our main obstacle is that we do not know all the eigenvalues of $H_{n,k}$, that is, we do not know the eigenvalues that depend on k, which are the ones we care about. We know even less about the corresponding eigenvectors. Therefore later we have to do some approximations and make some assumptions.

Again, let n be even and let $\lambda(k)$ be the $\frac{n+2}{2}$-th largest k-dependent eigenvalue of $H_{n,k}$. From the discussions in the beginning of Section 3.2.2 and Section 3.2.3 we know that $\lambda(k)$ is holomorphic, and there exists a holomorphic function $|\psi(k)\rangle$ such that $H(|\tilde{k}\rangle \otimes |\psi(k)\rangle) = \lambda(k)\,|\tilde{k}\rangle \otimes |\psi(k)\rangle$ and $\langle \psi(k) | \psi(k) \rangle = 1$ for all $k \in \mathbb{R}$, and $\langle \psi(\frac{\pi}{2}) | \psi'(\frac{\pi}{2}) \rangle = 0$. In this section we lift the restriction that k is in $[0, 2\pi)$.

For $z \in \mathbb{Z}$, consider the state

$$|\xi_z\rangle = c_\sigma \int_{-\frac{\pi}{2}}^{\frac{3\pi}{2}} e^{-\frac{(k-\frac{\pi}{2})^2}{2\sigma^2}} e^{-\mathrm{i}kz} \, |\tilde{k}\rangle \otimes |\psi(k)\rangle \, \mathrm{d}k, \tag{3.72}$$

where $c_\sigma > 0$ is the normalization factor and we assume that the parameter $\sigma > 0$ is small (we should think of σ^2 as a variance). Other than $\langle \psi(\frac{\pi}{2}) | \psi'(\frac{\pi}{2}) \rangle = 0$, we have no information about the global phases of vectors $|\psi(k)\rangle$ at all. It is not obvious that the integral in (3.72) even converges. However, we show later that it does, assuming that σ^2 is small enough and we can use certain approximations.

We claim that the state $|\xi_z\rangle$ under the evolution governed by H behaves as a wave packet moving in the negative direction of X-axis (the line) with momentum $\frac{8}{n+2}$. In order to show that, we consider two cases: one, when the time of the evolution is small, and other, when the time is asymptotically large.

3.3.1 Short-time approximation

The time evolution of $|\xi_z\rangle$ is given by

$$e^{-\mathrm{i}Ht}|\xi_z\rangle = c_\sigma \int_{-\frac{\pi}{2}}^{\frac{3\pi}{2}} e^{-\frac{(k-\frac{\pi}{2})^2}{2\sigma^2}} e^{-\mathrm{i}kz} e^{-\mathrm{i}t\lambda(k)} \, |\tilde{k}\rangle \otimes |\psi(k)\rangle \, \mathrm{d}k. \tag{3.73}$$

When σ is small, the most contribution to the integral in (3.73) comes from the values k which are close to $\frac{\pi}{2}$. Because of that, we choose to use a first order approximation and approximate $|\psi(k)\rangle$ by $|\psi(\frac{\pi}{2})\rangle + (k-\frac{\pi}{2})|\psi'(\frac{\pi}{2})\rangle$ and $\lambda(k)$ by $\lambda(\frac{\pi}{2}) + (k-\frac{\pi}{2})\lambda'(\frac{\pi}{2})$. (We could use a second order approximation instead, and it would not complicate things too much since we already know that $\lambda''(\frac{\pi}{2}) = 0$. Careful, but relatively simple derivations similar to those in Section 3.2.3 can give us the expression for $|\psi''(\frac{\pi}{2})\rangle$.) Our approximation is valid when the time t is not too large and we still have $e^{\mathrm{i}t\lambda(k)} \approx e^{\mathrm{i}t(\,\lambda(\frac{\pi}{2}) + (k-\frac{\pi}{2})\lambda'(\frac{\pi}{2})\,)}$ for the values of k which give considerable contribution to (3.73). The upper bound for such t is yet unknown.

Let $|\psi^{(0)}\rangle = |\psi(\frac{\pi}{2})\rangle$, $|\psi^{(1)}\rangle = |\psi'(\frac{\pi}{2})\rangle$, $\lambda^{(0)} = \lambda(\frac{\pi}{2})$ and $\lambda^{(1)} = \lambda'(\frac{\pi}{2})$. Similarly, for a hat vector $|\widehat{m}\rangle$, which is k-dependent, let $|\widehat{m}^{(0)}\rangle$ denote its value at $k = \frac{\pi}{2}$ and let $|\widehat{m}^{(1)}\rangle$ denote the value of its derivative at $k = \frac{\pi}{2}$, where $m \in [0\,..\,2^n - 1]$. Note that $\{\, |\widehat{m}^{(0)}\rangle \,:\, m \in [0\,..\,2^n - 1] \,\}$ is an orthonormal basis. In Section 3.2.3 we showed $\lambda^{(0)} = 0$, $\lambda^{(1)} = -\frac{8}{n+2}$,

$$|\psi^{(0)}\rangle = \sqrt{\frac{2}{n+2}} \left(|\widehat{0}^{\,(0)}\rangle + \sum_{\substack{y=2 \\ y \text{ is even}}}^{n} \mathrm{i}^y \, |\widehat{2^{y-1}\,^{(0)}}\rangle \right) \tag{3.74}$$

and

$$|\psi^{(1)}\rangle = \sqrt{\frac{2}{n+2}} \left(\frac{2}{n+2} \sum_{\substack{y=2 \\ y \text{ is even}}}^{n} \mathrm{i}^y \, y \, |\widehat{2^{y-2}\,^{(0)}}\rangle - \sum_{\substack{y=0 \\ y \text{ is even}}}^{n-2} \sum_{j=1}^{n-y-1} \mathrm{i}^{y-j} |\widehat{2^y(2^{j+1} - 1)\,^{(0)}}\rangle \right), \tag{3.75}$$

for which we have

$$\langle\psi^{(0)}|\psi^{(0)}\rangle = 1, \quad \langle\psi^{(0)}|\psi^{(1)}\rangle = 0 \quad \text{and} \quad \langle\psi^{(1)}|\psi^{(1)}\rangle = \frac{n(3n^2 + 14n + 8)}{6(n+2)^2} \approx \frac{n}{2}. \tag{3.76}$$

Let $\kappa = k - \frac{\pi}{2}$. Hence

$$\begin{aligned}
e^{-\mathrm{i}Ht}|\xi_z\rangle &\approx c_\sigma \int_{-\frac{\pi}{2}}^{\frac{3\pi}{2}} e^{-\frac{(k-\frac{\pi}{2})^2}{2\sigma^2}} e^{-\mathrm{i}kz} e^{\mathrm{i}t(k-\frac{\pi}{2})\frac{8}{n+2}} |\tilde{k}\rangle \otimes \Big(|\psi^{(0)}\rangle + \big(k-\frac{\pi}{2}\big)|\psi^{(1)}\rangle\Big)\,\mathrm{d}k \\
&= \frac{c_\sigma}{\sqrt{2\pi}} \sum_{x\in\mathbb{Z}} \mathrm{i}^{x-z}|x\rangle \otimes \int_{-\pi}^{\pi} e^{-\frac{\kappa^2}{2\sigma^2}} e^{\mathrm{i}(x-z+\frac{8}{n+2}t)\kappa} \Big(|\psi^{(0)}\rangle + \kappa|\psi^{(1)}\rangle\Big)\,\mathrm{d}\kappa \\
&= \frac{c_\sigma}{\sqrt{2\pi}} \sum_{x\in\mathbb{Z}} \mathrm{i}^{x-z}\sqrt{2\pi}\sigma e^{-\frac{\left(x-z+\frac{8}{n+2}t\right)^2}{2/\sigma^2}} \mathrm{erf}\Big(\frac{\pi}{\sqrt{2}\sigma}\Big)|x\rangle \otimes |\psi^{(0)}\rangle \\
&- \frac{c_\sigma}{\sqrt{2\pi}} \sum_{x\in\mathbb{Z}} \mathrm{i}^{x-z} 2\mathrm{i}\sigma^2 e^{-\frac{\pi^2}{2\sigma^2}} \sin\Big(\pi\big(x-z+\frac{8t}{n+2}\big)\Big)|x\rangle \otimes |\psi^{(1)}\rangle \\
&+ \frac{c_\sigma}{\sqrt{2\pi}} \sum_{x\in\mathbb{Z}} \mathrm{i}^{x-z}\mathrm{i}\sqrt{2\pi}\sigma^3 \Big(x-z+\frac{8t}{n+2}\Big) e^{-\frac{\left(x-z+\frac{8}{n+2}t\right)^2}{2/\sigma^2}} \mathrm{erf}\Big(\frac{\pi}{\sqrt{2}\sigma}\Big)|x\rangle \otimes |\psi^{(1)}\rangle \\
&\approx c_\sigma \sum_{x\in\mathbb{Z}} \mathrm{i}^{x-z}\sigma e^{-\frac{\left(x-z+\frac{8}{n+2}t\right)^2}{2(1/\sigma)^2}} |x\rangle \otimes \left(|\psi^{(0)}\rangle + \mathrm{i}\sigma^2\big(x-z+\frac{8t}{n+2}\big)|\psi^{(1)}\rangle\right),
\end{aligned} \tag{3.77}$$

where we use integrals (2.9) and (2.10), and the last approximation is due to the fact that $e^{-\frac{\pi^2}{2\sigma^2}}$ and $1 - \mathrm{erf}(\frac{\pi}{\sqrt{2}\sigma})$ rapidly decreases as σ decreases; for $\sigma = 1$ we already have $e^{-\frac{\pi^2}{2}} = 0.0072$ and $\mathrm{erf}(\frac{\pi}{\sqrt{2}}) = 0.9983$.

We can see that for small σ the state $|\xi_z\rangle$ corresponds to the superposition of snakes which are concentrated around the position z on the line, and then, as time passes, this superposition moves in the negative direction of X-axis with momentum $\frac{8}{n+2}$. Since $\langle\psi^{(0)}|\psi^{(1)}\rangle = 0$, $\langle\psi^{(0)}|\psi^{(0)}\rangle = 1$ and $\langle\psi^{(1)}|\psi^{(1)}\rangle \approx \frac{n}{2}$, we have

$$\begin{aligned}
\langle\xi_z|\xi_z\rangle &\approx \sigma^2 c_\sigma^2 \sum_{x-z\in\mathbb{Z}} e^{-(x-z)^2\sigma^2}(1 + (x-z)^2\sigma^4 n/2) \\
&\approx \sigma^2 c_\sigma^2 \int_{-\infty}^{\infty} e^{-x^2\sigma^2}(1 + x^2\sigma^4 n/2)\,\mathrm{d}x \\
&= \sigma^2 c_\sigma^2 (\sqrt{\pi}/\sigma + n\sqrt{\pi}\sigma/4),
\end{aligned} \tag{3.78}$$

which gives us $c_\sigma \approx 1/\sqrt{\sigma(1 + n\sigma^2/4)\sqrt{\pi}}$. We choose $\sigma \in \Omega(1/\operatorname{poly} n)$ small enough so that we can ignore the term corresponding to the vector $|\psi^{(1)}\rangle$ in (3.77). In that case, $|\xi_z\rangle$ looks like a Gaussian-shaped wave packet of length $c/\sigma \in O(\operatorname{poly} n)$, where c is a constant; that is, $|\xi_z\rangle$ can be well approximated with a state $\sum_{x=z-c/\sigma}^{z+c/\sigma} \alpha_x|x\rangle \otimes |\psi^{(0)}\rangle$ for some amplitudes α_x. The fact that this state 'occupies' only a polynomial length interval of the line is important for algorithmic purposes.

3.3.2 Asymptotic approximation

Now we want to show that the same type of motion with momentum $\frac{8}{n+2}$ remains even when we do not restrict ourselves to small values of the time t. A good way how to describe a location of the snake after time t would be to calculate the norm of the vector $(\langle x| \otimes \mathbb{I})e^{-\mathrm{i}Ht}|\xi_z\rangle$ for every value $x \in \mathbb{Z}$. Unfortunately, this seems to be a hard thing to do because we do not know the value of $\langle\psi(k_1)|\psi(k_2)\rangle$ for $k_1 \neq k_2$ (and this value depends on how we choose the global phase of $|\psi(k)\rangle$). We already know that the state $|\xi_x\rangle$ is concentrated on the line around the position x, therefore we choose to calculate $\langle\xi_x|e^{-\mathrm{i}Ht}|\xi_z\rangle$, where $x \in \mathbb{Z}$, instead.

Let $x = z + \omega t$, and let us think of ω as the momentum. We have the following:

$$\begin{aligned}\langle\xi_{z+\omega t}|e^{-\mathrm{i}Ht}|\xi_z\rangle =& c_\sigma \int_{-\frac{\pi}{2}}^{\frac{3\pi}{2}} e^{-\frac{(k_1-\frac{\pi}{2})^2}{2\sigma^2}} e^{\mathrm{i}k_1(z+\omega t)} \langle\tilde{k_1}| \otimes \langle\psi(k_1)| \,\mathrm{d}k_1 \\ & \cdot c_\sigma \int_{-\frac{\pi}{2}}^{\frac{3\pi}{2}} e^{-\frac{(k_2-\frac{\pi}{2})^2}{2\sigma^2}} e^{-\mathrm{i}\lambda(k_2)t} e^{-\mathrm{i}k_2 z} |\tilde{k_2}\rangle \otimes |\psi(k_2)\rangle \,\mathrm{d}k_2 \\ =& c_\sigma^2 \int_{-\frac{\pi}{2}}^{\frac{3\pi}{2}} e^{-\frac{(k-\frac{\pi}{2})^2}{\sigma^2}} e^{\mathrm{i}t(\omega k - \lambda(k))} \,\mathrm{d}k. \end{aligned} \tag{3.79}$$

When t is large, $e^{\mathrm{i}t(\omega k-\lambda(k))}$ rapidly changes as $f(k) = \omega k - \lambda(k)$ changes. This means that in an interval where $f(k)$ changes the contribution from adjacent subintervals to the integral (3.79) nearly cancels out [25]. Therefore the most contribution to the integral comes from values of k where the function $f(k)$ is stationary, that is, where $f'(k) = 0$. The method of stationary phase approximation makes this statement more rigorous, therefore let us present this method here.

Consider an integral

$$I(k) = \int_a^b g(k) e^{\mathrm{i}tf(k)} \,\mathrm{d}k, \tag{3.80}$$

where $g(k)$ and $f(k)$ are smooth real-valued functions in the interval $[a, b]$, $g(a) \neq 0$, and t is some large argument. We call k_0 a stationary point of $f(k)$ of order q if $f'(k_0) = f''(k_0) = \ldots = f^{(q)}(k_0) = 0$ and $f^{(q+1)}(k_0) \neq 0$. The method of stationary phase approximation states [3, 25]:

- if there are no stationary points of any order in the interval $[a, b]$, then

$$I(k) \in o(1/t^d) \tag{3.81}$$

  for any $d \in \mathbb{R}$;

- if a is a stationary point of order $q - 1$ and there are no other stationary points in the interval $[a, b]$ of order $q - 1$ or higher, then

$$I(k) \approx g(a)\, e^{\mathrm{i}tf(a)\pm\mathrm{i}\frac{\pi}{2q}} \sqrt[q]{\frac{q!}{\pm t f^{(q)}(a)}}\, \frac{\Gamma(1/q)}{q}, \tag{3.82}$$

  where Γ is the Gamma function and $f^{(q)}(a) = \pm|f^{(q)}(a)|$.

Any integral of form (3.80) may be expressed as a sum of multiple integrals such that for each of them one of the two above cases applies.

Now let us use the method of stationary phase approximation for (3.79), the integral of our interest; we have $f_\omega(k) = \omega k - \lambda(k)$ and $g(k) = e^{-\frac{(k-\frac{\pi}{2})^2}{\sigma^2}}$, where we use the subscript ω to clarify which momentum we are talking about and we ignore the normalizing constant c_σ^2. From Section 3.2.2 we have $\lambda'(\pm\frac{\pi}{2}) = \mp\frac{8}{n+2}$ and $\lambda'''(\pm\frac{\pi}{2}) = \pm\frac{8(3n^2+4)}{(n+2)^3} \approx \pm\frac{24}{n}$. Because we do not know much about the function $\lambda(k)$, let us assume Hypothesis 3.6, which, first of all, implies that $\lambda'(k) \in [-\frac{8}{n+2}, \frac{8}{n+2}]$ for all $k \in \mathbb{R}$. Since $\lambda(k) = \lambda(-k)$, we have

$$\begin{array}{lll} f_\omega(k) = \omega k - \lambda(k) & \text{and} & f_\omega(-k) = -\omega k - \lambda(k), \\ f'_\omega(k) = \omega - \lambda'(k) & \text{and} & (f_\omega(-k))' = -\omega - \lambda'(k), \\ f''_\omega(k) = -\lambda''(k) & \text{and} & (f_\omega(-k))'' = -\lambda''(k), \\ f'''_\omega(k) = -\lambda'''(k) & \text{and} & (f_\omega(-k))''' = -\lambda'''(k). \end{array} \tag{3.83}$$

We consider four following cases.

- If $\omega \notin [-\frac{8}{n+2}, \frac{8}{n+2}]$, then $f'_\omega(k) \neq 0$ for all k, and therefore $f_\omega(k)$ has no stationary points. This, according to (3.81), implies that

$$\int_{-\frac{\pi}{2}}^{\frac{3\pi}{2}} g(k)\, e^{\mathrm{i}t f_\omega(k)}\, \mathrm{d}k \in o(1/t^d) \tag{3.84}$$

  for any $d \in \mathbb{R}$, which basically means that no part of the wave packet moves faster than with momentum $\frac{8}{n+2}$. To be more precise, there might be a part which moves faster, but stays orthogonal to $|\xi_y\rangle$ for all $y \in \mathbb{Z}$.

- If $\omega = -\frac{8}{n+2}$, then $k = \frac{\pi}{2}$ is the unique stationary point of $f_\omega(k)$ in the interval $[-\frac{\pi}{2}, \frac{3\pi}{2}]$, having order 2. (3.82) and (3.83) give us

$$\begin{aligned} \int_{-\frac{\pi}{2}}^{\frac{3\pi}{2}} g(k)\, e^{\mathrm{i}t f_\omega(k)}\, \mathrm{d}k &= \int_{-\frac{\pi}{2}}^{\frac{\pi}{2}} g(-k)\, e^{\mathrm{i}t f_\omega(-k)}\, \mathrm{d}k + \int_{\frac{\pi}{2}}^{\frac{3\pi}{2}} g(k)\, e^{\mathrm{i}t f_\omega(k)}\, \mathrm{d}k \\ &\approx e^{\mathrm{i}t\frac{24}{n} + \mathrm{i}\frac{\pi}{6}} \sqrt[3]{\frac{3!}{t\frac{24}{n}}}\, \frac{\Gamma(1/3)}{3} + e^{-\mathrm{i}t\frac{24}{n} - \mathrm{i}\frac{\pi}{6}} \sqrt[3]{\frac{3!}{t\frac{24}{n}}}\, \frac{\Gamma(1/3)}{3} \\ &\approx 1.125 \cos\left(\frac{24t}{n} + \frac{\pi}{6}\right) \frac{1}{\sqrt[3]{t/n}}\,. \end{aligned} \tag{3.85}$$

- If $\omega = \frac{8}{n+2}$, then $k = -\frac{\pi}{2}$ and $k = \frac{3\pi}{2}$ are the only two stationary points of $f_\omega(k)$ in the interval $[-\frac{\pi}{2}, \frac{3\pi}{2}]$, both having order 2. Similarly as for $\omega = -\frac{8}{n+2}$ we get

$$\begin{aligned} \int_{-\frac{\pi}{2}}^{\frac{3\pi}{2}} g(k)\, e^{\mathrm{i}t f_\omega(k)}\, \mathrm{d}k &= \int_{-\frac{\pi}{2}}^{\frac{\pi}{2}} g(k)\, e^{\mathrm{i}t f_\omega(k)}\, \mathrm{d}k + \int_{-\frac{3\pi}{2}}^{-\frac{\pi}{2}} g(-k)\, e^{\mathrm{i}t f_\omega(-k)}\, \mathrm{d}k \\ &\approx 1.125\, e^{-\frac{\pi^2}{\sigma^2}} \cos\left(\frac{24t}{n} + \frac{\pi}{6}\right) \frac{1}{\sqrt[3]{t/n}}\,, \end{aligned} \tag{3.86}$$

which is almost 0, because the factor $e^{-\frac{\pi^2}{\sigma^2}}$ is very small for small σ (for $\sigma = 1$ it is already $5.172 \cdot 10^{-5}$).

- If $\omega \in (-\frac{8}{n+2}, \frac{8}{n+2})$, then $f'_\omega(k) = \omega - \lambda'(k) = 0$ has exactly two solutions in the interval $[-\frac{\pi}{2}, \frac{3\pi}{2}]$: they are $\frac{\pi}{2} + \kappa_\omega$ and $\frac{\pi}{2} - \kappa_\omega$ for some $\kappa_\omega > 0$, and the order of these two stationary points is 1. That is so due to the fact that, according to Hypothesis 3.6, $\lambda'(k)$ strictly decreases in the interval $(-\frac{\pi}{2}, \frac{\pi}{2})$ and increases in the interval $(\frac{\pi}{2}, \frac{3\pi}{2})$, and $\lambda(\frac{\pi}{2} - \kappa) = -\lambda(\frac{\pi}{2} + \kappa)$ implies $\lambda'(\frac{\pi}{2} - \kappa) = \lambda'(\frac{\pi}{2} + \kappa)$ for all κ. Let $\lambda^{(2)}_\omega = \lambda''(\frac{\pi}{2} + \kappa_\omega) > 0$. Since $\lambda''(-\frac{\pi}{2} - \kappa_\omega) = \lambda''(\frac{\pi}{2} + \kappa_\omega) = -\lambda''(\frac{\pi}{2} - \kappa_\omega) = -\lambda''(-\frac{\pi}{2} + \kappa_\omega)$, we have

$$\begin{aligned}
&\int_{-\frac{\pi}{2}}^{\frac{3\pi}{2}} g(k)\, e^{\mathrm{i}tf_\omega(k)}\, \mathrm{d}k \\
&= \int_{-\frac{\pi}{2}+\kappa_\omega}^{\frac{\pi}{2}} g(-k)\, e^{\mathrm{i}tf_\omega(-k)}\, \mathrm{d}k + \int_{\frac{\pi}{2}-\kappa_\omega}^{\frac{\pi}{2}} g(k)\, e^{\mathrm{i}tf_\omega(k)}\, \mathrm{d}k \\
&+ \int_{-\frac{\pi}{2}-\kappa_\omega}^{-\frac{\pi}{2}} g(-k)\, e^{\mathrm{i}tf_\omega(-k)}\, \mathrm{d}k + \int_{\frac{\pi}{2}+\kappa_\omega}^{\frac{3\pi}{2}} g(k)\, e^{\mathrm{i}tf_\omega(k)}\, \mathrm{d}k \\
&\approx 5.013\, e^{\frac{-\kappa_\omega^2}{\sigma^2}}\, \cos(t\lambda^{(2)}_\omega + \pi/4) \frac{1}{\sqrt{t\lambda^{(2)}_\omega}}.
\end{aligned} \tag{3.87}$$

  In order to analyze this quantity, it is useful to look at Figure 3.5 on page 25. When ω is close to $-\frac{8}{n+2}$, κ_ω is close to 0 and so is $\lambda^{(2)}_\omega$. Thus, the value of (3.87) is likely to be close to the value of (3.85). However, $\lambda^{(2)}_\omega$ increases as ω moves further from $-\frac{8}{n+2}$ because $\lambda'''(k)$ is relatively large for k close to $\frac{\pi}{2}$ (see Hypothesis 3.6). Also, since $(n+2)|\lambda''(k)| \leq 8$ by Hypothesis 3.6, we have $\kappa_\omega > (\omega - (-\frac{8}{n+2}))/\frac{8}{n+2} = \frac{n+2}{8}\omega + 1$. Therefore, the value of the integral (3.87) exponentially decays as $\omega + \frac{8}{n+2}$ increases.

Hence, if we restrict our interest to the projection of the state $e^{-\mathrm{i}Ht}|\xi_z\rangle$ on the space $\mathcal{X} = \mathrm{span}\{|\xi_x\rangle : x \in \mathbb{Z}\}$, then we see a wave packet which moves in the negative direction of X-axis with momentum $\frac{8}{n+2}$. Let us call this projection $|\xi_z\rangle_{t,\mathcal{X}}$. The norm of $|\xi_z\rangle_{t,\mathcal{X}}$ can be shown to be in $\Omega(1/\operatorname{poly} n)$ assuming that $\sigma \in \Omega(1/\operatorname{poly} n)$ and that we can use the approximation $\cos^2(t\lambda^{(2)}_{\omega_x} + \pi/4) \approx 1/2$ in the sum

$$\sum_{\substack{x=-\frac{8}{n+2}t \\ \Delta x \,|\, x}}^{x=-\frac{8}{n+2}t} \left(5.013\, e^{\frac{-\kappa^2_{\omega_x}}{\sigma^2}}\, \cos(t\lambda^{(2)}_{\omega_x} + \pi/4) \frac{1}{\sqrt{t\lambda^{(2)}_{\omega_x}}} \right)^2 \leq || \, |\xi_z\rangle_{t,\mathcal{X}} \, ||^2, \tag{3.88}$$

where $\Delta x \in \mathbb{N}$ is a constant and $\omega_x = (x - z)/t$, which seems a reasonable approximation to make since t is large. The gap Δx appears in the sum (3.88) because we cannot sum over all consecutive values of x due to the fact that $\{|\xi_x\rangle : x \in \mathbb{Z}\}$ is not an orthogonal basis of $\mathcal{X}$. Hence, assuming Hypothesis 3.6 and that we can use $\cos^2(t\lambda^{(2)}_{\omega_x} + \pi/4) \approx 1/2$ in (3.88), a substantially large part of the initial state $|\xi_z\rangle$ propagates as a wave packet with momentum $\frac{8}{n+2}$.

However, it might as well be the case that the norm of $|\xi_z\rangle_{t,\mathcal{X}}$ is 1. That would be the case if $\Pi = \int_0^{2\pi} |\tilde{k}\rangle\langle\tilde{k}| \otimes |\psi(k)\rangle\langle\psi(k)| \,\mathrm{d}k$ were the projector on the space $\mathcal{X}$, because it can be easily seen that $\Pi\, e^{-\mathrm{i}Ht}|\xi_z\rangle = e^{-\mathrm{i}Ht}|\xi_z\rangle$. We could also consider what are the inner products between $e^{-\mathrm{i}Ht}|\xi_z\rangle$ and elements of the set

$$\left\{ \int_{\mu-\pi}^{\mu+\pi} e^{-\frac{(k-\mu)^2}{2\sigma_2^2}} e^{-\mathrm{i}kx} \,|\tilde{k}\rangle \otimes |\psi(k)\rangle \,\mathrm{d}k \,:\, x \in \mathbb{Z}, \sigma_2 \in \mathbb{R}, \mu \in [-\pi/2, 3\pi/2] \right\}, \tag{3.89}$$

because it seems that vectors from this set span the space Π projects to (consider $\sigma_2 \to 0$).

3.3.3 Span of a snake

Definition. Let $s = (v_0, \ldots, v_n) \in \mathbb{Z}^{n+1}$ be a snake on the line. We define the *span* of s to be the pair $\mu(s) = (s_m, s_M) = (\min(v_0, \ldots, v_n), \max(v_0, \ldots, v_n))$, and the *span length* of s to be $\bar{\mu}(s) = s_M - s_m$.

This definition easily generalizes to superpositions over snakes: for a unit vector $|\chi\rangle \in \mathbb{C}^{S_n(G)}$ let the span of $|\chi\rangle$ be a random variable $\mu(|\chi\rangle)$ which for every pair $(t_m, t_M) \in \mathbb{Z}^2$ assigns the probability that in the event of measuring $|\chi\rangle$ in the standard basis $\{|s\rangle \,:\, s \in S_n(G)\}$ we obtain a snake s such that $\mu(s) = (t_m, t_M)$. Similarly we define $\bar{\mu}(|\chi\rangle)$, the span length of $|\chi\rangle$, which is an integer-valued random variable. For algorithmic purposes described in Chapter 4 we are interested that the span length of $|\xi_z\rangle$ is large. To be more precise, we want that with probability $\Omega(1/\operatorname{poly} n)$ we have $n \in O(\operatorname{poly} \bar{\mu}(|\xi_z\rangle))$.

Now again let us consider every snake s to be given as a pair $s = (x, j) \in \mathbb{Z} \times \{0,1\}^n$. The span length of s is determined by j alone. That is,

$$\bar{\mu}(j) = \bar{\mu}(s) = \left(\max\left\{ -\sum_{b=1}^{l} (-1)^{j_b} \,:\, l \in [0\,..\,n] \right\} - \min\left\{ -\sum_{b=1}^{l} (-1)^{j_b} \,:\, l \in [0\,..\,n] \right\} \right). \tag{3.90}$$

Hence, $\bar{\mu}(j) \geq |\,2||j||_1 - n\,|$ holds for every $j \in \{0,1\}^n$. Again, let us generalize it for superpositions: for $|\psi\rangle \in \mathbb{C}^{\{0,1\}^n}$ let us define $\bar{\mu}(|\psi\rangle) = \bar{\mu}(|\upsilon\rangle \otimes |\psi\rangle)$, where $|\upsilon\rangle \in \mathbb{C}^{\mathbb{Z}}$ can be chosen arbitrarily.

In Section 3.3.1 we show that we can choose σ small enough, but still in $\Omega(1/\operatorname{poly} n)$, so that $|\xi_z\rangle \approx |\upsilon_z\rangle \otimes |\psi^{(0)}\rangle$, where $|\upsilon_z\rangle \in \mathbb{C}^{\mathbb{Z}}$ and $|\psi^{(0)}\rangle$ is given on page 27. We have

$$\begin{aligned} |\psi^{(0)}\rangle &= \sqrt{\frac{2}{n+2}} \left(|\widehat{0}^{\,(0)}\rangle + \sum_{\substack{y=2 \\ y \text{ is even}}}^{n} \mathrm{i}^y \, |\widehat{2^{y-1}\,(0)}\rangle \right) \\ &= (-\mathrm{i})^{n+1} \sqrt{\frac{2}{n+2}} \sum_{l=0}^{n/2} (|-\rangle \otimes |-\rangle)^{\otimes \frac{n}{2}-l} (|+\rangle \otimes |+\rangle)^{\otimes l} \end{aligned} \tag{3.91}$$

(the expressions for $|\widehat{0}^{\,(0)}\rangle$, $|\widehat{2}^{\,(0)}\rangle$, $|\widehat{8}^{\,(0)}\rangle$ etc. are from (3.65)).

Let $p(j) = |\langle j|\psi^{(0)}\rangle|^2$ and $q(j) = 1/2^n$ be two probability distributions. Numerical results suggest that the trace distance between them $||p-q||_1$ is quite precisely 1, which which would mean that $E(\bar{\mu}(|\psi^{(0)}\rangle)) \in \Omega(\sqrt{n})$. Instead of trying to prove that this holds, let us do something easier which is still sufficient for our purposes: in the case where 4 divides n, we have $|\langle j|\psi^{(0)}\rangle|^2 \geq \frac{1}{2^n}\frac{2}{n+2}$ for all $j \in \{0,1\}^n$; therefore with probability at least $\frac{1}{n+2}$ we have $\bar{\mu}(|\psi^{(0)}\rangle) \geq c\sqrt{n}$ for some constant c ($\sqrt{n}$ comes from the standard deviation of the binomial distribution). Since $\bar{\mu}(|\xi_z\rangle) \approx \bar{\mu}(|\psi^{(0)}\rangle)$, with probability $\Omega(1/n)$ the span length $\bar{\mu}(|\xi_z\rangle)$ is large enough.

It might be the case that a more general result holds, that is, it might be that $E(\bar{\mu}(|\psi(k)\rangle)) \in \Omega(\sqrt{n})$ for all k. That, in turn, (using the partial trace) would imply that $E(\bar{\mu}(|\xi_z\rangle)) \in \Omega(\sqrt{n})$ for an arbitrary choice of σ (when we cannot make certain approximations). However, we do not try to prove it here.

3.3.4 Other momenta and other eigenvalues

We have shown that there is an initial state of the continuous-time quantum snake walk on the line which, under certain assumptions, propagates as a wave packet moving with momentum $-\frac{8}{n+2}$ in the positive direction (therefore the minus sign) of X-axis, assuming n is even. However, it seems that for any chosen ω in $[-\frac{8}{n+2}, \frac{8}{n+2}]$ there is an initial state which propagates with momentum ω, similarly as it is in the case of the regular continuous-time quantum walk on the line (see Section 2.1.2). At least, when the time of the evolution is small. Indeed, choose $k_\omega \in [\frac{\pi}{2}, \frac{3\pi}{2}]$ such that $\lambda'(k_\omega) = \omega$, and for small σ consider a state

$$|\xi_\omega\rangle = c_\sigma \int_{k_\omega-\pi}^{k_\omega+\pi} e^{-\frac{(k-k_\omega)^2}{2\sigma^2}} |\tilde{k}\rangle \otimes |\psi(k)\rangle \,\mathrm{d}k \tag{3.92}$$

and its time evolution

$$\begin{aligned} e^{-\mathrm{i}Ht}|\xi_\omega\rangle &\approx c_\sigma \int_{k_\omega-\pi}^{k_\omega+\pi} e^{-\frac{(k-k_\omega)^2}{2\sigma^2}} e^{-\mathrm{i}t(\lambda_\omega^{(0)}+(k-k_\omega)\omega)} |\tilde{k}\rangle \otimes \Big(|\psi_\omega^{(0)}\rangle + \big(k-k_\omega\big)|\psi_\omega^{(1)}\rangle\Big) \,\mathrm{d}k \\ &= \frac{c_\sigma e^{-\mathrm{i}t\lambda_\omega^{(0)}}}{\sqrt{2\pi}} \sum_{x\in\mathbb{Z}} e^{\mathrm{i}k_\omega x}|x\rangle \otimes \int_{-\pi}^{\pi} e^{-\frac{\kappa^2}{2\sigma^2}} e^{\mathrm{i}(x-\omega t)\kappa} \Big(|\psi_\omega^{(0)}\rangle + \kappa|\psi_\omega^{(1)}\rangle\Big) \,\mathrm{d}\kappa \end{aligned} \tag{3.93}$$

where $\kappa = k - k_\omega$ and we use approximations $\lambda(k) \approx \lambda_\omega^{(0)} + (k-k_\omega)\omega$ and $|\psi(k)\rangle \approx |\psi_\omega^{(0)}\rangle + (k-k_\omega)|\psi_\omega^{(1)}\rangle$, $\lambda_\omega^{(0)} = \lambda(k_\omega)$, $|\psi_\omega^{(0)}\rangle = |\psi(k_\omega)\rangle$ and $|\psi_\omega^{(1)}\rangle = |\psi'(k_\omega)\rangle$. By doing similar derivations to (3.93) as we do in (3.77) we can see that $|\xi_\omega\rangle$ propagates as a wave packet moving in the positive direction of X-axis with momentum ω. (Without loss of generality we can assume that $|\psi_\omega^{(0)}\rangle$ and $|\psi_\omega^{(1)}\rangle$ are orthogonal, yet we do not know what is the norm of $|\psi_\omega^{(1)}\rangle$.) This analysis is far from being rigorous, and more work is required in the future.

We also do not need to restrict ourselves to the median eigenvalue and restrict n to be even. We can easily use (3.92) and (3.93) for any of $n+1$ k-dependent eigenvalues and their corresponding eigenvectors, as far as the derivative of this eigenvalue has the value

ω at some point k_ω. The reason why we consider the median eigenvalue in more detail in the case when n is even is not only because it makes calculations easier, but also because this eigenvalue seems to have the largest range for the value of its derivative (see Figure 3.4), therefore we can construct initial states having highest momenta.

Regarding the span length: it is not clear what the span length of $|\xi_\omega\rangle$ is. We know that an eigenvector of $H_{n,k}$ corresponding to a k-dependent eigenvalue is a superposition of k-dependent vectors $|\widehat{0}\rangle$, $|\widehat{1}\rangle$, $|\widehat{2}\rangle$, $|\widehat{4}\rangle$, $|\widehat{8}\rangle$, etc. That would be really useful if we could show that for any such superposition the expected value of the span length is in $\Theta(\sqrt{n})$, since it would imply $E(\bar{\mu}(|\xi_\omega\rangle)) \in \Theta(\sqrt{n})$. So far we can neither prove nor disprove it.

This concludes our discussion about quantum snakes on the line. Later in Chapter 4 we show how the analysis of the quantum snake walk on the line can be useful for analyzing the quantum snake walk on the glued trees graph.

Chapter 4

Snakes on the glued trees graph

In this chapter we discuss how the continuous-time quantum snake walk might lead to an efficient algorithm solving the extended glued trees problem defined in Section 2.2. We say 'might' because we do not have an algorithm which provably works efficiently yet.

Recall that in the extended glued trees problem we are given a glued trees graph $G = (V, E)$ via a black-box oracle. The graph G consists of two complete binary trees of height N having roots r_1 and r_2, and the leaves of the trees are connected by a randomly chosen cycle of length $2 \cdot 2^N$. We are also given the label of the root r_1. Our aim is to obtain a path connecting r_1 to r_2. The complexity of the computation is measured in terms of how many oracle queries the algorithm makes, and we want it to be in $O(\text{poly}\, N)$.

In Section 4.1 we discuss several approaches how to solve the extended glued trees problem using the quantum snake walk. We also explain how to construct the initial state of the walk so that the behaviour of the walk does not depend on which cycle in particular glues the trees. This allows us to reduce the continuous-time quantum snake walk on a graph of our consideration (a slight modification of the glued trees graph) to the regular continuous-time quantum walk on some simpler graph. In Section 4.2 we present the Hamiltonian governing this simpler walk. Then in Sections 4.3 and 4.4 we show how this walk behaves under certain circumstances, and point out multiple similarities to the quantum snake walk on the line. We conclude by presenting an algorithm solving the extended glued trees problem, but without knowing anything about its efficiency.

Due to technical difficulties, the analysis used in Sections 4.3.2 and 4.4 are very approximate.

4.1 Potential approaches

The way we plan to tackle the extended glued trees problem is by running the continuous-time quantum snake walk started from some easily constructable initial superposition over snakes. What we hope for is that after running the quantum snake walk for a certain amount of time $t \in O(\text{poly}\, N)$ and measuring the state of the snake, with a high probability

we obtain a path which includes both r_1 and r_2, from which we then can extract a solution to the problem. Thus, we require that the length of the snake n is at least $2N + 1$.

One choice we have to make is which state to use as the initial state for the walk. First of all, not all states can be prepared efficiently, because preparing any superposition over snakes requires us to know the labels of all of their vertices. Plus, the evolution of many states depends on the structure of the cycle gluing the trees. In this section we show how to choose the initial state so that we do not need to worry about the latter, the dependence on the random cycle. After that we discuss how we can modify our graph, still using the same black-box oracle, so that we have more freedom in terms of which initial states we can choose from.

4.1.1 Glued trees graph alone

As we see in the Section 2.2, the regular quantum walk solving the glued trees problem always remains in a subspace spanned by certain superpositions. Therefore it is possible to reduce that walk to a walk on a much simpler graph, and the analysis of the walk does not have to depend on which cycle in particular glues the trees. Now we show that we can do the same for the quantum snake walk on the glued trees graph.

For every vertex $v \in V$ let $\delta(v) \in [0\,..\,2N + 1]$ denote the distance between v and the root r_1. Similarly as in the case of quantum snakes on the line (see Section 3.1), for every snake $s = (v_0, \ldots, v_n) \in V^{n+1}$ on G let us assign a pair $\eta(s) = (x, j) \in \mathbb{Z}_{2N+2} \times \{0, 1\}^n$ such that $x = \delta(v_0)$ and for $l \in [1\,..\,n]$ let $j_l \in \{0, 1\}$ be such that $\delta(v_l) = \delta(v_{l-1}) - (-1)^{j_l}$. The difference form the case of the line is that in this case every pair (x, j) corresponds to more than one snake. Let $S(x, j) = \{s \in S_n(G) : \eta(s) = (x, j)\}$, and let $|x, j\rangle$ denote the uniform superposition over the snakes of $S(x, j)$ (assuming $S(x, j) \neq \emptyset$).

Due to the symmetry among the snakes in a set $S(x', j')$, for any snake $s \in S(x', j')$ the number of snakes t in a set $S(x'', j'')$ for which $m_b(s, t)$ holds depends only on the values of x', x'', j' and j'', but not on which particular snake in $S(x', j')$ we consider (here primes do not denote derivatives as in the previous chapter). The same is true for $m_f(s, t)$. This, according to Lemma 2.2, implies that the subspace $\mathcal{Z} = \mathrm{span}(\{|x, j\rangle : S(x, j) \neq \emptyset\})$ is invariant under $A_n(G)$. As we can see, if we choose the initial state to be in the subspace $\mathcal{Z}$, the walk always stays in this subspace, and it proceeds exactly the same way for all possible cycles gluing the trees.

However, it is not obvious for which values of x and j we can prepare the superposition $|x, j\rangle$ efficiently. For a snake $s = (v_0, \ldots, v_n) \in S(x, j)$ let $\delta_{\mathrm{m}} = \min(\delta(v_0), \ldots, \delta(v_n))$ and $\delta_{\mathrm{M}} = \max(\delta(v_0), \ldots, \delta(v_n))$. It is easy to see that both δ_{m} and δ_{M} depend only on the values of x and j. We say that the snake is *stretched* if $\delta_{\mathrm{M}} - \delta_{\mathrm{m}} \in \Omega(N)$ and *folded* if $\delta_{\mathrm{M}} - \delta_{\mathrm{m}} \in O(\mathrm{poly}(\log N))$. Let X_q be the set of vertices which are at the distance q from the root r_1. Since all the vertices of the snake s are connected, for every $q \in [\delta_{\mathrm{m}}\,..\,\delta_{\mathrm{M}}]$ there is a vertex of s which is in X_q. Therefore, it is not clear if there is a way how to prepare the state $|x, j\rangle$ other than learning the labels of all the vertices in the sets $X_{\delta_{\mathrm{m}}}$, $X_{\delta_{\mathrm{m}}+1}$, $\ldots$, $X_{\delta_{\mathrm{M}}}$. But we can do it efficiently only if δ_{M} or $2N + 1 - \delta_{\mathrm{m}}$ is in $O(\mathrm{poly}(\log N))$. This highly restricts which initial superpositions we can start form. For example, for a state

$|x, j\rangle$ to be constructed in this manner efficiently we require snakes in $S(x, j)$ to be folded and therefore $\left|\sum_{l=a}^{b} (-1)^{j_l}\right| \in O(\mathrm{poly}(\log N))$ for all $1 \leq a \leq b \leq n$. But, in the end, we need to obtain a stretched snake, that is, a snake connecting r_1 to r_2. Nonetheless, these restrictions on the initial j can be lifted if we consider the glued trees graph being a part of a larger graph.

4.1.2 Glued trees graph with semi-infinite lines attached

There is a way to make the initial state of the walk be stretched. This requires us to introduce ancillary vertices. Let us attach a semi-infinite line to the root r_1, for which we can choose labels of vertices as we like. (In practice, we attach a finite line segment which is much longer than both the length of the snake n and the time for which we intend to run the walk, but length of which is still in $O(\mathrm{poly}\, N)$.) In order for labels of the original and the ancillary vertices not to overlap, we can add 0 and 1 in front of them, respectively. Then we can make any initial state on the semi-infinite line we like, including ones which correspond to stretched snakes, without querying the black-box oracle at all. (Technically we have defined what it means for a snake to be stretched only on the glued trees graph, but this definition can be generalized in the obvious way.)

We can make a wave packet described in Section 3.3, and make to move towards the glued trees graph with the momentum $\frac{8}{n+2}$ (again, under certain assumptions). Since we already have an efficient algorithm which finds the label of r_2, we can attach a semi-infinite line to the root r_2 as well, therefore making the graph more symmetric. Our hope is that the packet would propagate through the glued trees graph giving us a snake which connects r_1 and r_2.

In order to simulate the continuous-time quantum snake walk on this new graph we need an oracle which for every its vertex v, given as an input, outputs the list of vertices adjacent to v. But, since we already know the labels of r_1, r_2 and the ancillary vertices, we can implement such an oracle efficiently by using the black-box oracle of the glued trees graph as a subroutine.

The problem with this graph is that it seems to be hard to analyze how the snake walk behaves on it. The reason for that is that the attached lines introduces some irregularities. While each vertex in the glued trees graph has the degree 3, each vertex in the semi-infinite lines has the degree 2. It is not even clear if the wave packet (or another initial state we decide to use) gets through the part where the line connects to the tree; it might be reflected back. To overcome these problems we propose a bit more complex graph, but which seems to be much easier to analyze.

4.1.3 Expanded glued trees graph

For every vertex v of the glued trees graph G let $\bar{v}$ denote its label, which we assume is a bit string of length $L \in \Omega(N)$. We also assume that $w_\emptyset = 1 \ldots 1$ is not the label of any vertex. Suppose we have run the algorithm solving the original glued trees problem, and

now we know $\bar{r}_1$ and $\bar{r}_2$, the labels of both roots. Let $n \in O(\text{poly}\, N)$, as usual, be the length of the snake, $n \geq 2N + 1$, and let $M \in O(\text{poly}\, N)$ be such that $M \gg n + N$.

Now step by step we are going to construct a graph each vertex of which has a unique $M - N + 1 + L$ bit label. Let T_{tmp} be a complete binary tree of height $M - N - 1$. The unique $M - N + 1$ bit label of each vertex of T_{tmp} is assigned as follows. For an integer $a \in [1 \,..\, 2^{M-N+1} - 1]$ let $(a)_2$ be its binary representation using $M - N + 1$ bits. We assign the label $(1)_2$ to the root, and then, recursively, for every node having label $(a)_2$ we assign label $(2a)_2$ to one of its children, and $(2a+1)_2$ to the other. Therefore the vertices of T_{tmp} have labels $(1)_2, (2)_2, \ldots, (2^{M-N} - 1)_2$, and the distance between the root and the vertex with a label $(a)_2$ is $\lfloor \log_2(a) \rfloor$. Let T_1 also be a complete binary tree of height $M - N - 1$ obtained from T_{tmp} by simply adding $\bar{r}_1$ at the end of each label of T_{tmp}. (As an example, T_1 is shown in Figure 4.1 for the case when $M - N = 4$.) The same way we define a tree T_2, just by adding $\bar{r}_2$ instead of $\bar{r}_1$. The vertices of T_1 and T_2 have $M - N + 1 + L$ bit labels.

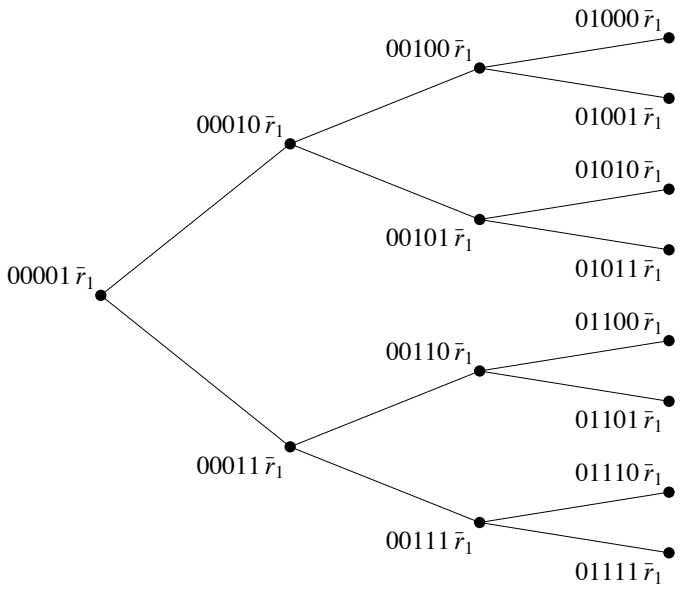

Figure 4.1: Tree T_1 when $M - N = 4$.

For every $a \in [2^{M-N} \,..\, 2^{M-N+1} - 1]$ let $G_{(a)}$ be the same as G just with a difference that we add $(a)_2$ in front of each label of G. This gives us 2^{M-N} graphs of this form. Now for every $a \in [2^{M-N-1} \,..\, 2^{M-N} - 1]$, let us connect:

- the leaf of T_1 having the label $(a)_2\bar{r}_1$ to the root of $G_{(2a)}$ having the label $(2a)_2\bar{r}_1$,
- the leaf of T_1 having the label $(a)_2\bar{r}_1$ to the root of $G_{(2a+1)}$ having the label $(2a+1)_2\bar{r}_1$,
- the leaf of T_2 having the label $(a)_2\bar{r}_2$ to the other root of $G_{(2a)}$ having the label $(2a)_2\bar{r}_2$,
- the leaf of T_2 having the label $(a)_2\bar{r}_2$ to the other root of $G_{(2a+1)}$ having the label $(2a+1)_2\bar{r}_2$.

This way we have obtained a graph G^M consisting of two complete binary trees of height M which are connected by 2^{M-N} cycles that alternates between the leaves of the two trees. We call G^M the *expanded glued trees graph*. For example, for the case $N = 2$ and $M = 4$, a glued trees graph G and the expanded graph G^M are shown in Figure 4.2.

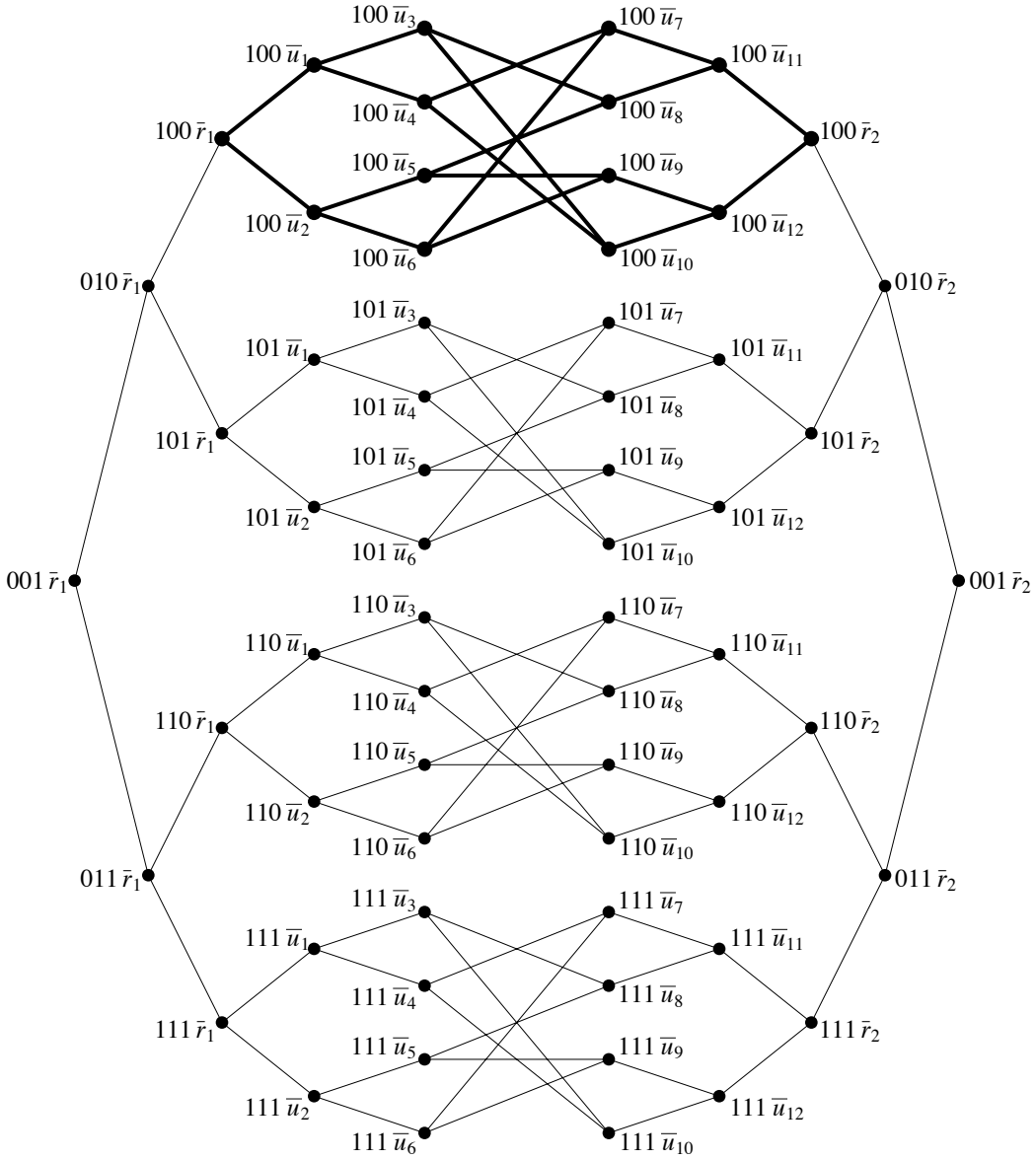

Figure 4.2: An expanded glued trees graph G^M for $N = 2$ and $M = 4$. A copy of the original glued trees graph G is shown using thick edges.

We need to implement the oracle which, given the label $\tilde{w} \in \{0,1\}^{M-N+1+L}$ of a vertex w of G^M, returns the list of three labels corresponding to vertices adjacent to w. In case $\tilde{w}$ is either $(1)_2\bar{r}_1$ or $(1)_2\bar{r}_2$, w has only two adjacent vertices, but this case can be easily checked and handled. Another special case is when $\tilde{w} = (a)_2\bar{r}$ for some $a \in [2^{M-N} .. 2^{M-N+1} - 1]$ and $r \in \{r_1, r_2\}$. The occurrence of this case can also be checked efficiently: it occurs whenever the first bit of $\tilde{w}$ is 1 and the last L bits are either $\bar{r}_1$ or $\bar{r}_2$. Let v_1 and v_2

be the two vertices adjacent to r in G. The oracle simply returns $(\lfloor a/2 \rfloor)_2\bar{r}$, $(a)_2\bar{v}_1$ and $(a)_2\bar{v}_2$. For the rest of the vertices we can distinguish two following cases. If the first bit of $\tilde{w}$ is 0, then $\tilde{w} = (a)_2\bar{r}$ for some $a \in [2\,..\,2^{M-N}-1]$ and $r \in \{r_1, r_2\}$, and the oracle returns $(\lfloor a/2 \rfloor)_2\bar{r}$, $(2a)_2\bar{r}$ and $(2a+1)_2\bar{r}$. But if the first bit is 1, then $\tilde{w} = (a)_2\bar{v}$ for some $a \in [2^{M-N}\,..\,2^{M-N+1}-1]$ and a vertex v of G. The oracle uses the black-box oracle of G to find the three vertices v_1, v_2 and v_3 adjacent to v, and returns $(a)_2\bar{v}_1$, $(a)_2\bar{v}_2$ and $(a)_2\bar{v}_3$. Hence, we can implement the oracle for G^M efficiently. This also allows us to simulate the continuous-time quantum snake walk on G^M efficiently.

The advantage of considering the walk on G^M rather than one on G is that, first of all, we do not need to worry what happens close to the roots of both trees, since we can choose M to be much larger than the time for how long we intend to run the walk. The exact value of M, as we show later, does not matter as long as we assume it is very large, and for analytical purposes it is useful to work in the limit $M \to \infty$. But most importantly, we know the labels of all vertices which are at distance up to $M-N$ from either root of G^M, that is, from a vertex with the label $(1)_2\bar{r}_1$ or $(1)_2\bar{r}_2$. This allows us to prepare a large variety of initial states efficiently. For that reason, from now on let us consider the continuous-time quantum snake walk on G^M.

4.2 Reduction to a simpler walk

Let R_1 be the root of G^M having the label $(1)_2\bar{r}_1$. The same way as for G, for any vertex w of G^M let $\delta(w)$ denote its distance from R_1 and let X_q be the set of all vertices w having $\delta(w) = q$. The structure of G^M is basically the same as the structure of G, except that instead of one cycle gluing the trees now we have many. However, the important thing is that cycles still connect each vertex in X_M to two vertices in X_{M+1} and vice versa (a vertex in X_{M+1} to two in X_M). This means that the subspace $\mathcal{Z} = \mathrm{span}(\,\{|x,j\rangle \,:\, S(x,j) \neq \emptyset\}\,) \subset \mathbb{C}^{S_n(G^M)}$, where $S(x,j)$ and $|x,j\rangle$ are defined the same way as for G (see Section 4.1.1), is invariant under $A_n(G^M)$. If we restrict ourselves to this subspace, the continuous-time quantum snake walks on the graph G^M and on a glued trees graph of height M are equal.

What we need to achieve here is that after a polynomial amount of time with a high probability we can obtain a snake for which at least one vertex is in X_{M-N}, and one in X_{M+N+1}. For every such a snake s there is a subgraph $G_{(a)}$, where $a \in [2^{M-N}\,..\,2^{M-N+1}-1]$, such that s goes through $G_{(a)}$ connecting both its roots having labels $(a)_2\bar{r}_1$ and $(a)_2\bar{r}_2$. Thus, knowing such a snake reveals us a path in G connecting r_1 and r_2.

Both the start vertex and the end vertex of a snake $s \in S_n(G^M)$ have 3 adjacent vertices; unless one of the two is a root of G^M, but we assume this is not the case for now. This means that there are three distinct snakes t such that $m_f(s,t)$ and three distinct snakes t such that $m_b(s,t)$ (two out of those six snakes can be equal, which is the case if and only if $s = (u,v,u,v,\ldots)$ for some vertices u and v). Let $x \in [1\,..\,2M]$ and $j_1, \ldots, j_n \in \{0,1\}$ be such that $s \in S(x, j_1 \ldots j_n)$. The snake s can move backward to one snake in $S(x-1, 1j_1 \ldots j_{n-1})$ and two in $S(x+1, 0j_1 \ldots j_{n-1})$ or, vice versa, two in $S(x-1, 1j_1 \ldots j_{n-1})$ and one in $S(x+1, 0j_1 \ldots j_{n-1})$. Which of those two is the case is determined by whether $x \leq M$ or

$x \geq M+1$. That is, if $x \leq M$, then the start vertex w_0 (which is at distance x from R_1) has one adjacent vertex closer to R_1 than w_0 (in terms of the distance) and two adjacent vertices which are further than w_0. The opposite happens if $x \geq M+1$. For $x', x'' \in [0\,..\,2M+1]$ and $j', j'' \in \{0,1\}^n$ let $m_b[\,(x', j'),\,(x'', j'')\,]$ be the number of snakes $s'' \in S(x'', j'')$ for which $m_b(s', s'')$, where s' is an arbitrary snake in $S(x', j')$ (due to symmetry, such a number always exists). The same way we define $m_f[\,(x', j'),\,(x'', j'')\,]$ using $m_f(s', s'')$ instead of $m_b(s', s'')$. We define $m_b[\,(x', j'),\,(x'', j'')\,] = m_f[\,(x', j'),\,(x'', j'')\,] = 0$ if $S(x', j') = \emptyset$ or $S(x'', j'') = \emptyset$, or both. We have

$$m_b[\,(x, j_1 \dots j_n),\,(x-1, 1 j_1 \dots j_{n-1})\,] = \begin{cases} 1 & \text{if } x \leq M \\ 2 & \text{if } x \geq M+1, \end{cases} \tag{4.1}$$

$$m_b[\,(x, j_1 \dots j_n),\,(x+1, 0 j_1 \dots j_{n-1})\,] = \begin{cases} 2 & \text{if } x \leq M \\ 1 & \text{if } x \geq M+1. \end{cases} \tag{4.2}$$

If x were 0 or $2M+1$, then the start vertex of the snake would have only two adjacent vertices, and only, respectively, (4.2) or (4.1) would hold.

For a binary vector $j \in \{0,1\}^l$ of length l let $|j|_\pm = -\sum_{y=1}^{l} (-1)^{j_y}$. Note that for all snakes in $S(x, j)$ the distance between their end vertices and R_1 is $x + |j|_\pm$. Something very similar as for backward motion also holds for forward motion: the snake s can move forward to one snake in $S(x - (-1)^{j_1}, j_2 \dots j_n 0)$ and two in $S(x - (-1)^{j_1}, j_2 \dots j_n 1)$ or vice versa. Which is the case now is determined by whether $x + |j_1 \dots j_n|_\pm \leq M$ or $x + |j_1 \dots j_n|_\pm \geq M+1$. That is,

$$m_f[\,(x, j_1 \dots j_n),\,(x - (-1)^{j_1}, j_2 \dots j_n 0)\,] = \begin{cases} 1 & \text{if } x + |j_1 \dots j_n|_\pm \leq M \\ 2 & \text{if } x + |j_1 \dots j_n|_\pm \geq M+1, \end{cases} \tag{4.3}$$

$$m_f[\,(x, j_1 \dots j_n),\,(x - (-1)^{j_1}, j_2 \dots j_n 1)\,] = \begin{cases} 2 & \text{if } x + |j_1 \dots j_n|_\pm \leq M \\ 1 & \text{if } x + |j_1 \dots j_n|_\pm \geq M+1. \end{cases} \tag{4.4}$$

Again, if $x + |j_1 \dots j_n|_\pm$ were 0 or $2M+1$, then the end vertex of the snake would have only two adjacent vertices, and only (4.4) or (4.3) would hold, respectively. Therefore we have described all the possible ways how the snake s can move.

Let H be the operator $A_n(G^M)$ reduced to the subspace $\mathcal{Z} = \mathrm{span}(\{|x, j\rangle \,:\, S(x, j) \neq \emptyset\}) \subset \mathbb{C}^{S_n(G^M)}$, and let $S(x', j')$ and $S(x'', j'')$ be two non-empty sets. According to Lemma 2.2 and the definition of $A_n(G^M)$ (see Section 2.3 for latter) we have

$$\begin{aligned} \langle x'', j''|H|x', j'\rangle = &\sqrt{m_b[\,(x', j'),\,(x'', j'')\,] + m_f[\,(x', j'),\,(x'', j'')\,]} \\ &\cdot \sqrt{m_b[\,(x'', j''),\,(x', j')\,] + m_f[\,(x'', j''),\,(x', j')\,]}. \end{aligned} \tag{4.5}$$

Since for any two snakes s' and s'' we have $m_b(s', s'')$ if and only if $m_f(s'', s')$, we have $m_b[\,(x', j'),\,(x'', j'')\,] \neq 0$ if and only if $m_f[\,(x'', j''),\,(x', j')\,] \neq 0$. Also, similarly as $m_b(s', s'')$ and $m_b(s'', s')$ both hold simultaneously if and only if there are two vertices u and v such

that $s' = (u, v, u, v, \ldots)$ and $s'' = (v, u, v, u, \ldots)$, one can see that both $m_b[\,(x', j'),\,(x'', j'')\,]$ and $m_b[\,(x'', j''),\,(x', j')\,]$ are non-zero simultaneously if and only if $j' = (1010\ldots)$, $x'' = x' + 1$ and $j'' = (0101\ldots)$ or vice versa. Hence, if this in not the case, then

$$\begin{aligned}&\sqrt{m_b[(x', j'), (x'', j'')] + m_f[(x', j'), (x'', j'')]} \cdot \sqrt{m_b[(x'', j''), (x', j')] + m_f[(x'', j''), (x', j')]} \\ &= \sqrt{m_b[(x', j'), (x'', j'')] \cdot m_f[(x'', j''), (x', j')]} + \sqrt{m_b[(x'', j''), (x', j')] \cdot m_f[(x', j'), (x'', j'')]}.\end{aligned} \tag{4.6}$$

Suppose for now that (4.6) holds even if we have $j' = (1010\ldots)$, $x'' = x' + 1$ and $j'' = (0101\ldots)$ (we show later on page 48 that it indeed does hold). Then

$$\begin{aligned}H &= \sum_{x',\,j',\,x'',\,j''} \Bigg(\sqrt{m_b[\,(x', j'),\,(x'', j'')\,] \cdot m_f[\,(x'', j''),\,(x', j')\,]} \\ &\qquad + \sqrt{m_b[\,(x'', j''),\,(x', j')\,] \cdot m_f[\,(x', j'),\,(x'', j'')\,]} \Bigg) \cdot |x'', j''\rangle\langle x', j'| \\ &= \sum_{x',\,j',\,x'',\,j''} \sqrt{m_b[(x', j'), (x'', j'')] \cdot m_f[(x'', j''), (x', j')]} \cdot (\,|x'', j''\rangle\langle x', j'| + |x', j'\rangle\langle x'', j''|\,)\,,\end{aligned} \tag{4.7}$$

where the summation is over all $x', x'' \in [0\,..\,2M{+}1]$ and $j', j'' \in \{0,1\}^n$ such that $S(x', j') \neq \emptyset$ and $S(x'', j'') \neq \emptyset$.

We can split the sum (4.7) into four sums for each of which particular values of the last bit of j' and the first bit of j'' are required. For example, suppose we require $j'_n = 0$ and $j''_1 = 0$. Then $m_b[\,(x', j'_1 \ldots j'_{n-1}0),\,(x'', 0j''_2 \ldots j''_n)\,]$ according to (4.1) and (4.2) is 0 unless $j'_l = j''_{l+1}$ for all $l \in [1\,..\,n-1]$ and $x'' = x' + 1$, in which case

$$m_b[\,(x', j'_1 \ldots j'_{n-1}0),\,(x'+1, 0j'_1 \ldots j'_{n-1})\,] = \begin{cases} 2 & \text{if } x' \leq M \\ 1 & \text{if } x' \geq M+1 \end{cases} \tag{4.8}$$

assuming $S(x', j') \neq \emptyset$ and $S(x'', j'') \neq \emptyset$. From (4.3) we get

$$m_f[\,(x'+1, 0j'_1 \ldots j'_{n-1}),\,(x', j'_1 \ldots j'_{n-1}0)\,] = \begin{cases} 1 & \text{if } x'+1+|0j'_1 \ldots j'_{n-1}|_{\pm} \leq M \\ 2 & \text{if } x'+1+|0j'_1 \ldots j'_{n-1}|_{\pm} \geq M+1. \end{cases} \tag{4.9}$$

To make following equations shorter, let $\mathrm{If}_c[q_1; q_0]$ be q_1, if the condition c is true, and q_0, if it is false. For the sake of convenience let us define $|x, j\rangle$ to be 0, if $S(x, j) = \emptyset$. Therefore, according to (4.8) and (4.9), we have

$$\sum_{\substack{x',\,j',\,x'',\,j'' \\ j'_n=0,\,j''_1=0}} \sqrt{m_b[\,(x', j'),\,(x'', j'')\,] \cdot m_f[\,(x'', j''),\,(x', j')\,]} \cdot (\,|x'', j''\rangle\langle x', j'| + |x', j'\rangle\langle x'', j''|\,) =$$

$$= \sum_{j\in\{0,1\}^{n-1}} \Bigg(\sqrt{2} \sum_{x=0}^{M-\max(|j|_\pm,0)} (\,|x+1,0j\rangle\langle x,j0| + |x,j0\rangle\langle x+1,0j|\,) \\ + \mathrm{If}_{|j|_\pm>0}[2;1] \sum_{x=M+1-\max(|j|_\pm,0)}^{M-\min(|j|_\pm,0)} (\,|x+1,0j\rangle\langle x,j0| + |x,j0\rangle\langle x+1,0j|\,) \\ + \sqrt{2} \sum_{x=M+1-\min(|j|_\pm,0)}^{2M+1} (\,|x+1,0j\rangle\langle x,j0| + |x,j0\rangle\langle x+1,0j|\,) \Bigg). \tag{4.10}$$

(For some values of $x \in [0\,..\,2M+1]$ and $j \in \{0,1\}^{n-1}$ either or both of $|x,j0\rangle$ and $|x+1,0j\rangle$ can be 0. For example, $|2,000111\rangle = 0$ because the distance between the middle vertex of a snake in $S(2,000111)$ and R_1 should be -1, which is clearly not possible, and therefore this set $S(2,000111)$ is empty.)

For the three remaining sums, when $(j'_n, j''_1) = (0,1)$, $(j'_n, j''_1) = (1,0)$ and $(j'_n, j''_1) = (1,1)$, similar derivations can be done. In the end we get

$$H = \sum_{j\in\{0,1\}^{n-1}} \Bigg(\sum_{x=0}^{M-\max(|j|_\pm,0)} \Big(2\,(\,|x+1,0j\rangle\langle x,j1| + |x,j1\rangle\langle x+1,0j|\,) \\ + (\,|x-1,1j\rangle\langle x,j0| + |x,j0\rangle\langle x-1,1j|\,) \\ + \sqrt{2}\,(\,|x+1,0j\rangle\langle x,j0| + |x,j0\rangle\langle x+1,0j|\,) \\ + \sqrt{2}\,(\,|x-1,1j\rangle\langle x,j1| + |x,j1\rangle\langle x-1,1j|\,)\Big) \\ + \sum_{x=M+1-\max(|j|_\pm,0)}^{M-\min(|j|_\pm,0)} \Big(\sqrt{2}\,(\,|x+1,0j\rangle\langle x,j1| + |x,j1\rangle\langle x+1,0j|\,) \\ + \sqrt{2}\,(\,|x-1,1j\rangle\langle x,j0| + |x,j0\rangle\langle x-1,1j|\,) \\ + \mathrm{If}_{|j|_\pm>0}[2;1]\,(\,|x+1,0j\rangle\langle x,j0| + |x,j0\rangle\langle x+1,0j|\,) \\ + \mathrm{If}_{|j|_\pm>0}[1;2]\,(\,|x-1,1j\rangle\langle x,j1| + |x,j1\rangle\langle x-1,1j|\,)\Big) \\ + \sum_{x=M+1-\min(|j|_\pm,0)}^{2M+1} \Big((\,|x+1,0j\rangle\langle x,j1| + |x,j1\rangle\langle x+1,0j|\,) \\ + 2\,(\,|x-1,1j\rangle\langle x,j0| + |x,j0\rangle\langle x-1,1j|\,) \\ + \sqrt{2}\,(\,|x+1,0j\rangle\langle x,j0| + |x,j0\rangle\langle x+1,0j|\,) \\ + \sqrt{2}\,(\,|x-1,1j\rangle\langle x,j1| + |x,j1\rangle\langle x-1,1j|\,)\Big)\Bigg). \tag{4.11}$$

What is left to do is to show that (4.6) holds even if $j' = (1010\ldots)$, $x'' = x' + 1$ and

$j'' = (0101\ldots)$. For the backward motion from (4.1) and (4.2) we get

$$m_b[\,(x+1, 0101\ldots),\,(x, 1010\ldots)\,] = \begin{cases} 1 & \text{if } x \leq M-1 \\ 2 & \text{if } x \geq M, \end{cases} \tag{4.12}$$

$$m_b[\,(x, 1010\ldots),\,(x+1, 0101\ldots)\,] = \begin{cases} 2 & \text{if } x \leq M \\ 1 & \text{if } x \geq M+1. \end{cases} \tag{4.13}$$

For the forward motion, however, we need to consider two cases. If n is odd, then (4.3) and (4.4) give

$$m_f[\,(x, 1010\ldots1),\,(x+1, 0101\ldots0)\,] = \begin{cases} 1 & \text{if } x \leq M-1 \\ 2 & \text{if } x \geq M, \end{cases} \tag{4.14}$$

$$m_f[\,(x+1, 0101\ldots0),\,(x, 1010\ldots1)\,] = \begin{cases} 2 & \text{if } x \leq M \\ 1 & \text{if } x \geq M+1, \end{cases} \tag{4.15}$$

while, if n is even, we have

$$m_f[\,(x+1, 0101\ldots01),\,(x, 1010\ldots10)\,] = \begin{cases} 1 & \text{if } x \leq M-1 \\ 2 & \text{if } x \geq M, \end{cases} \tag{4.16}$$

$$m_f[\,(x, 1010\ldots10),\,(x+1, 0101\ldots01)\,] = \begin{cases} 2 & \text{if } x \leq M \\ 1 & \text{if } x \geq M+1. \end{cases} \tag{4.17}$$

Using (4.12-4.17) one can verify that (4.6) holds for all values of x and n.

Now that we have found the Hamiltonian (4.11) which governs the continuous-time quantum snake walk on G^M restricted to subspace $\mathcal{Z}$, we can start to examine how this walk behaves for specific initial states.

4.3 Quantum snakes on infinite binary trees

The description of the Hamiltonian H is quite complex, and it is not clear how the quantum evolution governed by H behaves. Because of that, let us restrict our attention to superpositions $|x, j\rangle$ such that $0 \ll x - n$ and $x + n \ll M$.

Consider an operator

$$\begin{aligned} \hat{H} = \sum_{j\in\{0,1\}^{n-1}} \sum_{x\in\mathbb{Z}} \big(& 2\,(\,|x+1, 0j\rangle\langle x, j1| + |x, j1\rangle\langle x+1, 0j|\,) \\ & + (\,|x-1, 1j\rangle\langle x, j0| + |x, j0\rangle\langle x-1, 1j|\,) \\ & + \sqrt{2}\,(\,|x+1, 0j\rangle\langle x, j0| + |x, j0\rangle\langle x+1, 0j|\,) \\ & + \sqrt{2}\,(\,|x-1, 1j\rangle\langle x, j1| + |x, j1\rangle\langle x-1, 1j|\,)\,\big), \end{aligned} \tag{4.18}$$

where, unlike in the definition of H, we assume $\{\,|x,j\rangle \;:\; (x,j) \in \mathbb{Z}\times\{0,1\}^n\,\}$ is an orthonormal basis ($|x,j\rangle$ is not defined to be 0 of $S(x,j)\neq\emptyset$).

On our states of interest both operators H and $\hat{H}$ act equally. Therefore, similarly as the continuous-time quantum walk on a finite line segment can be approximated by the continuous-time quantum walk on the infinite line (see [20]), assuming the time of evolution t is not too large, $e^{-\mathrm{i}\hat{H}t}$ well approximates how $e^{-\mathrm{i}Ht}$ acts on the states of our interest. (Indeed, if we neglect the higher terms starting from the same degree of both Taylor series $U_t = e^{-\mathrm{i}Ht} = \mathbb{I} - \mathrm{i}Ht - \frac{(Ht)^2}{2!} + \mathrm{i}\frac{(Ht)^3}{3!} + \ldots$ and $\tilde{U}_t = e^{-\mathrm{i}\hat{H}t} = \mathbb{I} - \mathrm{i}\hat{H}t - \frac{(\hat{H}t)^2}{2!} + \mathrm{i}\frac{(\hat{H}t)^3}{3!} + \ldots$, which can be done without causing significant errors, we obtain two operators which act equally on our states of interest.) $\hat{H}$ can be thought of as a Hamiltonian governing the walk on infinite binary tree restricted to certain superpositions, where each vertex has two children and one parent (there is no root). In this section let us analyze the operator $\hat{H}$.

4.3.1 Analogies to snakes on line

It turns out that the structure of $\hat{H}$ is very similar to the Hamiltonian (3.4) governing the continuous-time quantum snake walk on the line. Here we present many similar results as in Chapter 3, but without going into too much details explaining them.

Note that we can rewrite $\hat{H}$ as

$$\begin{aligned}\hat{H} =& \sum_{x\in\mathbb{Z}} |x-1\rangle\langle x| \otimes \sum_{j\in\{0,1\}^{n-1}} (\,\sqrt{2}\,|j0\rangle\langle 0j| + 2\,|j1\rangle\langle 0j| + |1j\rangle\langle j0| + \sqrt{2}\,|1j\rangle\langle j1|\,)\\ &+ \sum_{x\in\mathbb{Z}} |x+1\rangle\langle x| \otimes \sum_{j\in\{0,1\}^{n-1}} (\,|j0\rangle\langle 1j| + \sqrt{2}\,|j1\rangle\langle 1j| + \sqrt{2}\,|0j\rangle\langle j0| + 2\,|0j\rangle\langle j1|\,)\\ &= \int_0^{2\pi} |\tilde{k}\rangle\langle\tilde{k}| \otimes \hat{H}_{n,k}\,\mathrm{d}k,\end{aligned} \tag{4.19}$$

where $|\tilde{k}\rangle = \frac{1}{\sqrt{2\pi}}\sum_{x\in\mathbb{Z}} e^{\mathrm{i}kx}|x\rangle$ as usual and

$$\begin{aligned}\hat{H}_{n,k} =& \sum_{j\in\{0,1\}^{n-1}} e^{\mathrm{i}k}(\,\sqrt{2}\,|j0\rangle\langle 0j| + 2\,|j1\rangle\langle 0j| + |1j\rangle\langle j0| + \sqrt{2}\,|1j\rangle\langle j1|\,)\\ &+ \sum_{j\in\{0,1\}^{n-1}} e^{-\mathrm{i}k}(\,|j0\rangle\langle 1j| + \sqrt{2}\,|j1\rangle\langle 1j| + \sqrt{2}\,|0j\rangle\langle j0| + 2\,|0j\rangle\langle j1|\,).\end{aligned} \tag{4.20}$$

Hence, eigenvalues and eigenvectors of $\hat{H}_{n,k}$ give us eigenvalues and eigenvectors of $\hat{H}$. For unit vectors $|u_{0,k}\rangle = \frac{1}{\sqrt{3}}\left(\sqrt{2}e^{-\mathrm{i}k}|0\rangle + e^{\mathrm{i}k}|1\rangle\right)$, $|u_{1,k}\rangle = \frac{1}{\sqrt{3}}\left(e^{-\mathrm{i}k}|0\rangle - \sqrt{2}e^{\mathrm{i}k}|1\rangle\right)$, $|v_0\rangle = \frac{1}{\sqrt{3}}\left(|0\rangle + \sqrt{2}\,|1\rangle\right)$ and $|v_1\rangle = \frac{1}{\sqrt{3}}\left(\sqrt{2}\,|0\rangle - |1\rangle\right)$ we have

$$\hat{H}_{n,k} = 3\sum_{j\in\{0,1\}^{n-1}} (|u_{0,k}\rangle|j\rangle\langle j|\langle v_0| + |j\rangle|v_0\rangle\langle u_{0,k}|\langle j|). \tag{4.21}$$

Similarly as before, we define $|\widehat{0}\rangle = |u_{0,k}\rangle^{\otimes n}$ (here we do not use the factor $-\mathrm{i}$ because, unlike in the case of the line, it does not make any expressions simpler) and for $m \in [1\,..\,2^n-1]$

we define

$$|\widehat{m}\rangle = |u_{0,k}\rangle^{\otimes n-\lfloor \log_2(m)\rfloor -1}|u_{1,k}\rangle|v_{m_{\lfloor \log_2(m)\rfloor}}\rangle \dots |v_{m_1}\rangle, \tag{4.22}$$

where $1m_{\lfloor \log_2(m)\rfloor} \dots m_1$ is m written binary using $\lfloor \log_2(m)\rfloor + 1$ bits. Since $\langle u_{0,k}|u_{1,k}\rangle = 0$ and $\langle v_0|v_1\rangle = 0$, $B_{n,k} = \{|\widehat{0}\rangle, \dots, |\widehat{2^n-1}\rangle\}$ is an orthonormal basis. By proceeding in the same way as in the case of the line (see Section 3.1.1), we obtain

$$\begin{aligned}\hat{H}_{n,k} =& 2\sqrt{2}(e^{\mathrm{i}k} + e^{-\mathrm{i}k})\,|\widehat{0}\rangle\langle\widehat{0}| + (e^{\mathrm{i}k} - 2e^{-\mathrm{i}k})|\widehat{1}\rangle\langle\widehat{0}| + (e^{-\mathrm{i}k} - 2e^{\mathrm{i}k})|\widehat{0}\rangle\langle\widehat{1}| \\ &+ 3\sum_{m=1}^{2^{n-1}-1} (|\widehat{2m}\rangle\langle\widehat{m}| + |\widehat{m}\rangle\langle\widehat{2m}|).\end{aligned} \tag{4.23}$$

Again we can show that only $n+1$ eigenvalues of $\hat{H}_{n,k}$ depend on k and those are the eigenvalues we care about. k-dependent eigenvalues of $\hat{H}_{n,k}$ are the eigenvalues of

$$\begin{aligned}\Phi_k = U_k^* \hat{H}_{n,k} U_k =& 3\sum_{y=1}^{n-1} (|\overline{y+1}\rangle\langle\overline{y}| + |\overline{y}\rangle\langle\overline{y+1}|) + 2\sqrt{2}(e^{\mathrm{i}k} + e^{-\mathrm{i}k})\,|\overline{n+1}\rangle\langle\overline{n+1}| \\ &+ (e^{-\mathrm{i}k} - 2e^{\mathrm{i}k})|\overline{n+1}\rangle\langle\overline{n}| + (e^{\mathrm{i}k} - 2e^{-\mathrm{i}k})|\overline{n}\rangle\langle\overline{n+1}|,\end{aligned} \tag{4.24}$$

where U_k is a linear isometry defined as

$$U_k = \sum_{y=1}^{n} |\widehat{2^{n-y}}\rangle\langle\overline{y}| + |\widehat{0}\rangle\langle\overline{n+1}|. \tag{4.25}$$

Now let us state the analogue of Lemma 3.1 and the p-condition (3.27) for the case of the binary tree. Without loss of generality let $\langle\overline{1}|\phi\rangle \geq 0$ for all eigenvectors of Φ_k.

Lemma 4.1. *For any k let $|\phi\rangle \in \mathbb{R}^{n+1}$ be a unit vector such that $\Phi_k|\phi\rangle = \lambda|\phi\rangle$ for some eigenvalue $\lambda \in \mathbb{R}$. There exist unique $p \in (0,\pi)$ and $c > 0$ such that $|\phi\rangle = c\sum_{y=1}^{n} \sin yp|\overline{y}\rangle + c\frac{3\sin(n+1)p}{e^{\mathrm{i}k}-2e^{-\mathrm{i}k}}|\overline{n+1}\rangle$, $\lambda = 6\cos p$, and p satisfies*

$$6(3\cos p - 2\sqrt{2}\cos k)\sin(n+1)p = (1 + 8\sin^2 k)\sin np. \tag{4.26}$$

Proof. First let us show that $|\lambda| < 6$. Suppose $\lambda = 6$. It can be easily shown that $\langle\overline{1}|\phi\rangle \neq 0$ (for any value of λ), therefore $\langle\overline{1}|\phi\rangle = b$ for some constant $b > 0$. We have

$$6b = \lambda\langle\overline{1}|\phi\rangle = \langle\overline{1}|\Phi_k|\phi\rangle = 3\langle\overline{2}|\phi\rangle, \tag{4.27}$$

which gives us $\langle\overline{2}|\phi\rangle = 2b$. Then, the induction used in a similar fashion as in the proof of Lemma 3.1 gives us $\langle\overline{y}|\phi\rangle = by$ for $y \in [1\,..\,n]$. By combining this with

$$\lambda\langle\overline{n}|\phi\rangle = \langle\overline{n}|\Phi_k|\phi\rangle = 3\langle\overline{n-1}|\phi\rangle + (e^{\mathrm{i}k} - 2e^{-\mathrm{i}k})\langle\overline{n+1}|\phi\rangle \tag{4.28}$$

and

$$\lambda\langle\overline{n+1}|\phi\rangle = \langle\overline{n+1}|\Phi_k|\phi\rangle = (e^{-\mathrm{i}k} - 2e^{\mathrm{i}k})\langle\overline{n}|\phi\rangle + 2\sqrt{2}(e^{\mathrm{i}k} + e^{-\mathrm{i}k})\langle\overline{n+1}|\phi\rangle \tag{4.29}$$

we get

$$(6 - 4\sqrt{2}\cos k)(3n+3)b = (9 - 8\cos^2 k)nb, \tag{4.30}$$

which has solutions $\cos k = 3\sqrt{2}(n+1\pm 1)/(4n) \notin [-1,1]$. This contradiction gives us $\lambda \neq 6$ for any value of k; similarly $\lambda \neq -6$. It can be shown quite easily that for $k = \frac{\pi}{2}$ we have $\lambda \in \{6\cos\frac{\pi}{n+2}, 6\cos\frac{2\pi}{n+2}, \ldots, 6\cos\frac{(n+1)\pi}{n+2}\}$, therefore the continuity of eigenvalues as a functions of k implies $|\lambda| < 6$.

Let p be a unique value in $(0,\pi)$ satisfying $\lambda = 6\cos p$ and let $c > 0$ be such that $\langle\overline{1}|\phi\rangle = c\sin p$. By using induction in the same way as in the proof of the Lemma 3.1 we get

$$|\phi\rangle = c\sum_{y=1}^{n}\sin yp|\overline{y}\rangle + c\frac{3\sin(n+1)p}{e^{\mathrm{i}k} - 2e^{-\mathrm{i}k}}|\overline{n+1}\rangle. \tag{4.31}$$

Finally, the condition (4.26) comes from substituting the expression (4.31) for $|\phi\rangle$ and $\lambda = 6\cos p$ in (4.29). □

Since each eigenvalue of Φ_k uniquely determines its corresponding eigenvector, Lemma 4.1 implies that all the eigenvalues of Φ_k are distinct. If using numerical computation we plot how k-dependent eigenvalues of $\hat{H}_{n,k}$ and their derivatives depend on k (see Figures 4.3 and 4.4 for the case when $n = 8$), we see that they behave very similarly as in the case of the line (Figures 3.3 and fig:deigenvalues).

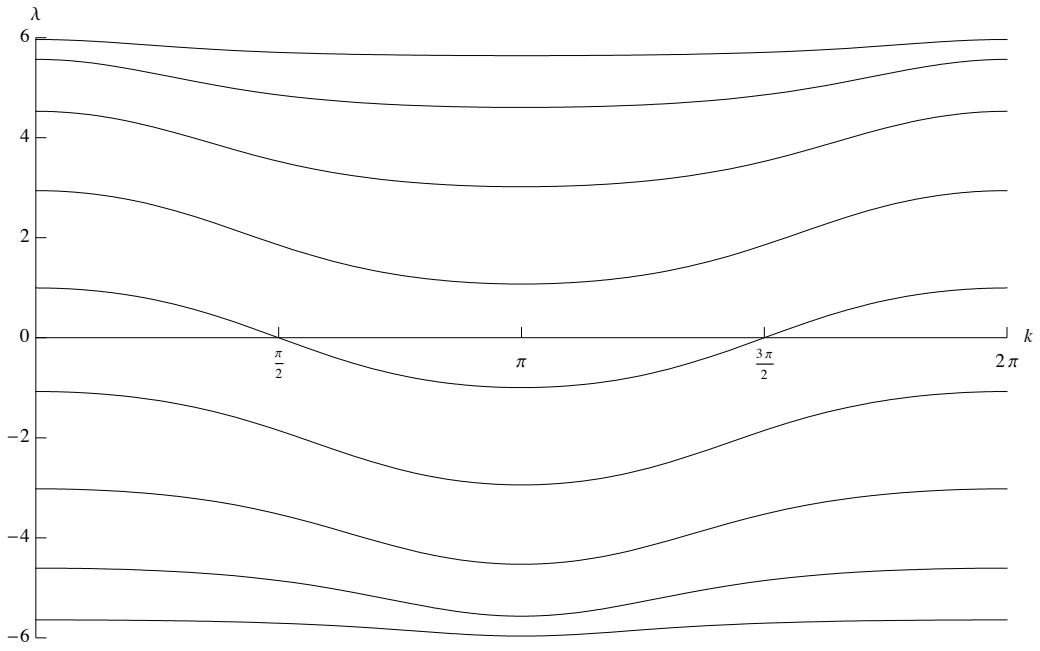

Figure 4.3: k-dependent eigenvalues in the case of the tree for $n = 8$.

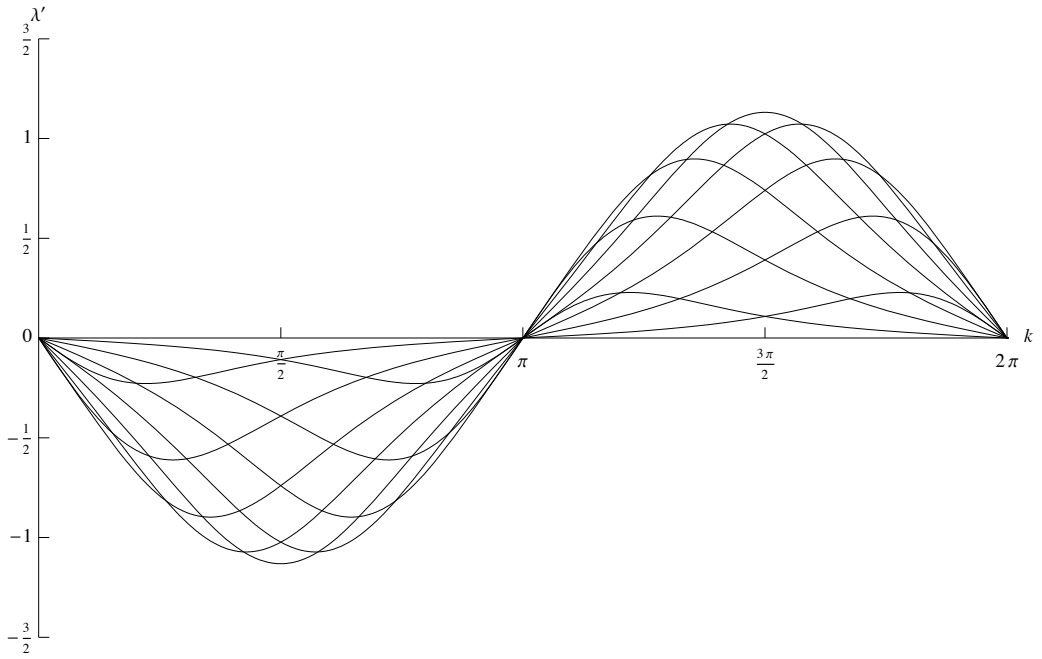

Figure 4.4: Derivatives of k-dependent eigenvalues in the case of the tree for $n = 8$.

4.3.2 Wave packets and the span length

As long as the derivative of any eigenvalue is ω at some point $k = k_\omega$, we can prepare a wave packet which for at least some amount of time moves with momentum ω up or down the tree. The technique to show this is very similar to one used in Section 3.3 for the case of the line, and still requires us to do some approximations.

For every $x \in \mathbb{Z}$ and $j \in \{0,1\}^n$ let us define the span length of the state $|x,j\rangle$, which can be thought of as a superposition over snakes, to be $\bar{\mu}(|x,j\rangle) = \bar{\mu}(j)$, where $\bar{\mu}(j)$ is defined in (3.90) on page 37. In some sense it means that all snakes in $|x,j\rangle$ connect two levels of tree which are apart from each other by the distance $\bar{\mu}(|x,j\rangle)$. We also define $\bar{\mu}(|\psi\rangle)$ for $|\psi\rangle \in \mathbb{C}^{\mathbb{Z}\times\{0,1\}^n}$ to be the random variable which for every $m \in \mathbb{Z}$ assigns the probability that the measurement of $|\psi\rangle$ in the standard basis results in a pair (x,j) such that $\bar{\mu}(|x,j\rangle) = m$.

In Section 3.3.3 we mention that we are interested in wave packets which have a large span length with a substantial probability, and now we see why: if such a wave packet is placed on the expanded glued trees graph and it goes down the tree, the hope is that it does not lose too much of its span length once it hits the center part of the graph. By the *center part* we mean the part of G^M which corresponds to the copies of the original glued trees graph G, that is, the part which is at distance at most N from the glued part. Then with a probability high enough we would get a snake which reveals the roots r_1 and r_2 of G.

However, there are still many issues we need to address. First of all, it might be the case that the wave packet is reflected form the center part, and it never 'reaches' levels deep enough to give a path connecting the roots r_1 and r_2 with substantially large probability.

And second, even if the wave packet propagates through the center part, while doing so it might lose its span length a lot (meaning that the span length is outside $O(\log n)$ with exponentially small probability). Whether it happens or not is not clear yet. Anyhow, let us consider a span length of one particular wave packet, which seems to be the one of the greatest importance.

Consider n to be even. Let $\lambda(k)$ be the $\frac{n+2}{2}$-th largest eigenvalue of Φ_k, and $|\phi(k)\rangle$ and $|\psi(k)\rangle = U_k|\phi(k)\rangle$ be its corresponding eigenvectors of Φ_k and $\hat{H}_{n,k}$, respectively. Operator Φ_k is holomorphic in k, therefore due to the Lemma 3.3 so are $\lambda(k)$, $|\phi(k)\rangle$ and $|\psi(k)\rangle$ (to be more precise, we can choose the eigenvectors to be holomorphic, because there is obviously some choice of global phases for which they are not). Let us consider the initial state

$$|\xi_z\rangle = c_\sigma \int_{\frac{\pi}{2}}^{\frac{5\pi}{2}} e^{-\frac{(k-\frac{3\pi}{2})^2}{2\sigma^2}} e^{-\mathrm{i}kz} \, |\tilde{k}\rangle \otimes |\psi(k)\rangle \, \mathrm{d}k, \tag{4.32}$$

where $c_\sigma > 0$ is a normalization factor. Let $\lambda'(k)$ and Φ'_k denote the derivatives of $\lambda(k)$ and Φ_k respectively. We assume that σ is small enough so that we can approximate $\lambda(k)$ by $\lambda(\frac{3\pi}{2}) + (k - \frac{3\pi}{2})\lambda'(\frac{3\pi}{2})$ and $|\psi(k)\rangle$ simply by $|\psi(\frac{3\pi}{2})\rangle$. Similarities to the case of the line (see page 33) suggests that choosing $\sigma \in \Omega(1/\operatorname{poly} n)$ might be enough for the latter approximation to be accurate. We have

$$\Phi_{3\pi/2} = 3\sum_{y=1}^{n-1} (|\overline{y+1}\rangle\langle\overline{y}| + |\overline{y}\rangle\langle\overline{y+1}|) + 3\mathrm{i}|\overline{n+1}\rangle\langle\overline{n}| - 3\mathrm{i}|\overline{n}\rangle\langle\overline{n+1}|, \tag{4.33}$$

for which the median eigenvalue is $\lambda(\frac{3\pi}{2}) = 0$ with corresponding eigenvector

$$|\phi(3\pi/2)\rangle = \sqrt{\frac{2}{n+2}}\left(\sum_{\substack{y=1 \\ y \text{ is odd}}}^{n-1} (-1)^{\frac{n+y-1}{2}} \, |\overline{y}\rangle + \mathrm{i}|\overline{n+1}\rangle \right). \tag{4.34}$$

We have $\Phi'_{3\pi/2} = -|\overline{n+1}\rangle\langle\overline{n}| - |\overline{n}\rangle\langle\overline{n+1}| + 4\sqrt{2}\,|\overline{n+1}\rangle\langle\overline{n+1}|$, and perturbation theory gives us $\lambda(\frac{3\pi}{2}) = \langle\phi(\frac{3\pi}{2})|\Phi'_{3\pi/2}|\phi(\frac{3\pi}{2})\rangle = \frac{8\sqrt{2}}{n+2}$ [21, Section 1.2]. As similar analysis (with similar assumptions) to the case of the line in Section 3.3.2 implies that $|\xi_z\rangle$ evolves under $\hat{H}$ as a wave packet moving with momentum $\frac{8\sqrt{2}}{n+2}$.

Since $|u_{0,3\pi/2}\rangle = \frac{1}{\sqrt{3}}\left(\sqrt{2}\mathrm{i}|0\rangle - \mathrm{i}|1\rangle\right) = \mathrm{i}|v_1\rangle$ and $|u_{1,3\pi/2}\rangle = \frac{1}{\sqrt{3}}\left(\mathrm{i}|0\rangle + \sqrt{2}\mathrm{i}|1\rangle\right) = \mathrm{i}|v_0\rangle$, we get

$$|\psi(3\pi/2)\rangle = U_{3\pi/2}|\phi(3\pi/2)\rangle = \mathrm{i}^{n+1}\sqrt{\frac{2}{n+2}}\sum_{l=0}^{n/2}(|v_1\rangle \otimes |v_1\rangle)^{\otimes\frac{n}{2}-l}(|v_0\rangle \otimes |v_0\rangle)^{\otimes l}. \tag{4.35}$$

It is not clear what is the span length $\bar{\mu}(|\upsilon, \psi(\frac{3\pi}{2})\rangle)$, where $|\upsilon\rangle \in \mathbb{C}^{\mathbb{Z}}$ can be chosen arbitrarily. On a positive note, numerical results suggest that $E(\bar{\mu}(|\upsilon, \psi(\frac{3\pi}{2})\rangle)) \in \Omega(\sqrt{n})$. However, even if it indeed holds, it does not mean that the span length of the snake remains sufficiently large when it hits the center part.

4.4 Reflection and transmission coefficients

Let us still assume that M is very large and $M \in O(\operatorname{poly} N)$. In Section 4.3 we restrict our attention to superpositions $|x, j\rangle$ satisfying $0 \ll x - n$ and $x + n \ll M$, and therefore we can approximate H by $\hat{H} = \int_0^{2\pi} |\tilde{k}\rangle\langle\tilde{k}| \otimes \hat{H}_{n,k}$, where $\hat{H}_{n,k}$ is given in (4.20). Similarly, if we place the restriction that $M \ll x - n$ and $x + n \ll 2M$, then we can approximate H by $\check{H} = \int_0^{2\pi} |\tilde{k}\rangle\langle\tilde{k}| \otimes \check{H}_{n,k}$, where

$$\begin{aligned}\check{H}_{n,k} = &\sum_{j\in\{0,1\}^{n-1}} e^{\mathrm{i}k}(\,\sqrt{2}\,|j0\rangle\langle 0j| + |j1\rangle\langle 0j| + 2\,|1j\rangle\langle j0| + \sqrt{2}\,|1j\rangle\langle j1|\,)\\ &+ \sum_{j\in\{0,1\}^{n-1}} e^{-\mathrm{i}k}(\,2\,|j0\rangle\langle 1j| + \sqrt{2}\,|j1\rangle\langle 1j| + \sqrt{2}\,|0j\rangle\langle j0| + |0j\rangle\langle j1|\,).\end{aligned} \tag{4.36}$$

We can see that $\check{H}_{n,k}$ is the conjugate of the operator $\hat{H}_{n,k}$ with its rows and columns reversed. That is not a big surprise since the expanded glued trees graph is symmetric and the same properties should hold for the both binary trees (asymmetries in the glued part have no effect since we are working only over certain superpositions). Therefore $\hat{H}_{n,k}$ and $\check{H}_{n,k}$ have the same eigenspectrum. Also note that $\hat{H}_{n,k}$ and $\hat{H}_{n,-k}$ have the same eigenspectrum as well.

Now let us consider superpositions $|x, j\rangle$ such that $0 \ll x - n$ and $x + n \ll 2M$. In this case we may approximate the Hamiltonian H governing the continuous-time quantum snake walk on the expanded glued trees graph by one which we obtain by changing summation boundaries in (4.11) for x from 0 and $2M + 1$ to $-\infty$ and $+\infty$, respectively, where now we assume $\{\, |x, j\rangle \,:\, (x, j) \in \mathbb{Z} \times \{0, 1\}^n \,\}$ is an orthonormal basis, that is, we sum over all values of $j \in \{0, 1\}^{n-1}$ and $x \in \mathbb{Z}$ (the argument why we can do it is similar to one in the beginning of Section 4.3 for approximating H by $\hat{H}$). Let us call this new operator $\tilde{H}$. The eigenspectrum of $\tilde{H}$ does not depend on the value of M because for different values of M this operator differs only up to some power of the translation $\sum_{x\in\mathbb{Z}} |x + 1\rangle\langle x| \otimes \mathbb{I}$, where $\mathbb{I}$ is the identity operator on the space $\mathbb{C}^{\{0,1\}^n}$. Even though the eigenvectors depend on the value of M, this dependence is trivial. Because of this M-independence, we choose to analyze the operator $\tilde{H}$ instead of H.

Let us fix $l \in [1\,..\,n+1]$, let $\lambda(k)$ be l-th largest k-dependent eigenvalue of $\hat{H}_{n,k}$, and let $|\hat{\psi}_k\rangle$, $|\hat{\psi}_{-k}\rangle$ and $|\check{\psi}_k\rangle$ be the eigenvectors of $\hat{H}_{n,k}$, $\hat{H}_{n,-k}$ and $\check{H}_{n,k}$, respectively, corresponding to the eigenvalue $\lambda(k)$. This means that $|\hat{\chi}_k\rangle = |\tilde{k}\rangle \otimes |\hat{\psi}_k\rangle$ and $|\hat{\chi}_{-k}\rangle = |\widetilde{-k}\rangle \otimes |\hat{\psi}_{-k}\rangle$ are eigenvectors of $\hat{H}$ and $|\tilde{k}\rangle \otimes |\check{\psi}_k\rangle$ is an eigenvector of $\check{H}$. Finally, let $\hat{\Pi} = \sum_{x\le M-n+1} |x\rangle\langle x| \otimes \mathbb{I}$ and $\check{\Pi} = \sum_{x\ge M+n} |x\rangle\langle x| \otimes \mathbb{I}$ be two projectors. We look for eigenvectors of $\tilde{H}$ in the from

$$|\theta_k\rangle = \hat{\Pi}(\,|\hat{\chi}_k\rangle + R_k|\hat{\chi}_{-k}\rangle\,) + \check{\Pi}(\,T_k|\check{\chi}_k\rangle\,) + \sum_{x=M-n+2}^{M+n-1} \sum_{j\in\{0,1\}^n} \alpha_{x,j}|x, j\rangle \tag{4.37}$$

with corresponding eigenvalue $\lambda(k)$, where $R_k, T_k, \alpha_{x,j} \in \mathbb{C}$ for all $j \in \{0, 1\}^n$ and $x \in [M-n+2\,..\,M+n-1]$. In some sense the vector $|\theta_k\rangle$ represents a wave packet which moves towards the center part of the expanded glued trees graph with momentum $\lambda'(k)$, then

hits the center part, and then gets reflected with the probability $|R_k|^2$ or gets transmitted through the center part with the probability $|T_k|^2$ (numerical results agree with $|R_k|^2 + |T_k|^2 = 1$); the wave packet maintains its previous momentum $\lambda'(k)$ after being reflected or transmitted (see [11] for a similar argument about the scattering on graphs).

Since $\hat{\Pi}\tilde{H}\hat{\Pi} = \hat{\Pi}\hat{H}\hat{\Pi}$, $\check{\Pi}\tilde{H}\check{\Pi} = \check{\Pi}\check{H}\check{\Pi}$ and $(\langle x_1| \otimes \mathbb{I})\tilde{H}(|x_2\rangle \otimes \mathbb{I}) = 0$ whenever $|x_1 - x_2| \neq 1$, we already know that $\langle x, j|\tilde{H}|\theta_k\rangle = \lambda(k)\langle x, j|\theta_k\rangle$ for all $x \in \mathbb{Z} \setminus [M - n + 1 \,..\, M + n]$ and all $j \in \{0, 1\}^n$ no matter what the values of R_k and T_k are. Hence, $|\theta_k\rangle$ is an eigenvector of $\tilde{H}$ if and only if $\tilde{\Pi}_1\tilde{H}|\theta\rangle = \tilde{\Pi}_1|\theta\rangle$, where $\tilde{\Pi}_1 = \sum_{x=M-n+1}^{M+n} |x\rangle\langle x| \otimes \mathbb{I}$.

Let $\tilde{\Pi}_2 = \sum_{x=M-n}^{M+n+1} |x\rangle\langle x| \otimes \mathbb{I}$, and note that $\tilde{\Pi}_1\tilde{H}|\theta\rangle = \tilde{\Pi}_1\tilde{H}\tilde{\Pi}_2\tilde{\Pi}_2|\theta\rangle$. Let us think of $\tilde{\Pi}_1|\theta\rangle$ and $\tilde{\Pi}_2|\theta\rangle$ as column vectors of the dimension $n2^{n+1}$ and $(n+1)2^{n+1}$, respectively, and of $\tilde{\Pi}_1 H \tilde{\Pi}_2$ as a matrix with dimensions $n2^{n+1} \times (n+1)2^{n+1}$. The both vectors and the matrix do not depend on the value of M. Assuming that we know $|\hat{\psi}_k\rangle$, $|\hat{\psi}_{-k}\rangle$ and $|\check{\psi}_k\rangle$, we can get the coefficients R_k, T_k and $\alpha_{x,j}$ for all $x \in [M - n + 1 \,..\, M + n]$ and $j \in \{0, 1\}^n$ by solving the system of linear equations

$$(\tilde{\Pi}_1\tilde{H}\tilde{\Pi}_2)(\tilde{\Pi}_2|\theta\rangle) = \tilde{\Pi}_1|\theta\rangle. \tag{4.38}$$

The problem is that we do not know the how to calculate $|\hat{\psi}_k\rangle$ (the other two vectors $|\hat{\psi}_{-k}\rangle$ and $|\check{\psi}_k\rangle$ can be easily obtained from $|\hat{\psi}_k\rangle$). If we run symbolic computations for the two simplest cases when $n = 1$ and $n = 2$, what we get is that the system (4.38) has a unique solution satisfying $|R_k|^2 + |T_k|^2 = 1$. There is also one even more interesting observation: $|T_k|^2 = \frac{8\sin^2 k}{1+8\sin^2 k}$, and it holds in both cases for all $n + 1$ values of l (that is, it does not matter which k-dependent eigenvalue of $\hat{H}_{n,k}$ we consider). Numerical results for $n = 3, 4, 5, 6, 7$ also agree with this (up to the precision of order 10^{-12}), which suggests that it might be true in general.

The function $\frac{8\sin^2 k}{1+8\sin^2 k}$ reaches its maximal value $\frac{8}{9}$ at $k = \frac{\pi}{2}$ and $k = \frac{3\pi}{2}$ (see Figure 4.5). That is good because from Section 4.3.2 we already know that in case n is even we can prepare a wave packet $|\xi_z\rangle$, satisfying $0 \ll z - n$ and $z + n \ll M$ and being a superposition mostly over vectors $|\tilde{k}\rangle \otimes |\hat{\psi}_k\rangle$ such that k is close to $\frac{3\pi}{2}$, which (for at least some amount of time) moves with momentum $\frac{8\sqrt{2}}{n+2}$ on the expanded glued trees graph G^M towards the center part. Let us choose $|\hat{\psi}_k\rangle$, $|\hat{\psi}_{-k}\rangle$ and $|\check{\psi}_k\rangle$ to be holomorphic. Assuming that $\arg(R_k)$ is differentiable and the derivative of $\arg(R_k)$ is not too large, the state

$$|\xi_z^*\rangle = c_\sigma^* \int_{\frac{\pi}{2}}^{\frac{5\pi}{2}} e^{-\frac{(k-\frac{3\pi}{2})^2}{2\sigma^2}} e^{-\mathrm{i}kz} |\theta_k\rangle \,\mathrm{d}k \tag{4.39}$$

most likely has a large overlap with the state $|\xi_z\rangle$ (given in (4.32)), therefore it seems that the wave packet $|\xi_z\rangle$ propagates through the center part with high probability. This statement is vague because of the fact that we do not know even approximately the values of $\arg(R_k)$ and $\arg(T_k)$, which highly determine the value of the integral in (4.39). Note that, even though the absolute values of T_k and R_k seem not to depend on l, their arguments do.

Assuming that the wave packet $|\xi_z\rangle$ propagates through the center part, which seems to be the case, it is important to know how much time it takes for the wave packet do so.

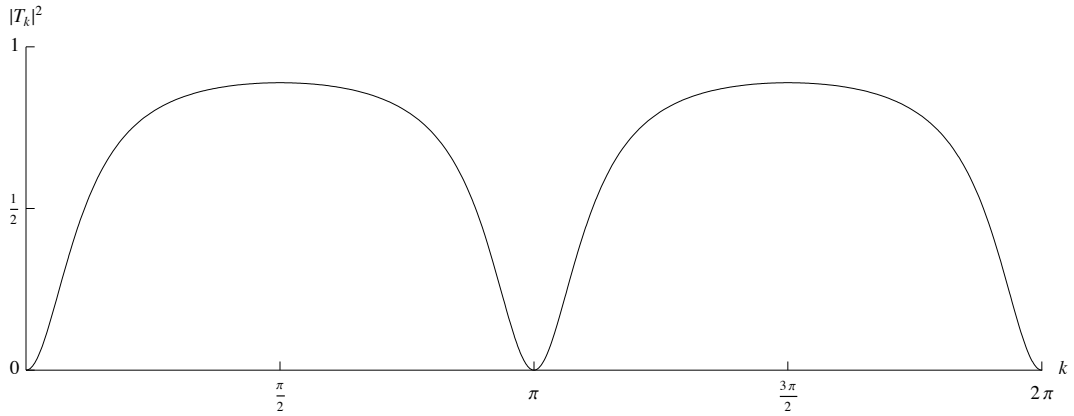

Figure 4.5: The absolute value of the transmission coefficient T_k squared.

This is why we talk about the effective length of the center part defined below. Since we do not know for what global phases $|\hat{\psi}_k\rangle$, $|\hat{\psi}_{-k}\rangle$ and $|\check{\psi}_k\rangle$ can be considered as holomorphic functions in k, we define the effective length in a way which is useful for the numerical computation.

Definition. Let us fix $l \in [1\,..\,n+1]$ and $k \in [0, 2\pi)$. Suppose that the first elements of vectors $|\hat{\psi}_k\rangle$, $|\hat{\psi}_{-k}\rangle$ and $|\check{\psi}_k\rangle$ (i.e., the amplitudes corresponding to $|0\ldots0\rangle$) are non-zero. Then there exists $\epsilon > 0$ such that for all $\delta < \epsilon$ we may uniquely choose the global phases of vectors $|\hat{\psi}_{k\pm\delta}\rangle$, $|\hat{\psi}_{-k\mp\delta}\rangle$ and $|\check{\psi}_{k\pm\delta}\rangle$ so that the first elements of all $e^{\mathrm{i}(M-n+1)k}|\hat{\psi}_{k\pm\delta}\rangle$, $e^{-\mathrm{i}(M-n+1)k}|\hat{\psi}_{-k\mp\delta}\rangle$ and $e^{\mathrm{i}(M+n)k}|\check{\psi}_{k\pm\delta}\rangle$ are strictly positive; let us choose the global phases in this way and, in turn, obtain states $|\theta_{k+\delta}\rangle$ and $|\theta_{k-\delta}\rangle$ having transmission coefficients $T_{k-\delta}$ and $T_{k+\delta}$, respectively. We define the *effective length* of the center part for k and l to be $\beta_{l,k} = \lim_{\delta\to 0} \frac{\arg(T_{k+\delta})-\arg(T_{k-\delta})}{2\delta}$ if this limit exists.

Let us explain a possible meaning of the effective length by talking about a simpler walk first. Suppose we have an arbitrary finite graph W, and we obtain another graph by attaching a semi-infinite line to two vertices of W. For $k \in [0, 2\pi)$ the effective length β_k of W can be defined similarly as we have defined it above (detailed description about the scattering on graphs and, in particular, how precisely we define β_k can be found in [11]). As described in Section 2.1, we can prepare a wave packet on one of the two semi-infinite lines which moves towards W with momentum $\nu_k = 2\sin k$ (here we are talking about the regular continuous-time quantum walk). The time it takes for this wave packet to propagate through the graph W, assuming it is not reflected, is β_k/ν_k; therefore the name the effective length.

Not enough analytical work has been done yet to tell whether the effective length of the center part $\beta_{l,k}$ has exactly the same meaning, but it might be so. Numerical results for $n \in [1\,..\,7]$ and $l \in [1\,..\,n+1]$ indicates that the effective length of the center part for $k = \frac{3\pi}{2}$ grows linearly in n (see Figure 4.6). That suggests that there are wave packets which traverse the center part in time $\Theta(n^2)$, since the wave packets corresponding to $k = \frac{3\pi}{2}$ and the median eigenvalue move with momentum $\Theta(\frac{1}{n})$.

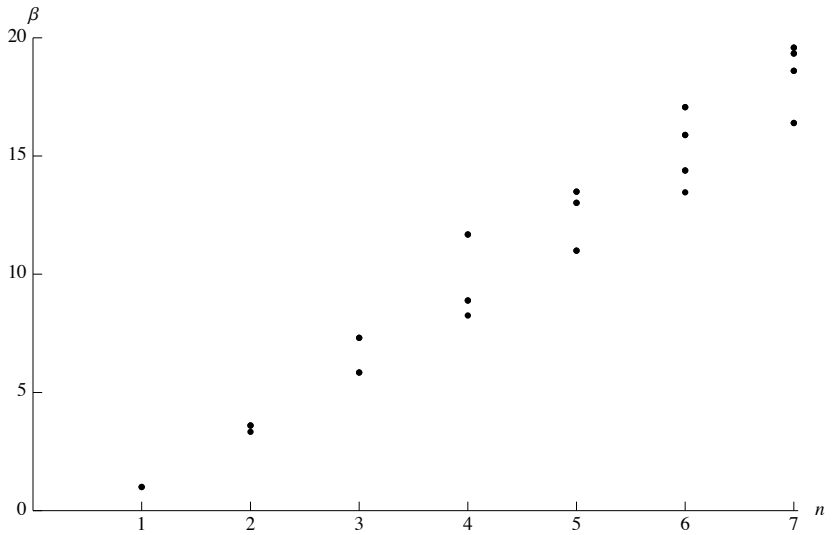

Figure 4.6: The effective length $\beta_{l,k}$ of the center part for $n \in [1\,..\,7]$, $l \in [1\,..\,n+1]$ and $k = \frac{3\pi}{2}$. The value of $\beta_{l,k}$ is the same for $l = l_0$ and $l = n + 2 - l_0$.

Not all eigenvectors of $\tilde{H}$ can be written in form $|\theta_k\rangle$ given in (4.37), but it seems that those other eigenvectors are not as important.

4.4.1 Potential algorithm for the extended glued trees problem

Now that we have seen that we can prepare a wave packed which moves on the expanded glued trees graph toward the center part with momentum $\Theta(\frac{1}{n})$ and most likely propagates through it with high probability, let us present a sketch of an algorithm that might solve the extended glued trees problem efficiently. We say 'might' mostly because of the fact that we do not know what happens with the span length of the wave packet once it hits the center part. It seams to be $\Omega(\sqrt{n})$ on average before and after that (see Section 4.3.2), but there might be some interesting reason why the span length decreases exponentially around the center part. Hopefully there is not.

Let N be the height of the original glued trees graph G which we have an access to via the black-box oracle, and we know the label of one of its two roots r_1. Our algorithm is going to be parametrized by seven following parameters which all may depend on the value of N:

- $n \in \mathbb{N}$, the length of the snake, satisfying $n \geq 2N + 1$ and $n \in O(\operatorname{poly} N)$;
- $l \in \mathbb{N}$, the number which determines which k-dependent eigenvalue of $\hat{H}_{n,k}$ we consider, satisfying $l \in [1\,..\,n+1]$;
- $k_0 \in [0, 2\pi)$, $\sigma \in \mathbb{R}$ and $z \in \mathbb{Z}$, the parameters determining the initial state of the walk, satisfying $z \in O(\operatorname{poly} N)$, $\sigma \in \Omega(1/\operatorname{poly} N)$, $z \ll -n - 1/\sigma$ and $\lambda'(k_0) \in \Omega(1/\operatorname{poly} N)$, where $\lambda'(k)$ is the derivative of l-th largest k-dependent eigenvalue of $\hat{H}_{n,k}$;

- $M \in \mathbb{N}$, the height of the expanded glued trees graph, satisfying $M \in O(\operatorname{poly} N)$ and $M \gg z + n + 1/\sigma$;
- $\tau \in \mathbb{R}$, the time of evolution, satisfying $\tau \in O(\operatorname{poly} N)$ and being approximately $z/\lambda'(k_0)$.

The algorithm for solving the extended glued trees problem then consists of four following steps.

1. Run the algorithm which solves the original glued trees problem, and obtain the label of the second root r_2. This can be done efficiently [12]. Then construct the oracle for the expanded glued trees graph G^M as shown in Section 4.1.3.
2. Prepare the initial state
$$|\xi_z\rangle = c_\sigma \Pi \int_{k_0-\pi}^{k_0+\pi} e^{-\frac{(k-k_0}{2\sigma^2}} e^{-\mathrm{i}kz} |\tilde{k}\rangle \otimes |\hat{\psi}(k)\rangle \,\mathrm{d}k, \tag{4.40}$$
where $\Pi = \sum_{x=0}^{M-N-n} |x\rangle\langle x| \otimes \mathbb{I}$ is a projector, $\mathbb{I}$ is the identity operator on the space $\mathbb{C}^{\{0,1\}^n}$, and $|\hat{\psi}(k)\rangle$ is the eigenvector of $\hat{H}_{n,k}$ corresponding to its l-th largest k-dependent eigenvalue. Here we already restrict our attention to superpositions $|x, j\rangle$. Note that we can construct the state $|\xi_z\rangle$ without any oracle queries.
3. Using $|\xi_z\rangle$ as the initial state, run the continuous-time quantum snake walk on G^M for time τ. This walk can be simulated efficiently using the circuit model and the oracle for G^M we have just constructed. Then measure the state of the walk in the standard basis, thus obtaining a list of labels of vertices, which corresponds to a path in G^M of length n.
4. If the list produced in Step 3 or its reverse contains a sub-list $(1a\bar{r_1}, 1a\bar{w}_1, 1a\bar{w}_2, \ldots, 1a\bar{r_2})$, where $a \in \{0,1\}^{M-N}$, then return $(\bar{r_1}, \bar{w}_1, \bar{w}_2, \ldots, \bar{r_2})$; otherwise go back to Step 2.

If this algorithm returns an answer, then it is obviously correct. The algorithm is also efficient, assuming it has to execute Steps 2, 3 and 4 only $O(\operatorname{poly} N)$ times in order to terminate with a high probability. The question is: is this assumption true?

If transmission coefficients really are as given in Figure 4.5, then for most of the values of k_0 their corresponding wave packets propagate throught the center part with probability at least $\Omega(1/\operatorname{poly} N)$. It is not clear for which values of k_0 and l the momentum $\lambda'(k_0)$ of the wave packet is in $\Omega(1/\operatorname{poly} N)$, but it seems that we can choose k_0 and l in a wide range to satisfy that. This gives us the hope that for some choice of the parameters of the algorithm the span length of the wave packet is sufficiently large during its traversal of the center part of the graph. Then again, it might as well be the case that choosing even n, $l = \frac{n+2}{2}$ and $k_0 = \frac{3\pi}{2}$ is good enough.

Another issue we must address is the precision of our approximations. That is, we have shown that the states of form $|\xi_z\rangle$ behaves as wave packets moving with momentum

$\lambda'(k_0)$ only when we assume that the time of evolution is small enough. We do not know how small this time should be in order for the approximations to be precise, plus, what kind of disturbances the irregularities at the center part causes to the behavior of the wave packet.

Chapter 5

Conclusion

In this thesis we have introduced a new type of quantum walk on graphs which we call the continuous-time quantum snake walk. We have analyzed the behavior of this walk on the line and the glued trees graph. Even though there are still caveats left to consider, the quantum snake walk has a potential to become a useful tool in quantum algorithm construction at least for some black-box oracle problems. Solving those caveats is the first problem we should address in the future.

Assuming the algorithm described in Chapter 4 indeed finds a path connecting both roots of the glued trees graph, it almost certainly does not find a shortest path. It would be interesting to see if there exists another algorithm which can efficiently do that. The problem of finding the shortest path connecting two vertices of a graph is known as *pathfinding*, and it has applications in many fields, for example, computer networking. It seems unrealistic that quantum methods can give us much faster algorithms for pathfinding in general weighted graphs than already known classical algorithms, because quantum algorithms generally perform better only on structures which feature some symmetry. Probably one can relatively simply prove this claim using some of quantum lower bound proving techniques (such as the adversary method [4]). However, superpolynomial separations might be possible for some specific classes of graphs.

The glued trees problem can also be easily turned into a decision problem (see [12]). One obvious way how to do that is to ask what is the first bit of the label of the root r_2, instead of asking the whole label. Another way would be to consider the following graph reachability problem. Suppose we are given a graph which consists of two copies of a same glued trees graph and we are given the labels of all four roots v_1, v_2, v_3 and v_4 without specifying which two of them belong to one copy of the glued trees graph and which two to the other. The problem is to find whether v_1 and v_2 are connected. Even though an algorithm solving the original glued trees problem also solves this problem, it does not necessarily provide a proof of the correctness of the answer which can be verified efficiently by a classical algorithm. On the other hand, an algorithm solving the extended glued trees problem efficiently would provide such a proof.

The reason why we care about such proofs can be understood by considering the following setting. Suppose are given a physically implemented quantum computer which we

do not trust. We would like this computer to be able to provide certificates that the results of its computations are correct which we then can verify with a trusted classical device (if BQP$\not\subseteq$NP, this is not generally possible). For example, we can classically and efficiently verify results of Shor's factoring algorithm [28]. While integer factoring is not yet proven to be classically hard, the glued trees problem is [12]. The quantum snake walk might be able to provide an algorithm which efficiently produces a required certificate for the version of the glued trees problem described in the previous paragraph. It would also be interesting, if it were impossible for a quantum computer to find a certificate efficiently.

Another potential direction for the future research is to consider discrete-time analogues of the continuous-time quantum snake walk and their applications. A recent paper by Mc Gettrick defines a discrete-time walk on the line similar to the continuous-time quantum snake walk on the line defined here, although snakes (according to our terminology) are allowed to move only forward (or, equivalently, only backward) [24].

Bibliography

[1] M. Abramowitz and I. A. Stegun, editors. *Handbook of Mathematical Functions with Formulas, Graphs, and Mathematical Tables*. U.S. Department of Commerce, 10th edition, 1972. 5

[2] D. Aharonov and A. Ta-Shma. Adiabatic quantum state generation and statistical zero knowledge. In *Proc. 35th ACM symposium on Theory of Computing*, pages 20–29, 2003. 3

[3] A. Ambainis. Quantum algorithms and complexity. Lecture notes, University of Waterloo, 2005. Available at www.math.uwaterloo.ca/∼ambainis/CO781.htm. 4, 5, 17, 34

[4] A. Ambainis. Quantum lower bounds by quantum arguments. *Journal of Computer and System Sciences*, 64:750–767, 2002. 61

[5] A. Ambainis, E. Bach, A. Nayak, A. Vishwanath, and J. Watrous. One-dimensional quantum walks. In *ACM Symposium on Theory of Computing*, pages 37–49, 2001. 4

[6] A. Ambainis, A. M. Childs, B. W. Reichardt, R. Špalek, and S. Zhang. Any AND-OR formula of size N can be evaluated in time $N^{1/2+o(1)}$ on a quantum computer. In *Proc. 48th IEEE Symposium on Foundations of Computer Science*, pages 363–372, 2007.

[7] D. ben Avraham, E. M. Bollt, and C. Tamon. One-dimensional continuous-time quantum walks. *Quantum Information Processing*, 3:295–308, 2004. 4

[8] E. Bernstein and U. Vazirani. Quantum complexity theory. In *Proc. 25th ACM Symposium on Theory of Computing*, pages 11–20, 1993. 1

[9] D. W. Berry, G. Ahokas, R. Cleve, and B. C. Sanders. Efficient quantum algorithms for simulating sparse Hamiltonians. *Communications in Mathematical Physics*, 270(2):359–371, 2007. 3

[10] A. M. Childs. *Quantum Information Processing in Continuous Time*. PhD thesis, Massachusetts Institute of Technology, 2004. 3, 5, 9

[11] A. M. Childs. Universal computation by quantum walk. *Physical Review Letters*, 102(180501), 2009. Also available at arXiv:0806.1972v1. 2, 4, 7, 56, 57

[12] A. M. Childs, R. Cleve, E. Deotto, E. Farhi, S. Gutmann, and D. A. Spielman. Exponential algorithmic speedup by a quantum walk. In *Proc. 35th ACM symposium on Theory of Computing*, pages 59–68, 2003. 2, 7, 8, 9, 59, 61, 62

[13] A. M. Childs, R. Cleve, S. P. Jordan, and D. Yeung. Discrete-query quantum algorithm for NAND trees. *Theory of Computing*, 5:119–123, 2009.

[14] A. M. Childs and J. Goldstone. Spatial search by quantum walk. *Physical Review A*, 70(022314), 2004. 2

[15] A. M. Childs and R. Kothari. Limitations on the simulation of non-sparse Hamiltonians. Available at arXiv:0908.4398v1.

[16] A. M. Childs, L. J. Schulman, and U. V. Vazirani. Quantum algorithms for hidden nonlinear structures. In *Proc. 48th IEEE Symposium on Foundations of Computer Science*, pages 395–404, 2007. 2

[17] D. Deutsch. Quantum theory, the Church-Turing principle and the universal quantum computer. *Proc. Roy. Soc. London*, 400:97–117, 1985. 1

[18] E. Farhi, J. Goldstone, and S. Gutmann. A quantum algorithm for the Hamiltonian NAND tree. *Theory of Computing*, 4:169–190, 2008. 2, 7

[19] E. Farhi and S. Gutmann. Analog analogue of a digital quantum computation. *Physical Review A*, 57:2403–2406, 1998. 2

[20] E. Farhi and S. Gutmann. Quantum computation and decision trees. *Physical Review A*, 58:915–928, 1998. 2, 50

[21] F. M. Fernández. *Introduction to Perturbation Theory in Quantum Mechanics*. CRC Press, 2001. 28, 54

[22] T. Kato. *A Short Introduction to Perturbation Theory for Linear Operators*. Springer, 1982. 20

[23] A. Markushevich and R. A. Silverman. *Theory of Functions of a Complex Variable*, volume I. Prentice Hall, 1965. 20

[24] M. Mc Gettrick. One dimensional quantum walks with memory. Available at arXiv:0911.1653v1. 62

[25] A. Nayak and A. Vishwanath. Quantum walk on the line (extended abstract). Available at arXiv:quant-ph/0010117v1. 4, 34

[26] H. T. Nguyen and G. S. Rogers. *Fundamentals of Mathematical Statistics*, volume I: Probability for Statistics. Springer-Verlag, 1989. 6

[27] M. A. Nielsen and I. L. Chuang. *Quantum Computation and Quantum Information*. Cambridge University Press, 2000. 11

[28] P. W. Shor. Algorithms for quantum computation: discrete logarithms and factoring. In *Proc. 35th IEEE Symposium on Foundations of Computer Science*, pages 124–134, 1994. 1, 62

[29] D. R. Simon. On the power of quantum computation. In *Proc. 35th IEEE Symposium on Foundations of Computer Science*, pages 116–123, 1994. 1

[30] R. Wong. *Asymptotic Approximations of Integrals*. SIAM, 2001.